UNIVERSITÄT HAMBURG

DEPARTMENT BIOLOGIE

Functional consequences of interactions between the neural cell adhesion molecule NCAM, the receptor protein tyrosine kinase TrkB and the inwardly rectifying K^+ channel Kir3.3 in *Mus musculus* (Linnaeus, 1758)

DISSERTATION

zur Erlangung des akademischen Grades eines
Doktors der Naturwissenschaften
(*doctor rerum naturalium*)

des Departments Biologie
der Fakultät für Mathematik, Informatik und Naturwissenschaften
an der Universität Hamburg

Vorgelegt von

Claas Cassens

Hamburg, Mai 2008

Genehmigt vom Department Biologie
der Fakultät für Mathematik, Informatik und Naturwissenschaften
an der Universität Hamburg
auf Antrag von Frau Professor Dr. M. SCHACHNER
Weiterer Gutachter der Dissertation:
Professor Dr. K. WIESE
Tag der Disputation: 04. Juli 2008

Hamburg, den 20. Juni 2008

Professor Dr. Jörg Ganzhorn
Leiter des Departments Biologie

1 Introduction

The nervous system obtains sensory information from the environment, evaluates significance of the information, and generates appropriate behavioral responses. Accomplishing these tasks requires an anatomical plan of considerable complexity. The human nervous system is comprised of several hundreds of billions of neurons, each of which receives and gives rise to tens of thousands of connections. Some of these connections are located nearly a meter from the cell bodies of origin (Brodmann, 1908; Amaral, 2000).

The diverse functions of the vertebrate nervous system, which range from sensory perception and motor coordination to motivation and memory, depend on precise connections formed between distinct types of nerve cells. This developmental program culminates in a great variety of neural cell types – both neurons and glial cells. There are now thought to be many hundreds of different neuronal types, far more than in any other organ of the body (Jessell and Sanes, 2000).

The manifold functions of the mature nervous system depend critically on the establishment of regionally distinct subdivisions of the neural tube. The early pattern of cell differentiation in the neural tube can be viewed as a series of inductive interactions, in which signals provided by one group of cells direct the fate of neighboring cells. Despite the differences in the organization of the nervous systems of invertebrates and vertebrates, the signaling molecules responsible for the differentiation and patterning of developing neurons have been conserved throughout animal evolution to a surprisingly high degree, reflecting an economical use of genetic information (Jessell and Sanes, 2000). It is also becoming apparent that studies of the inductive signaling pathways and transcriptional responses that control development of the vertebrate nervous system can provide important insights into the molecular basis of human neurological disorders.

Development and maintenance of nervous system functions depend on cues that are molecularly distinct, but interact with each other in morphogenetic processes, such as cell proliferation, migration, differentiation and survival, neuritogenesis, synaptogenesis and regulation of synaptic activity in the adult. Cell adhesion molecules have been shown to play an important role in these interactions (Maness and Schachner, 2007). Equally

important are neurotrophic factors that regulate neuronal survival and neuritogenesis not only during development, but also in the adult, when the nervous system is under constraint to regenerate after injury and during synaptic plasticity, underlying learning and memory (Kaplan and Miller, 2000). Signal transduction triggered by cell adhesion molecules and neurotrophin receptors are pivotal in integrating the various signals from the cell surface to the cell interior. Knowledge of the cross-talk between cell adhesion molecules and neurotrophin receptors is likely to yield important information on converging and diverging signal transduction events.

1.1 The neural cell adhesion molecule - NCAM

The neuronal cell adhesion molecule NCAM belongs to the immunoglobulin (Ig) superfamily and plays a fundamental role in the ontogenetic development of the nervous system. Discovered as the first neural cell adhesion molecule, NCAM was also the first cell adhesion molecule of the immunoglobulin superfamily to be isolated and characterized in detail (Brackenbury et al., 1977; Cunningham et al., 1983; Hoffman and Edelman, 1983; Doherty et al., 1990). A wide diversity of NCAM proteins are encoded by a single gene and generated on transcriptional level as well as through posttranlational modification.

1.1.1 Structure and isoforms of NCAM

Three major isoforms of NCAM (NCAM120, NCAM140 and NCAM180) are generated by alternative splicing of a primary transcript leading to the translation of proteins with an apparent molecular mass of 120, 140 and 180 kDa (Cunningham et al., 1987). NCAM140 and NCAM180 are transmembrane proteins and have cytoplasmatic domains differing only in a 261 amino acid long insertion in NCAM180 that is encoded by exon 18. NCAM120

has only the extracellular domain and is attached to the membrane via a glycosylphosphatidylinositol (GPI) anchor. The extracellular part of all NCAM isoforms consists of five immunoglobulin domains followed by two fibronectin type III (FNIII) domains.

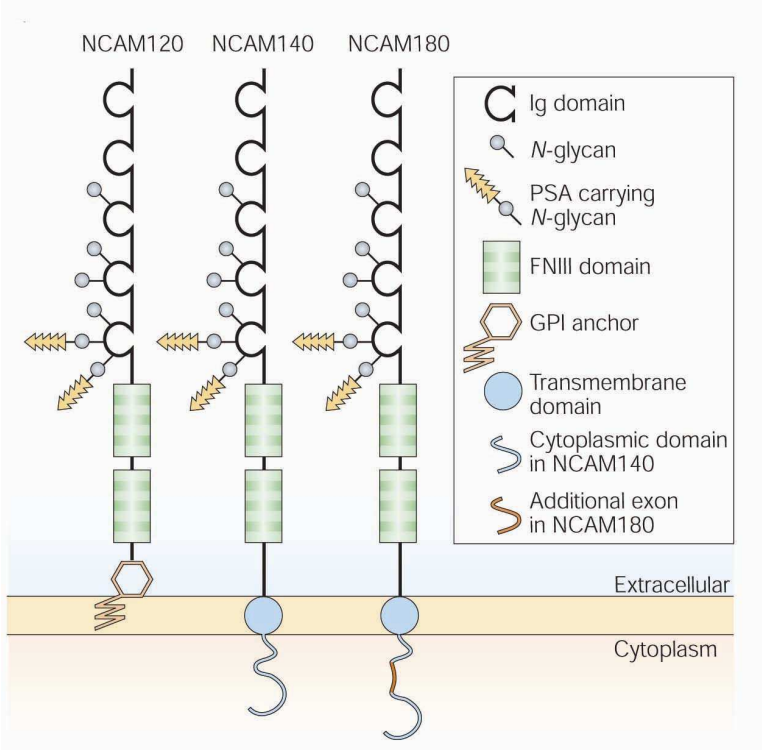

Figure 1 Structure of all NCAM isoforms

The glycosylphosphatidylinositol (GPI)-anchored NCAM120 and the transmembrane NCAM140 and NCAM180 consist of five immunoglobulin (Ig)-like domains and two fibronectin type III repeats (FNIII). The cytoplasmic domains of NCAM140 and NCAM180 differ in length owing to the presence of an additional exon sequence in NCAM180 that results from alternative splicing. All three isoforms of NCAM are carriers of PSA (Kleene and Schachner, 2004).

All isoforms are heavily glycosylated but especially worth mentioning is that NCAM carries an unusual carbohydrate, α-2,8-linked polysialic acid (PSA), which has not been found on any other recognition molecule in the nervous system (Kleene and Schachner, 2004). This glycan modifies functional properties of the NCAM protein backbone during neuronal migration, axon pathfinding and synaptic plasticity (Eckhardt et al., 2000; Angata et al., 2004; Weinhold et al., 2005).

1.1.2 Expression and function of NCAM

NCAM has been linked to human brain disorders such as schizophrenia, bipolar disorder and Alzheimer's disease and to learning and memory deficits in mice (Brennaman and Maness, 2008). NCAM-deficient mice also show behavioral abnormalities connected to serotonin-related aggression and anxiety (Stork et al., 1997; Stork et al., 1999).

Expression of NCAM persists into adulthood on both neurons and glial cells, but occurs in the nervous system mainly during neural tube closure. The three major isoforms show cell type-related and temporal differences in expression. Predominantly expressed in neurons late in development, NCAM180 is enriched at sites of cell contact and postsynaptic densities of mature neurons (Persohn et al., 1989). NCAM140 on the other hand is localized to migratory growth cones and axon shafts of developing neurons and mediate neurite outgrowth responses. The maturation of vesicle cycling has also been ascribed to NCAM140 (Polo-Parada et al., 2004). NCAM140 is expressed both by neurons and glia cells, whereas NCAM120 is predominantly expressed by glia.

Polysialylation of NCAM is regulated developmentally, decreasing during embryonic ages and into adulthood, when it remains detectable at sites where neurogenesis is active, such as on olfactory neurons in the rostral migratory stream and on neural stem cells in the dentate gyrus (Petridis et al., 2004). The existence of a α-2,8-linked polysialic acid on NCAM may decrease homophilic NCAM interactions because of its highly negative charge and large hydration volume (Johnson et al., 2005).

Molecular dissection of NCAM and identification of splice variants have revealed complex interactions of the extracellular region. The first fibronectin type III domain is important in mediating neurite outgrowth and plasticity. It contains the docking site for the polsialyltransferases that glycosylate the neighboring fifth immunoglobulin-like domain (Muhlenhoff et al., 1996; Mendiratta et al., 2005). The first and second fibronectin type III domains can bind fibroblast growth factor receptor FGFR, thereby competing with fibroblast growth factor FGF binding to the FGFR (Francavilla et al., 2007), and contain a putative motif for receptor activation and NCAM-mediated neurite growth, signaling and learning (Anderson et al., 2005; Kiselyov et al., 2005). The third immunoglobulin domain of NCAM is responsible for its binding to the glia cell line-derived neurotrophic factor

GDNF (Sjostrand et al., 2007), which leads to stimulation of neurite outgrowth (Paratcha et al., 2003) and synaptogenesis (Ledda et al., 2007) in hippocampal neurons, migration of neuronal precursors in the rostral migratory stream (Paratcha et al., 2003; Paratcha et al., 2006), and regulation of Schwann cell migration and function (Paratcha et al., 2003; Iwase et al., 2005). Additionally, alternative splicing can introduce a putative hinge between the two fibronectin type III domains in a muscle-specific isoform of NCAM that may modulate cell interactions or it can insert a sequence causing truncation and secretion of the entire NCAM extracellular region (Doherty et al., 2000; Johnson et al., 2004). A splice variant of NCAM that contains the VASE (variable alternatively spliced exon) in the fourth immunoglobulin-like domain arises postnatally in brain and has been proposed to downregulate axon growth (Doherty et al., 2000). Other domains of NCAM have also been shown to be involved in homophilic binding (Rao et al., 1994).

The intracellular domain of NCAM has a single tyrosine residue which is implicated to play a role in the formerly mentioned FGFR binding and thereby in neurite outgrowth through phosphorylation (Diestel et al., 2004). The 40 kDa cytoplasmic domain insert in NCAM180 is responsible for the interaction of this isoform with the cytoskeletal linker protein spectrin and therefore one of the initial proteins that stabilize intracellular organelles at nascent synapses (Sytnyk et al., 2002). The class I PDZ binding motif (aa ESKA) at the utmost C-terminus of NCAM, which is conserved throughout many species, is also suggested to be responsible for trafficking processes (Polo-Parada et al., 2005).

1.1.3 NCAM signaling and signal transduction

Transmembrane cell surface receptors of the immunoglobulin superfamily like NCAM are first of all signal transducers (Schuch et al., 1989; Rao et al., 1994). Activating these receptors at the cell surface through homophilic and/or heterophilic *trans*-interaction leads to a multitude of signaling responses. Many cell surface receptors form clusters on the cell surface in response to multivalent ligand binding or *cis*-interactions with other receptors, setting signal transduction into motion (Crossin and Krushel, 2000).

Neurite outgrowth is a major event in neural development mediated by several cell adhesion molecules. An important conceptual advance in the understanding of NCAM-triggered signaling mechanisms in regard to neurite outgrowth (Doherty et al., 1990) came with the finding that the Src-like non-receptor tyrosine kinase $p59^{fyn}$ is involved in NCAM-mediated signaling and neurite outgrowth (Beggs et al., 1994; Beggs et al., 1997). Within lipid rafts NCAM activates $p59^{fyn}$ and thereby leads to the phosphorylation cascade of the ERK-MAP kinase pathway, which in turn culminates in phosphorylation and activation of the transcription factor CREB required for neurite outgrowth (Schmid et al., 1999; Jessen et al., 2001). The transcriptional activator NF-κB is also known to be regulated by NCAM (Krushel et al., 1999). NCAM is furthermore able to signal through the FGFR and activation of phospholipase Cγ (PLCγ) (Saffell et al., 1997; Doherty et al., 2000). Interestingly, while some cell-types seem to be dependent on co-signaling of the NCAM-FAK-$p59^{fyn}$-Ras-MAP kinase and the NCAM-FGFR-PLCγ pathway, other cell-types seem to not require a convergence of the mentioned pathways for neuritogenesis (Schmid et al., 1999; Niethammer et al., 2002). Also worthy of note is, that NCAM can be an alternative signaling receptor for the ligand family of glia cell line-derived neurotrophic factor GDNF (Paratcha et al., 2003). In the absence of the GDNF family receptor GFRα, GDNF interacts with NCAM with low affinity. When GFRα is associated with NCAM, GDNF binds with high affinity to NCAM and activates in the cytoplasm $p59^{fyn}$ and focal adhesion kinase FAK. Interestingly, association of GFRα1 with NCAM also downregulates NCAM-mediated cell adhesion if GDNF is not present (Paratcha et al., 2003).

1.2 The receptor protein tyrosine kinase - TrkB

The Trk receptors (TrkA, TrkB, TrkC) are a family of three receptor tyrosine kinases deriving its name from the oncogene that led to its discovery (Martin-Zanca et al., 1986a; Martin-Zanca et al., 1986b; Barbacid et al., 1991). This oncogene was found to consist of the first seven of eight exons of nonmuscle topomyosin fused to the transmembrane and intracellular domains of a novel tyrosine kinase (Johnson et al., 1999; Huang and

Reichardt, 2003). Hence, the corresponding protooncogene was named *trk* – tropomyosin-receptor kinase (Martin-Zanca et al., 1986a; Barbacid, 1994). TrkB is a glycoprotein of an apparent molecular weight of 145 kDa and was discovered as the second member of the family due to its high homology to the original Trk, which is now commonly referred to as TrkA (Klein et al., 1989; Middlemas et al., 1991). Specific patterns of expression within the nervous system suggested roles in neuronal development and function, but the Trk receptors were originally only a small percentage of the large number of orphan tyrosine kinases with high expression in the nervous system. The ligands binding and activating the Trk receptors are known as neurotrophins. Different neurotrophins show binding specificity for particular receptors – nerve growth factor (NGF) binds preferentially to TrkA; brain-derived neurotrophic factor (BDNF) and neurotrophin 4 (NT4) to TrkB; and neurotrophin 3 (NT3) to TrkC (Klein et al., 1991; Dechant et al., 1993; Kaplan and Miller, 2000; Huang and Reichardt, 2001). The discovery of the Trk receptors had a revolutionary impact on this field, because it provided essential tools for pursuing the signaling pathways controlled by neurotrophins.

1.2.1 Structure and isoforms of TrkB

All Trk receptors share a common structural organization of their extracellular domain, which clearly distinguishes them from other receptor tyrosine kinases. An array of three tandem leucine-rich 24-residue motifs flanked by two cysteine clusters in their amino termini and two C2-type immunoglobulin-like domains in the more membrane-proximal region make up the extracellular region; a transmembrane domain and a tyrosine kinase domain containing cytosolic region are adjacent to these structures (Patapoutian and Reichardt, 2001). It was shown that Trk receptors interact with their ligands through the second immunoglobulin-like domain (Urfer et al., 1998; Ultsch et al., 1999). The unusual and unique combination of extracellular motifs adds up to the ligand-binding region and is also suggested to mediate adhesive interactions in addition to neurotrophin signaling (Tannahill et al., 1995). The region of highest sequence homology among the Trk family is in the kinase domain and like other tyrosine kinases, the phosphorylation of cytoplasmic

tyrosines regulates tyrosine kinase activity and provides phosphorylation dependent recruitment sites for enzymes and adaptor molecules that mediate initiation of intracellular signaling cascades (Kaplan and Miller, 2000; Sofroniew et al., 2001).

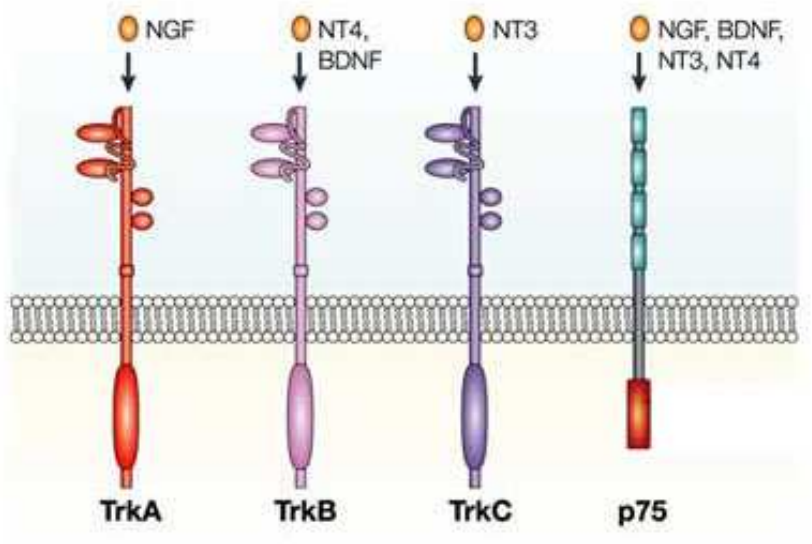

Figure 2 Models of Trk and p75 receptor

Trk receptors contain extracellular immunoglobulin G (IgG) domains for ligand binding and a catalytic tyrosine kinase sequence in the intracellular domain. Neurotrophins bind selectively to specific Trk receptors, whereas all neurotrophins bind to p75 (Chao, 2003).

Receptor isoforms resulting from splice variants of Trk mRNA transcripts exist for each family member. A specific deletion within the intracellular domain of TrkB leads to at least two truncated isoforms known as $TrkB_{TK-}$ ($TrkB_{T1}$ and $TrkB_{T2}$/ $TrkB_{T-Shc}$) in which the entire kinase domain is deleted (Middlemas et al., 1991). The truncated isoform $TrkB_{T2}$, which has the same splice site as $TrkB_{T1}$ but promotes a unique cytoplasmic tail region, has been described in rodent brain and is absent in human brain. The intracellular domains of $TrkB_{T1}$ and $TrkB_{T2}$ consist of 23 and 21 amino acids respectively. The first 12 amino acids of the cytoplasmic tail are identical to the full-length isoform, whilst the following 11 and 9 amino acids are specific for $TrkB_{T1}$ and $TrkB_{T2}$ respectively (Klein et al., 1990; Middlemas et al., 1991). The $TrkB_{T-Shc}$ isoform, which seem to be the human equivalent of the rodent $TrkB_{T2}$, is the only one of the truncated isoforms that contains, additionally, a Src homology domain containing transforming protein (Shc)-binding site in the juxtamembrane

domain, similar to the full-length $TrkB_{TK+}$ (Chao, 1992; Stoilov et al., 2002). Furthermore, a certain TrkB isoform ($TrkB_{ED}$) lacking a short insert within juxtamembrane region (exon 9) can be activated only by BDNF, whereas TrkB containing the insert is also activatable by NT3 and NT4 (Boeshore et al., 1999; Strohmaier et al., 1996).

1.2.2 Expression and function of TrkB

TrkB is the most abundant Trk receptor in the brain. Both full-length ($TrkB_{TK+}$) and kinase-deleted or truncated receptors ($TrkB_{TK-}$) are widely expressed on neurons throughout the nervous system as well as weakly in lung and ovaries. The expression of TrkB is detected in the central and peripheral nervous systems during embryogenesis, but while the full-length isoform ($TrkB_{TK+}$) stays almost at the same expression level throughout development until adulthood, the truncated splice variant is remarkably increased after birth and becomes the most abundant adult form of TrkB (Klein et al., 1989; Allendoerfer et al., 1994; Escandon et al., 1994; Armanini et al., 1995; Eide et al., 1996). In the peripheral nervous system it is expressed in dorsal root ganglia and the sympathetic plexus (Martin-Zanca et al., 1990), while in the central nervous system the full-length $TrkB_{TK+}$ is expressed in the cerebral cortex (Klein et al., 1990), the cerebellum (Kaplan et al., 1991; Segal et al., 1995; Lindholm et al., 1997; Ohira et al., 1999; Rico et al., 2002) and the pyramidal cell layer of the hippocampus (Klein et al., 1990; Minichiello and Klein, 1996; Yan et al., 1997; Shimada et al., 1998; Rabacchi et al., 1999). The truncated receptors $TrkB_{TK-}$ are also expressed on glial cells and were observed in the ependymal linings of the cerebral ventricles, astrocytes, and the choroid plexus (Middlemas et al., 1991; Klein et al., 1990; Armanini et al., 1995; Biffo et al., 1995; Fryer et al., 1996). TrkB with and without the exon 9 insert ($TrkB_{ED}$) is expressed differentially in subpopulations of sensory neurons, which suggests that regulation of splicing of the exon encoding this insert is important for normal neuronal development or function in vivo (Boeshore et al., 1999).

The pathways regulated by neurotrophin-mediated activation of TrkB include cell proliferation, cell differentiation, and cell survival (Huang and Reichardt, 2003). Neurotrophin binding to TrkB results in receptor dimerization and kinase activation. The

aggregation of the receptors in turn allows them to phosphorylate one another on their intracellular domains, which then catalyzes the formation of large signaling complexes through the recruitment of cytosolic and membrane-associated proteins (Heumann, 1994). There are 10 evolutionarily conserved tyrosines in the cytoplasmic domain of full-length TrkB ($TrkB_{TK+}$), three of which are present in the autoregulatory loop of the kinase domain (Stephens et al., 1994; Inagaki et al., 1995; Cunningham et al., 1997). Phosphorylation of the other residues promotes signaling by creating docking sites for adaptor proteins that couple the receptor to intracellular signaling cascades (Patapoutian and Reichardt, 2001). The truncated receptors $TrkB_{TK-}$ can bind and internalize neurotrophins in the same ways as the full-length receptor $TrkB_{TK+}$, but they do not initiate the phosphorylation events required for signal transduction. As a result, the distribution and membrane concentration of truncated receptors could potentially modulate neurotrophin activity by restricting the availability of the ligand to full-length receptors (Biffo et al., 1995; Fryer et al., 1997; Li et al., 1998; Eide et al., 1996; Haapasalo et al., 2002).

1.2.3 TrkB signaling and signal transduction

Intracellular signaling events of TrkB are activated by adaptor proteins binding to specific phosphorylated tyrosine residues within the intracellular domain. Three of the proteins that bind to the phosphotyrosines have been identified as the launching sites of the primary pathways for Trk signal transduction (Segal and Greenberg, 1996). All adaptor proteins contain phosphotyrosine-binding (PTB) or src-homology-2 (SH-2) motifs specifically recognizing the phosphotyrosine residue and flanking sequences (Pawson and Nash, 2000). These proteins are amongst others phospholipase C (PLC-γ), phosphatidylinositol-3 kinase (PI-3K) and Shc (SH-2 containing protein) (Stephens et al., 1994). They couple the Trk receptor to intracellular signaling cascades including Ras/extracellular signal regulated kinase (ERK) protein kinase pathway, the phosphatidylinositol-3-OH kinase (PI-3 kinase)/Akt kinase pathway and phospholipase C (PLC)-γ1 (Kaplan and Miller, 2000; Pawson and Nash, 2000). More recent work has resulted in the identification of additional adaptor proteins (e.g. NFκB, atypical protein kinase C (PKC) (Wooten, 1999; Foehr et al.,

2000; Wooten et al., 2001)) that interact with Trk receptors at different tyrosine sites and has demonstrated that transfer of Trk receptors to various membrane compartments controls the efficiency with which Trk receptors can associate with and subsequently activate adaptor proteins and intracellular signaling pathways (Qian et al., 1998; Saragovi et al., 1998; York et al., 2000).

Binding by neurotrophins provides the primary mechanism for activation of Trk receptors, but the affinity and specificity of Trk receptor activation by neurotrophins can be strongly facilitated by the pan-neurotrophin receptor $p75^{NTR}$ (Chao, 1994; Chao and Hempstead, 1995; Bibel et al., 1999). It has been shown that the presence of $p75^{NTR}$ leads to an increase in the specificity of TrkB activation by brain-derived neurotrophic factor (BDNF) in comparison to neurotrophin 3 (NT3) and neurotrophin 4 (NT4) (Bibel et al., 1999).

1.3 The G protein-coupled inwardly rectifying potassium channel - Kir3

Potassium channels active near resting membrane potentials are critical determinants of cellular excitability. The Kir channels are a particularly interesting class of these resting potassium selective ion channels which form homotetrameric proteins through the cell membrane. They elicit rectifying currents down the electrochemical gradient by passing K^+ more readily in the inward direction of the cell than outwards (Fakler et al., 1995). The molecular constitution of the Kir channel was discovered, when the first two subunits (ROMK1/Kir1.1 and IRK1/Kir2.1) were cloned (Ho et al., 1993; Kubo et al., 1993). Since then numerous Kir proteins have been identified and developed into the gene family of Kir channels containing further seven subfamilies. They all share the feature of only two transmembrane domains in all of the four potassium channel subunits (Isomoto et al., 1997) (Fig. 3). Kir channel activity is strongly influenced and regulated by intracellular factors and secondary messengers (Nichols and Lopatin, 1997; Ruppersberg and Fakler, 1996; Ruppersberg, 2000). All Kir channels play a pivotal role in the maintenance of the

resting membrane potential and are believed to regulate the repolarization after action potentials and thereby to modify neuronal excitability.

1.3.1 Structure and isoforms of Kir3

In contrast to the constitutively active Kir1 and Kir2 channels, more than one subunit seems to be required for a functional Kir3 channel. They normally form heterotetrameres consisting of two Kir3.1 subunits and either two Kir3.2, Kir3.3 or Kir3.4 subunits (Fig. 3). Kir3.1 alone does not form functional channels when expressed in most cell lines (Chan et al., 1996b; Kennedy et al., 1996; Woodward et al., 1997) and is not transported to the cell surface in transfected oocytes (Stevens et al., 1997). Kir3.2 and Kir3.4 alone can form homotetrameric channels in different heterologous expression systems with rather divergent single channel properties. The presence of Kir3.1 rectifies the properties of the single channels to yield amplitudes and open times corresponding to those of cardial and nerve cells (Lesage et al., 1995). The Kir3.1 subunit coprecipitates with Kir3.2 and Kir3.4 (Krapivinsky et al., 1995; Lesage et al., 1995; Chan et al., 1996a) and has been shown by electrophysiological assays in heterologous expression systems to form functional channels with all other Kir3 subunits (Isomoto et al., 1997; Mark and Herlitze, 2000). However, there are also studies reporting of functional Kir3.2 homomers and Kir3.2/3.3 combinations (Wischmeyer et al., 1997; Inanobe et al., 1999; Jelacic et al., 2000).

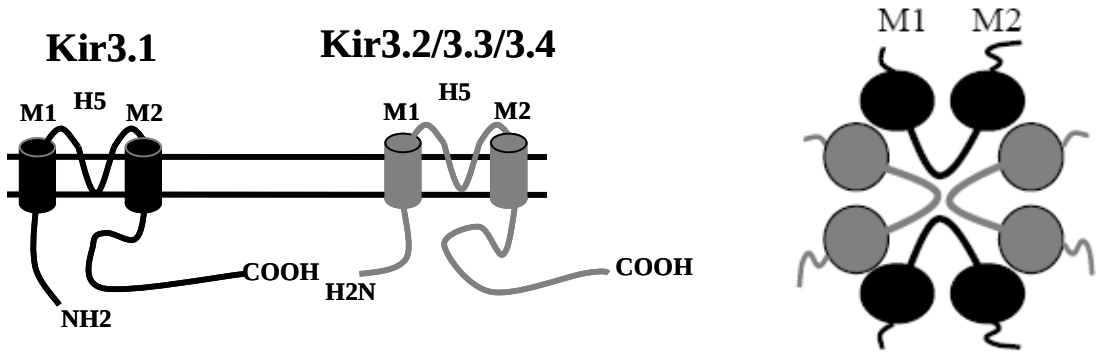

Figure 3 Schematic drawing of a Kir3 channel.

All Kir subunits consist of two transmembrane regions (M1 and M2 and a pore forming region (H5). Both the NH_2- and the COOH-terminus are located intracellularly. The vast majority of Kir3 channels forms heterotetramers consisting of two Kir3.1 subunits and two variable subunits (Delling, 2002).

1.3.2 Expression and function of Kir3

Kir3.1, Kir3.2 and Kir3.3 subunits are widely expressed throughout several brain regions and are especially abundant in the hippocampal region (Karschin and Karschin, 1997). Kir3.1/3.2 and Kir3.1/3.3 channels are supposed to be the main functional combinations found in the brain and are therefore considered as the neuronal Kir3 channels (Kofuji et al., 1995; Luscher et al., 1997). In contrast, the Kir3.1/3.4 combinations are mainly expressed in the heart, where they form the atrial K(ACh) channels, and for that reason are known as the cardiac Kir3 channels (Karschin and Karschin, 1997). While the Kir3.2 subunit is abundant throughout the whole hippocampus from an early embryonic stage on, Kir3.3 is selectively enriched in the stratum lucidum of the CA3 from between postnatal day 9 and 14 on, but mostly restricted to the distal part of axons and weakly in dendrites (Grosse et al., 2003). It was also proposed that the various Kir3 homotetramers and heterotetramers seem to display strikingly different trafficking patterns. While Kir3.2 and Kir3.4 exhibit an ER export motif that leads to their transport to the plasma membrane, this seems to be lacking in Kir3.1 and Kir3.3. In contrast, the Kir3.3 subunit seems to inhibit plasma membrane expression due to a lysosomal targeting sequence that diverts the

heterotetrameric channels at least partly to lysosomes (Ma et al., 2002). Still, these observations (i.e. a unique trafficking role of Kir3.3) cannot be supported overall (Grosse et al., 2003; Koyrakh et al., 2005).

The strongest stimulatory effect on Kir3 channels is caused through the $G_{\beta\gamma}$ subunits of the heterotrimeric G-protein binding to Kir3 channels and is activating them thereby (Huang et al., 1995; Slesinger et al., 1995; Wickman and Clapham, 1995; Lei et al., 2000). Inhibition of Kir channels by means of the G_{α} subunit has also been described (Slesinger et al., 1995; Lei et al., 2001) but seems to be of lesser potency than the activation by $G_{\beta\gamma}$ molecules. Microclusters, where Kir channels, G_{α} subunits and receptors are bound to each other to form complexes, may be the reason why Kir3 channels are opened only by certain receptors in several cell types (e.g. m2-receptors but not β1-receptors regulate Kir in atrial myocytes), even though Kir channels show no specificity for particular Gβγ subunits of certain G-protein subtypes (Yamada et al., 1998). These interactions have important physiological consequences. For example, the so called cardiac Kir3.1/3.4 channels are activated by acetylcholine via the mucarinic m2 receptor and are involved in the slowdown of the heart rate (Wickman et al., 1998; Mark and Herlitze, 2000). In the brain, various neurotransmitters can activate Kir3.2-containing channels, which mediate slow inhibitory postsynaptic potentials (Wickman and Clapham, 1995; Luscher et al., 1997; Signorini et al., 1997; Yamada et al., 1998).

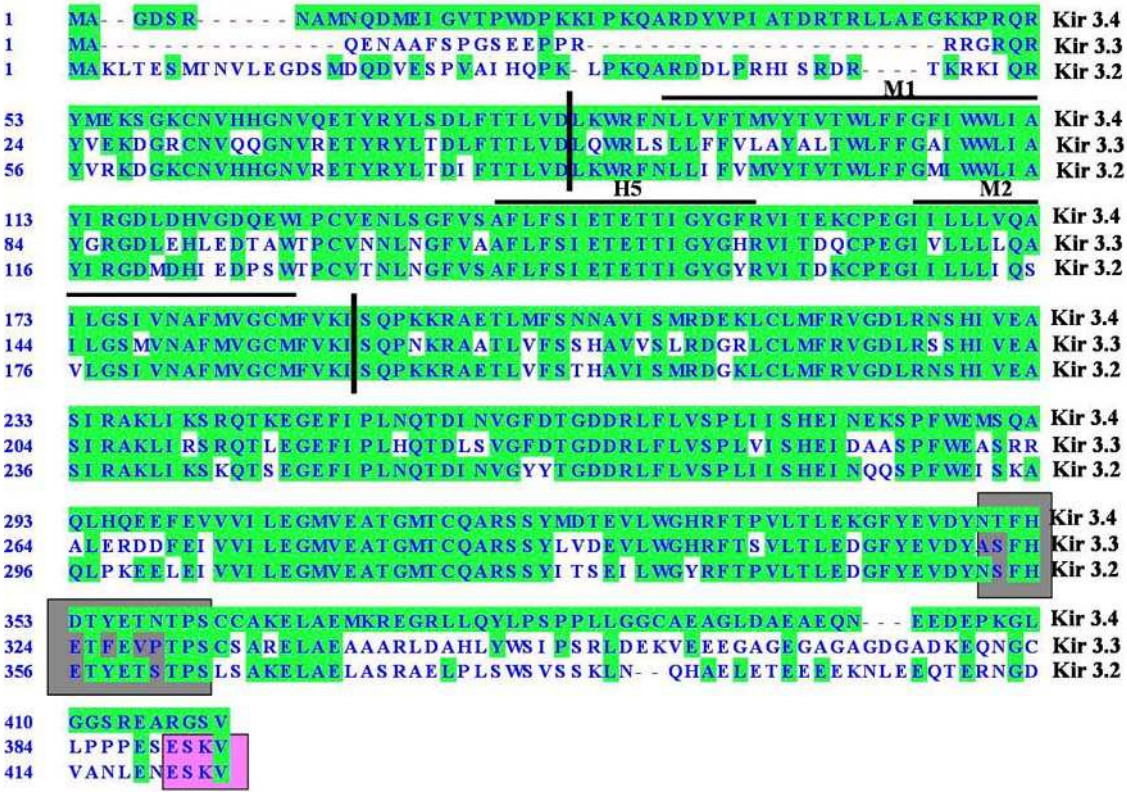

Figure 4 Alignment of the amino acids of the Kir3.4, Kir3.3 and Kir3.2 subunits.

Amino acids in Kir3.2 and Kir3.3 that are identical to Kir3.4 are in green. The PDZ-binding motif of Kir3.3 and Kir3.2 is shown in magenta. The identity between the Kir3 family members is 60-80%. M1, M2: membrane-spanning region; H5: pore-forming region. (Delling, 2002).

1.3.3 Kir3 signaling and signal transduction

In the brain Kir3 channels are linked to a multitude of G-protein coupled receptors (GPCRs) including opioid, adrenergic, muscarinic, dopaminergic, and GABAB receptors and are involved in regulating the excitability of neurons as well as in contributing to the maintenance of the resting potential (Hille, 1992). The disruption of these K+ channels could affect the signal transduction of several pathways in the central nervous system. The *weaver*-mouse (*wv*) was the first neurological abnormality directly related to a genetic point mutation in the Kir3.2 protein. Homozygous *wv* mice were initially characterized by their abnormal 'weaving' gait which appeared due to a substantial loss of cerebellar granule neurons (Hess, 1996). This weaver mutation is the result of a single glycine to serine

exchange in the highly conserved K^+ selectivity sequence (i.e. aa GYG). The mutated channel was no longer inhibited by specific K^+ channel antagonists, but could be blocked with the cation channel inhibitors verapamil, MK-801 and QX-314 (Kofuji et al., 1996). Similar properties could also be observed in cultured *wv* granule cells. Mutated cerebellar *wv* neurons appeared to be leaky in regard to Na^+ ions as well as chronically depolarized, unresponsive towards neurotransmitters (Kofuji et al., 1996) and to have elevated intracellular Ca^{2+} levels (Harkins et al., 2000).

Homozygous mutant mice lacking Kir3.2 (-/-) were morphologically indistinguishable from their wildtype litter-mates (+/+), but were prone to lethal seizures (Signorini et al., 1997). Deletion of Kir3.3 (-/-) yielded a rather modest electrophysiological phenotype in locus coeruleus, but apart from that were also indistinguishable from their wildtype litter-mates (+/+). Both Kir3.2 and Kir3.3 knockout mice showed a drastic decrease in Kir3.1 expression. This is an indication that Kir3.2 and Kir3.3, similar to Kir3.4, control Kir3.1 expression, assembly and/or surface localization to a Kir3 heteromer and are involved in control of neural excitability (Liao et al., 1996; Signorini et al., 1997; Kennedy et al., 1999). They furthermore exhibit a variety of additional behavioral abnormalities (Torrecilla et al., 2002; Wickman et al., 2002; Blednov et al., 2003; Morgan et al., 2003).

1.4 Indication for an interplay of NCAM and TrkB

The defective long-term potentiation (LTP) observed in NCAM deficient hippocampus can be selectively reduced by the neurotrophin BDNF and is linked to a reduced activation of the BDNF/TrkB signaling cascade. The same could be shown in organotypic slice cultures treated with EndoN, an enzyme that cleaves the PSA moiety of NCAM. Furthermore, TrkB phosphorylation, and thus BDNF signaling, is reduced in both NCAM knock-out mice and EndoN treated slice cultures. This suggests a mechanism through which PSA-NCAM could sensitize pyramidal neurons to BDNF, possibly through presenting and hence concentrating the neurotrophin close to the site of action, thereby modulating activity-dependent synaptic plasticity (Muller et al., 2000; Kiss et al., 2001). It is furthermore suggested, that the

promotion of cell survival through PSA-NCAM is also an effect mediated by the modulation of the increased responsiveness to BDNF and thus TrkB signaling (Vutskits et al., 2001).

On the other hand, recent observations could show that PSA-NCAM limits BDNF-induced choline acetyltransferase (ChAT) activity and BDNF-receptor interactions in cholinergic septal neurons. BDNF-induced ChAT activity is TrkB and $P75^{NTR}$ dependent, and upon PSA removal the additional binding of BDNF to its receptors contributes to the maximal ChAT activity observed (Burgess and Aubert, 2006).

1.5 Indication for an interplay of NCAM and Kir3

In hippocampal neurons of NCAM-deficient mice it could be observed that Kir3 currents were increased in comparison to wild-type controls. Furthermore recombinantly expressed NCAM140 and NCAM180 specifically reduced inward currents generated by the neuronal Kir3.1/3.2 and Kir3.1/3.3 channels, but not by the cardiac Kir3.1/3.4 channels, in *Xenopus* oocytes and in Chinese hamster ovary (CHO) cells. Interestingly, it could be shown that this effect appeared not due to a direct modulation of the channel activity itself but rather due to a reduced membrane surface localization of the Kir3 channels (Delling et al., 2002).

1.6 Indication for an interplay of TrkB and Kir3

It was shown that the neurotrophin BDNF, through activation of TrkB, strongly inhibited the basal activity of Kir3. The inhibition was subunit dependent as only the functional homomeric channels of Kir3.1 and Kir3.4 were significantly inhibited, whereas the

homomeric channels of Kir3.2 were insensitive. In this context BDNF was also found to directly stimulate channel phosphorylation through specific tyrosine residues in the amino terminus of Kir3.1 and Kir3.4 channels (Rogalski et al., 2000; Ippolito et al., 2002).

1.7 Aim of the Study

In the attempt to characterize binding partners for the intracellular domain of NCAM a peptide was identified by phage display that showed similarity to a peptide sequence in the intracellular domain of TrkB.

By this study, the question was addressed whether NCAM and TrkB functionally interact with each other and impinge on similar or distinct signal transduction events and whether they influence each others functions. During the ongoing study, the Kir3.3 channel became apparent as an involved player and the question arose, whether it is modulated by NCAM and/or TrkB.

The aim of the study was: a) to analyze whether there is an interaction between NCAM, TrkB and Kir3.3 and whether they bind directly to each other; b) to identify which region within NCAM, TrkB and Kir3.3 is responsible for the respective bindings; c) to determine functional consequences these bindings might have on neuritogenesis and d) to investigate whether NCAM and TrkB modulate Kir3.3 channel activity.

2 Materials

2.1 Chemicals

All chemicals were obtained from the following companies in p.a. quality: GibcoBRL (Life technologies, Karlsruhe, Germany), Macherey-Nagel (Düren, Germany), Merck (Darmstadt, Germany), Serva (Heidelberg, Germany), and Sigma-Aldrich (Deisenhofen, Germany). Restriction enzymes were obtained from New England biolabs (Frankfurt am Main, Germany) and MBI Fermentas (St. Leon-Rot, Germany), molecular weight standards were obtained from Gibco. DNA Purification kits were purchased from Life Technologies (Karlsruhe, Germany), Pharmacia Biotech (Freiburg, Germany), Macherey & Nagel and Qiagen (Hilden, Germany). Plasmids and molecular cloning reagents were obtained from Clontech (Heidelberg, Germany), Invitrogen (Groningen, The Netherlands), Pharmacia Biotech, Promega (Mannheim, Germany), Qiagen and Stratagene (La Jolla, California, USA). Oligonucleotides were ordered from metabion (Munich, Germany). All oligonucleotides used are listed in the appendix. Cell culture material was ordered from Nunc (Roskilde, Denmark) or Life Technologies. Protein peptides were ordered from Schafer-N (Copenhagen, Denmark).

2.2 Solutions and buffers

ABTS staining solution *(ELISA)*	2	% (w/v)	ABTS in 100 mM sodium acetate buffer, pH 4.2
	0.001	% (v/v)	H_2O_2

BCA Reagent A	1	% (v/v)	bicinchoninacid disodium salt
(BCA protein estimation)	1.7	% (w/v)	Na_2CO_3 x H_2O
	0.16	% (w/v)	tartaric acid
	0.4	% (w/v)	sodium tartrate
	0.95	% (w/v)	$NaHCO_3$, pH 11.25
BCA Reagent B	4	% (w/v)	$CuSO_4$ x 5 H_2O
(BCA protein estimation)			
Blocking buffer	1	% (w/v)	BSA in TBS, pH 7.4
(ELISA)			
Blocking buffer	3	% (w/v)	instant milk powder in TBS
(Western blot)			
Blotting buffer	25	mM	Tris
(Western blot)	192	mM	glycine
	20	% (v/v)	methanole
DNA sample buffer (5x)	50	% (v/v)	glycerol in TAE buffer
(DNA gel electrophoresis)	100	mg	Orange G
Elution buffer	1	x	PBS
(Protein expression)	150	mM	NaCl
	250	mM	imidazole

Ethidiumbromide-staining solution *(DNA gels)*	10	µg/ml	ethidiumbromide in 1x TAE
IPTG *(Protein expression)*	238	mg/ml	IPTG in ddH_2O for a 1 M stock solution
Lysis buffer	1	x	PBS
(Protein expression)	150	mM	NaCl
	10	mM	imidazole
	1	x	COMPLETE™
ND96 solution	96	mM	NaCl
(*Oocyte culture*)	2	mM	KCl
	1	mM	$MgCl_2$
	1	mM	$CaCl_2$
	5	mM	HEPES
PCR buffer	100	mM	KCl
(Taq polymerase)	100	mM	$(NH_4)_2SO_4$
	200	mM	Tris-HCl, pH 8.75
	20	mM	$MgSO_4$
PBS (Phosphate Buffered Saline)	150	mM	NaCl
(*Protein expression*)	20	mM	Na_3PO_4, pH 7.4

Phosphate buffered saline	150	mM	NaCl
supplemented with Ca^{2+}, Mg^{2+}	20	mM	Na_3PO_4, pH 7.4
(PBSCM)	0.2	mM	$CaCl_2$
(*Cell surface biotinylation*)	2	mM	MgCl
RIPA buffer	25	mM	Tris-HCl, pH 7.5
(Cell lysis)	150	mM	NaCl
	1	%	NP-40
	1	%	sodium deoxycholate
	0.1	%	SDS
Running gel (10 %)	3.45	ml	in ddH_2O
(Protein gel)	4.65	ml	1 M Tris-HCl, pH 8.8
	0.125	ml	10 % SDS
	4.17	ml	30 % acrylamide – Bis 29:1
	62.5	µl	10 % APS
	6.25	µl	TEMED
Sample buffer (5x)	0.312	M	Tris-HCl, pH 6.8
(*Protein gel*)	10	% (w/v)	SDS
	5	% (w/v)	β-mercaptoethanol
	50	% (v/v)	glycerol
	0.13	% (w/v)	bromphenol blue
SDS running buffer (10x)	0.25	M	Tris-HCl, pH 8.3
(Protein gel)	1.92	M	glycine

	1.0	M	SDS
Stacking gel (5 %)	3.515	ml	in ddH_2O
(Protein gel)	0.625	ml	1 M Tris-HCl, pH 6.8
	0.05	ml	10 % SDS
	0.830	ml	30 % acrylamide – Bis 29:1
	25.0	µl	10 % APS
	5.0	µl	TEMED
SDS sample buffer (5x)	185	mM	Tris-HCl, pH 6.8
(Protein gel)	50	% (v/v)	glycerol
	10	% (w/v)	SDS
	250	mM	DTT
	0.05	%	bromphenol blue
Stripping buffer	0.5	M	NaCl
(Western blot)	0.5	M	acetic acid
TAE	2	M	Tris actetate, pH 8.0
(*DNA gel*)	100	mM	EDTA
TBS (**Tris Buffered Saline)**	10	mM	Tris-HCl, pH 8.0
(ELISA)	150	mM	NaCl
TBST	10	mM	Tris-HCl, pH 8.0
(ELISA, IP and Western blot)	150	mM	NaCl

	0.05-0.1 % (v/v)		Tween-20
Wash buffer A	1	x	PBS
(Protein expression)	150	mM	NaCl
	10	mM	imidazole
Wash buffer B	1	x	PBS
(Protein expression)	150	mM	NaCl
	20	mM	imidazole
Wash buffer C	1	x	PBS
(Protein expression)	150	mM	NaCl
	40	mM	imidazole
Wash buffer D	1	x	PBS
(Protein expression)	150	mM	NaCl
	60	mM	imidazole

2.3 Bacterial media

(Media were autoclaved and antibiotics were supplemented prior to use)

Ampicillin stock solution	100	mg/ml	in ddH2O

IPTG/XGAL stock solution	238	mg/ml	IPTG in ddH_2O
	40	mg/ml	XGAL in Dimethyl formamide
LB medium	10	g/l	bacto tryptone, pH 7.4
	10	g/l	NaCl
	5	g/l	yeast extract
LB/Amp medium	100	mg/l	ampicillin in LB medium
LB/Amp plates	20	g/l	agar in LB medium
	100	mg/l	ampicillin
LB/IPTG/XGAL plates	15	g/l	agar in LB medium
	1	ml	IPTG/XGAL stock solution

2.4 Bacterial strains and cell lines

CHO	*Chinese hamster ovary* dehydrofolatreductase deficient hamster cell line
***E. coli* DH5α** *(Clontech)*	*deo*R, *end*A1, *gyr*A96, *hsd*R17($r_k^-m_k^+$), *rec*A1, *rel*A1, *sup*E44, *thi*-1, Δ(*lac*ZYA-*arg*FV169), Φ80*lac*ZΔM15, F^-

***E. coli* BL21 (DE3)** *(Novagen)*	F^-, *omp*T, *hsd*S_B ($r_B^-m_B^+$), *gal*, *dcm* (DE3)
***E. coli* M15 (pREP4)** *(Qiagen)*	NaI^S, Str^S, Rif^S, Lac^-, Ara^-, Gal^-, Mtl^-, F^-, $RecA^+$, Uvr^+, Lon^+
***E. coli* XL-1 Blue** *(Stratagene)*	*rec*A1, endA1, *gyr*A96, *thi*-1, *hsd*R17, *sup*E44 *rel*A1, *lac* [F' proAB *lac*$I^qZ\Delta$M15, *Tn*10(Ter^r)

2.5 Cell culture media

The cell culture media Gibco MEM (GMEM), Neurobasal-A and HAM's F-12 as well as all supplements and the trypsine were purchased from PAA-Laboratories.

CHO cell medium	50	ml	HAM's F-12/Gibco Medium (GMEM) supplemented with:
	10	% (v/v)	fetal calf serum (FCS)
	50	U/ml	penicillin/streptomycine
	1	mM	sodium pyruvate
	1	mM	L-glutamine
Primary culture dissection solution	50	ml	Neurobasal-A Medium supplemented with:
	1.0	ml	50x B-27 supplement

	0.5	ml	GlutaMAX
	25	µl	gentamycine (10 mg/ml)
Primary culture medium	50 ml		Neurobasal-A Medium
			supplemented with:
	1.0	ml	50x B-27 supplement
	0.5	ml	GlutaMAX
	10	µl	FGF (10 µg/ml)
Washing solution	Hanks' balanced salt solution (HBSS)		
Trypsine	1:5000		in PBS

2.6 Inhibitors and activators

All phosphatase inhibitors and the recombinant expressed brain-derived neurotrophic factor (BDNF) were ordered from Sigma-Aldrich (Deisenhofen, Germany). The protease inhibitor COMPLETE™ was purchased from Roche Diagnostics (Mannheim, Germany).

BDNF	100 µg/ml dissolved in ddH_2O
Brain-derived neurotrophic factor human, recombinantly expressed in *E. coli*)	
COMPLETE™ Protease inhibitor	One tablet diluted in 1 ml ddH_2O for a 50x stock.

A mixture of several protease inhibitors with broad inhibitory specificity. For the inhibition of serine, cysteine, and metalloproteases in bacterial, mammalian, yeast, and plant cell extracts.

Phosphatase Inhibitor Cocktail 1 5 ml DMSO solution used in 100-fold dilution

A mixture of inhibitors that will inhibit the L-isozymes of alkaline phosphatase as well as serine/threonine protein phosphatases such as PP1 and PP2A. Contains microcystin LR, cantharidin, and (−)-p-bromotetramisole.

Phosphatase Inhibitor Cocktail 2 1 ml aqueous solutions used in 100-fold dilution

A mixture of inhibitors that will inhibit acid and alkaline phosphatase as well as tyrosine protein phosphatases. Contains sodium vanadate, sodium molybdate, sodium tartrate, and imidazole.

2.7 Molecular weight standards

1 kb Plus DNA ladder 20 bands within the range from 100 und 12000 bp

(Invitrogen)

Precision Plus Protein™ Standards Dual Color 8 µl of the Prestained Protein Ladder were loaded on the SDS-PAGE gel.

(Bio-Rad)

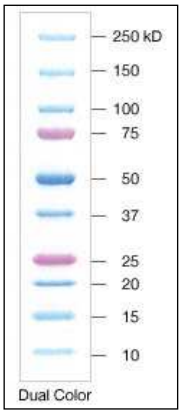

2.8 Plasmids

pcDNA3 *(Invitrogen)*	mammalian expression vector for transfection. Amp-resistance
pGEM®-T Easy *(Promega)*	vector for subcloning of PCR amplificated DNA fragments via T/A cloning. Amp-resistance
pQE-30® *(Qiagen)*	prokaryotic expression plasmid for recombinant expression of proteins carrying a polyhistidine-domain (6xHis) at the 5' end of the multiple cloning site for purification. Amp-resistance

2.9 Antibodies

2.9.1 Primary antibodies

GAPDH (6C5) *(Santa Cruz)*	mouse monoclonal antibody IB: 1:1000 (in blocking solution)
Kir3.3 (C-18) *(Santa Cruz)*	goat polyclonal antibody derived from the C-terminus of Kir3.3 IB: 1:1000 (in blocking solution)

NCAM (1B2)	polyclonal antibody derived from the extracellular domain of mouse NCAM IB: 1:5000 (in blocking solution) IP: 4 µg/sample
NCAM (D3)	mouse monoclonal antibody recognizing an epitope on the NCAM180 isoform within the intracellular domain encoded by exon 18 IB: 1:1000 (in blocking solution) ELISA: 1:1000 (in blocking solution) IP: 4 µg/sample
NCAM (P61)	rat monoclonal antibody recognizing the intracellular domain of NCAM ELISA: 1:1000 (in blocking solution)
NCAM (5B8)	mouse monoclonal antibody produced against the utmost C-terminus of the intracellular domain of NCAM IB: 1:1000 (in blocking solution) ELISA: 1:500 (in blocking solution)
PanTrk (C-14) *(Santa Cruz)*	rabbit polyclonal antibody against a peptide within the highly conserved C-terminus IB: 1:1000 (in blocking solution) ELISA: 1:100 (in blocking solution) IP: 4 µg/sample
TrkB (H-181) *(Santa Cruz)*	rabbit polyclonal antibody against a recombinant protein corresponding to amino acids 160-340 located within the extracellular domain of TrkB of human origin IB: 1:1000 (in blocking solution)

p-Tyr (PY20)	anti-phosphotyrosine mouse monoclonal
(Upstate)	antibody coupled to HRP, clone 4G10
	IB: 1:5000 (in blocking solution)
His-tag	rabbit polyclonal antibody recognizing the 6xHis-tag
(*NEB*)	IB: 1:1000 (in blocking solution)

2.9.2 Secondary antibodies

All HRP coupled secondary antibodies were purchased from The Jackson Laboratory and were used in a dilution of between 1:10000 and 1:20000 for Western blot and 1:5000 for ELISA experiments. Neutravidin-HRP was obtained from Pierce and was used in a dilution of 1:2000 for Western blot and ELISA.

2.10 Oligonucleotides

Name	Sequence 5'-3'	Amino acids	T_m (°C)
Kir3.3-ID-up-BamHI	GGATCCATGTTCGTCAAGATCTCGCAGCC	157-393	66,9/52,8
Kir3.3-ID-dn-HindIII	AAGCTTTCACACCTTGGACTCACTCTCTG	157-393	66,9/52,8
Kir3.2-ID-up-BamHI	GGATCCATGTTTGTGAAAATATCCCAACCC	191-425	66,9/52,8
Kir3.2-ID-dn-HindIII	AAGCTTCTATACTTTGGATTCATTCTCTAG	191-425	66,9/52,8
NCAM-Y734F-up	GGTCATGGACATCACCTGCT**T**CTTCCTGAA CAAGTGTGGCC	734	77,6/70,9
NCAM-Y734F-dn	GGCCACACTTGTTCAGGAAG**A**AGCAGGTG ATGTCCATGACC	734	68,3/57,1

Linker DNA is underlined and exchanged nucleotides for the site-directed mutagenesis are bold.

2.11 Synthesized peptides

The peptides were synthesized by Dr. Jochen Heukeshoven (Hamburg, Germany) and Dr. Christian Schafer (Copenhagen, Denmark).

2.11.1 NCAM peptides

Peptide	**Sequence**
NCAM 1	H-DITCYFLNKCGLLMCIAVNLCGKAGPGAKGKDMEEG-OH
NCAM 1a	H-DITCYFLNKCGLLMCIAVNLC-OH
NCAM 1b	H-NLCGKAGPGAKGKDMEEG-OH
NCAM 2	H-KAAFSKDESKEPIVEVRTEEERTPNHDGGKHTEPNETTPLTEPE-OH
NCAM 3	H-KGPVETKSEPQESEAKPAPTEVKTVPNEATQTKENESKA-OH
NCAM 3-Bio	Biotin-KGPVETKSEPQESEAKPAPTEVKTVPNEATQTKENESKA-OH

2.11.2 TrkB peptides

Peptide	**Sequence**
TrkB	H-CGMVYLASQHFVHRDLATRNCLVGC-OH

2.11.3 Kir3 peptides

Peptide	Sequence
Kir3.3 A	H-RLDAHLYWSIPSRLDEKVEEE-OH
Kir3.3 B	H-EEEGAGEGAGAGDGADKEHNG-OH
Kir3.3 C	H-DKEHNGCLPPPESESKV-OH
Kir3.3 C-Bio	Biotin-DKEHNGCLPPPESESKV-OH
Kir3.2	H-LTERNGDVANLENESKV-OH

2.12 siRNA

The siRNAs were purchased from Qiagen.

siRNA	Target Protein	MW
Ntrk2_2	TrkB	14,803.6
AllStars Neg. Control siRNA	unspecific	14,857.1

3 Methods

3.1 Molecular biology

3.1.1 **Polymerase chain reaction (PCR)** (Mullis et al., 1986)

3.1.1.1 Standard PCR

Amplification of DNA fragments was performed in a thin-walled PCR tube. For this procedure, the following reagents were mixed on ice, and the DNA was multiplied with the *Pfu*-polymerase (*Promega*), the AccuPrime™-polymerase (*Invitrogen*), or the Phusion™-polymerase (*Finnzymes*).

5	µl	10x PCR-buffer
1	µl	primer A (10 pmol/µl)
1	µl	primer B (10 pmol/µl)
1	µl	nucleotides (dNTPs) (40 mM, 10 mM per dNTP)
x	µl	DNA template (0,1-100 ng/µl)
1	µl	DNA-polymerase
ad 50	µl	ddH_2O

The polymerase chain reaction was performed according to reaction specific temperature profiles in MJ Research PTC-200 cycler. When using primers with different melting temperatures, the PCR was carried out at the lower T_m value. The PCR products were analyzed by gel electrophoresis and subsequently eluted from the gel.

Standard PCR program:

95°C	→	2	min	(initial denaturing)	
95°C	→	0,30	min	(denaturing)	25-35 cycles
50-70°C*	→	0,30	min	(annealing)	
72°C	→	#	min	(extension)	
72°C	→	10	min	(final extension)	
4°C	→	∞	min	(soak)	

*This temperature will be defined by the T_m value of the apporpriate primers.

#The extension time depends on the respective polymerase and the length of the amplicon (about 30 sec per kB DNA for the Phusion™-polymerase, about 1 min per kB DNA for the AccuPrime™-polymerase and about 2 min per kB DNA for the *Pfu*-polymerase).

3.1.1.2 Linker PCR

A possibility to include certain sequences for restriction enzymes at the ends of the DNA fragments is the so called linker PCR. Hereby, the primers must be designed so that at both the 5'- and the 3'-end of the PCR amplicon a specific cutting site for restriction enzymes (linker) will be inserted. To enable a directional cloning, two different cutting sites were used when possible. The same polymerases and the same reagent mixture as for the Standard PCR were used for the Linker PCR.

Linker-PCR program:

95°C	→	2	min	(initial denaturing)	
95°C	→	0,30	min	(denaturing)	5 cycles
50-70°C*	→	0,30	min	(annealing)	
(T_m calculation without considering the linker sequence)					
72°C	→	#	min	(extension)	
95°C	→	0,30	min	(denaturing)	25 cycles
50-70°C*	→	0,30	min	(annealing)	
(T_m calculation with considering the linker sequence)					
72°C	→	#	min	(extension)	
72°C	→	10	min	(final extension)	
4°C	→	∞	min	(soak)	

*This temperature will be defined by the T_m value of the approrpriate primers.

#The extension time depends on the respective polymerase and the length of the amplicon (about 30 sec per kB DNA for the Phusion^{TM}-polymerase, about 1 min per kB DNA for the AccuPrime^{TM}-polymerase and about 2 min per kB DNA for the *Pfu*-polymerase).

3.1.1.3 Touchdown PCR

A reason for the appearance of unspecific amplicons can be the suboptimal binding of the used primers. The Touchdown PCR was utilized to prevent unspecific bindings of the primers during the first PCR cycles. The principle is based on a stepwise reduction of the annealing temperature by 2°C for the first 10 PCR cycles. The initial annealing temperature

should be about 10°C above the calculated optimal T_m value. The same polymerases and the same reagent mixture as for the Standard PCR were used for the Touchdown PCR.

Touch Down-PCR program:

95°C	→	2	min	(initial denaturing)	
95°C	→	0,30	min	(denaturing)	15 cycles
50-70°C*	→	0,30	min	(annealing)	
Every third cycle the temperature will be reduced by 2°C for the primer annealing.					
72°C	→	#	min	(extension)	
95°C	→	0,30	min	(denaturing)	20 cycles
50-70°C*	→	0,30	min	(annealing)	
72°C	→	#	min	(extension)	
72°C	→	10	min	(final extension)	
4°C	→	∞	min	(soak)	

*This temperature will be defined by the T_m value of the apporpriate primers.

#The extension time depends on the respective polymerase and the length of the amplicon (about 30 sec per kB DNA for the Phusion™-polymerase, about 1 min per kB DNA for the AccuPrime™-polymerase and about 2 min per kB DNA for the *Pfu*-polymerase).

3.1.2 **Site-directed mutagenesis** (QuikChange® Site-directed mutagenesis kit)

For mutation of single amino acids within a DNA fragment, the QuikChange® Site-directed mutagenesis kit (*Stratagene*) was used. For detailed information, see the manufactures instruction. Primers were designed that they contain the desired mutation and anneal to the same sequence on opposite strands of the plasmid. In addition, they should have a length between 25 and 45 bases and a melting temperature greater than 78°C. The desired point mutation is in the middle of the primer with 10-15 bases of correct sequence on both sides. During PCR reaction, it is important to keep primer concentrations in excess. Therefore, the amount of template was varied while primer concentrations were kept constant.

5	µl	10x PCR-buffer
1	µl	mutation-primer A (10 pmol/µl)
1	µl	mutation-primer B (10 pmol/µl)
1	µl	nucleotides (dNTPs) (40 mM, 10 mM per dNTP)
x	µl	DNA template (0,1-100 ng/µl)
1	µl	*Pfu*-polymerase
ad 50	µl	ddH_2O

The number of cycles was set to 15 to minimize undesired mutations. For determining the extension time, the sizes of the insert and the plasmid have to be taken into account.

Standard PCR program:

95°C	→	2	min	(initial denaturing)	
95°C	→	0,30	min	(denaturing)	15 cycles
50-70°C*	→	0,30	min	(annealing)	
72°C	→	#	min	(extension)	
72°C	→	10	min	(final extension)	
4°C	→	∞	min	(soak)	

*This temperature will be defined by the T_m value of the approrpriate primers.

#The extension time depends on the length of the amplicon (about 2 min per kB DNA for the *Pfu*-polymerase).

After PCR reaction, 10 µl of the mixtures were applied on an agarose gel to check for sufficient amplification. The template DNA (e.g. non mutated DNA) in the amplification reaction was digested by adding 1 µl of DpnI restriction enzyme directly into the amplification reaction with subsequent incubation for 1h at 37°C. Afterwards, the amplification reaction was transformed into competent XL1-Blue bacteria as described. Single colonies were picked from the plate and inoculated into 3 ml cultures. Plasmid DNA was prepared and mutation was verified by sequencing.

3.1.3 **DNA Gel-electrophoresis** (Sambrook et al., 1989)

DNA fragments were separated by horizontal electrophoresis cambers (*BioRad*) using agarose gels. Agarose gels were prepared by heating 1 % (w/v) agarose in 1xTAE buffer. The gel was covered with 1xTAE buffer, and DNA sample buffer was added to the probes.

The DNA samples were pipetted in the sample pockets, and the gel was run at constant voltage (10V/cm gel length) until the orange G dye had reached the end of the gel. Afterwards, the gel was stained in an ethidiumbromide staining solution for 20 min. Finally, gels were documented using the E.A.S.Y. UV-light documentation system (E.A.S.Y. RH Imager, HEROLAB).

3.1.4 **Extraction of DNA from agarose gels** (QIAquick® Gel Extraction Kit)

For isolation and purification of DNA fragments from agarose gels, ethidiumbromide-stained gels were illuminated with UV-light, and the appropriate DNA band was excised from the gel with a clean scalpel and transferred into an Eppendorf tube. The fragment was isolated following the QIAquick®Gel Extraction Kit (*Qiagen*) protocol. The fragment was eluted from the column by addition of 50 µl prewarmed (70°C) Tris-HCl (10 mM, pH 8.0). The DNA-concentration was determined using the undiluted eluate.

3.1.5 **Determination of DNA concentration**

DNA concentrations were determined spectroscopically using an Amersham-Pharmacia spectrometer. The absolute volume necessary for measurement was 50 µl. For determining the concentration of DNA preparations, the eluate was diluted 1:50 with water and the solution was pipetted into a 50 µl cuvette. Concentration was determined by measuring the absorbance at 260 nm, 280 nm and 320 nm. Absorbance at 260 nm had to be higher than 0.1 but less than 0.6 for reliable determinations. A ratio of A260/A280 between 1.8 and 2 monitored a sufficient purity of the DNA preparation.

3.1.6 DNA Sequencing

DNA sequencing was performed by the sequencing facility of the ZMNH. For preparation, 1 µg of DNA was diluted in 7 µl ddH_20, and 1 µl of the appropriate sequencing primer (10 pM) was added.

3.1.7 **Digestion of DNA** (Sambrook et al., 1989)

For restriction, the DNA was incubated with twice the recommended amount of appropriate enzymes in the recommended buffer for 2 h. Restriction was terminated by addition of sample buffer and applied on an agarose gel. If two enzymes were incompatible with each other, the DNA was digested successively with the enzymes. The DNA was purified between the two digestions using the rapid purification kit (Life technologies).

3.1.8 **Dephosphorylation of plasmid-DNA** (Sambrook et al., 1989)

After restriction, the plasmid DNA was purified and SAP buffer (Boehringer Ingelheim) and 1 U SAP (scrimps alkaline phosphatase) per 100 ng plasmid DNA were added. The reaction was incubated at 37°C for 2 h and terminated by incubation at 70°C for 10 min. The plasmid DNA was used for ligation without further purification.

3.1.9 **Ligation of DNA-fragments** (Sambrook et al., 1989)

Ligation of DNA fragments was performed by mixing 50 ng vector DNA with the fivefold or tenfold molar excess of insert DNA. 1 µl of T4-Ligase, and 2 µl of ligation buffer were added, and the reaction mix was brought to a final volume of 20 µl. The reaction was incubated either for 2 h at room temperature or overnight at 16°C. The reaction mixture was used directly for transformation without any further purification.

3.1.10 **Production of competent bacteria** (Inoue et al., 1990)

DH5α and XL1-BLue bacteria were streaked on LB-plates, containing the appropriate antibiotics, and were incubated overnight at 37°C. Individual colonies were selected and used for inoculation of 5 ml LB-Medium for overnight. About 2.5 ml of the culture was subsequently added to 500 ml pre-warmed LB-Medium and growth continued at 37°C until an optical density (OD_{600}) of 0.5-0.6 was reached. After a cooling period on ice for 15 minutes, the culture was transferred to a pre-chilled sterile round-bottom tube and centrifuged at low speed (4,000 x g, 10 min, 4°C). The cells were gently resuspended in 500 ml ice-cold ddH_2O and were centrifuged again according to above mentioned conditions. Cells were once more resuspended in 500 ml H_2O, and HEPES was added (1 mM end concentration) slowly. The cells were centrifuged once again according to the above conditions, and the pellet was resuspended in 4 ml 1 mM HEPES. Aliquots were snap frozen in liquid nitrogen and stored at -70°C for no longer than a few months.

3.1.11 **Transformation of bacteria** (Sambrook et al., 1989)

For transformation of the competent *E. coli* strains BL21, M15, DH5α und XL1-Blue, either 50-100 ng of plasmid DNA or 20 µl of ligation mixture were added to 100 µl of cell

suspension and incubated for 30 min on ice. After a heat shock (1 min, 42°C) and successive incubation on ice (3 min), 800 µl of LB-medium were added to the bacteria and incubated at 37°C for 60 min. Cells were then centrifuged (10,000 x g, 1 min, RT) and the supernatant removed. Cells were resuspended 100 µl LB medium and plated on LB plates containing the appropriate antibiotics. Plates were incubated at 37°C overnight.

3.1.12 **Plasmid isolation from 1.5 ml *E. coli* cultures** (Plasmid-Miniprep)

To obtain rapidly higher amounts of DNA, the Macherey-Nagel Nucleospin kit was used. 15 ml LB/Amp-Medium (100 µg/ml ampicillin) were inoculated with a single colony and incubated over night at 37°C with constant agitation. Cultures were transferred into 15 ml Falcon tubes, and cells were pelleted by centrifugation (12,000 rpm, 1min, RT) in an Eppendorf centrifuge. Plasmids were isolated from the bacteria according to the manufactures protocol with the exception that twice the suggested amounts of buffers were used. DNA was eluted from the columns by adding twice 50 µl of prewarmed (70°C) Tris-HCl (10 mM, pH 8.0) with subsequent centrifugation (12,000 rpm, 2 min, RT). Finally, the concentration was determined.

3.1.13 **Plasmid isolation from 400 ml *E. coli* cultures** (Plasmid-Maxiprep)

For preparation of large quantities of DNA, the Qiagen Maxiprep kit was used. A single colony was inoculated in 2 ml LB/amp (100 µg/ml ampicillin) medium and grown at 37°C for 8 h with constant agitation. Afterwards, this culture was added to 500ml LB/amp medium (100 µg/ml ampicillin), and the culture was incubated at 37°C with constant agitation overnight. Cells were pelleted in a Beckmann centrifuge (6,000g, 15 min, 4°C) and DNA was isolated as described in the manufactures protocol. Finally, the DNA pellet was resuspended in 600 µl of prewarmed (70°C) Tris-HCl (10 mM, pH 8.0), and the DNA concentration was determined.

3.1.14 T/A cloning

DNA fragments amplified by PCR can be cloned into the pGEM®-T Easy Vector. This is advantageous because via transformation of the construct into competent *E.coli* cells and subsequent plasmid isolation, the inserted DNA fragment is multiplied manifold. With the help of suitable cutting sites, the fragment can be cut out of the pGEM®-T Easy Vector and afterwards cloned into the target vector. The pGEM®-T Easy Vector exhibit 3'-T overhangs at the insertion site. As the *Taq*-polymerase features a 3'-adenylation activity, PCR-fragments amplified by a *Taq*-polymerase (e.g. AccuPrime™-polymerase) were easily ligated into the vector. When polymerases with proofreading activity that do not attach 3'-adenosine to generate sticky ends were used for the amplification of the PCR product (e.g. Phusion™-polymerase or *Pfu*-polymerase), these had to be attached afterwards onto the purified PCR product with the help of a *Taq*-polymerase. For this purpose the PCR products were incubated with a *Taq*-polymerase for 30 min at 72°C in the presence of dATP. Then the modified fragments could be used for the T/A-cloning.

Scheme for the attachment of the adnenosine overhangs onto PCR fragments without 3'-adenosine:

7	µl	PCR product (purified via gel elution)
0,5	µl	dATP (10 mM)
1	µl	$MgCl_2$ (15 mM)
1	µl	10x buffer
0,5	µl	*Taq*-polymerase

Scheme for the ligation of PCR fragments into the pGEM®-T Easy Vector:

1	µl	pGEM®-T Easy Vector (50 ng)
x	µl	PCR product (with 3'-adenosine overhangs), 3x times excess
1	µl	T4 DNA-Ligase
5	µl	2x ligation buffer
ad 10	µl	ddH_2O

The ligation took place overnight at 4°C, and subsequently the whole mixing was transformed into competent *E.coli* cells. The plasmids carrying the desired insert could be distinguished from those not carrying it through blue/white screening. If the cloning was successful and the DNA fragment cloned into the vector, the reading frame of the lacZ gene would be disrupted and the bacterial colonies would appear white on the respective medium (IPTG/X-Gal). Colonies carrying plasmids without the inserted DNA fragment read the lacZ gene successfully and thereby marked the colony with a blue coloration.

3.2 Biochemistry

3.2.1 Determination of protein concentration (BCA) (Smith et al., 1985)

To determine the concentration of solutions (cell lysate, recombinantly expressed proteins etc.) the BCA kit was used (*Pierce*). Reagent A and B were mixed in a ratio of 1:50. 10 µl of each protein containing solution were mixed with 200 µl of this BCA solution in microtiter plates and incubated for 30 min at 37°C. A BSA standard curve was co-incubated ranging from a concentration of 50 µg/ml to 1 mg/ml. Afterwards, the extinction

of the samples was measured at 560 nm in an ELISA reader, and the protein concentration of the solutions was determined by comparison to the BSA standard curve.

3.2.2 **SDS-polyacrylamide gel elektrophoresis** (Laemmli, 1970)

For the separation and analysis of proteins SDS-polyacrylamide gels in Mini-Protean III chambers (*BioRad*) were used. The SDS-polyacrylamide gel with a thickness of 1 mm consisted of a 0.8 cm stacking gel containing 5% (v/v) acrylamide and covered a 4.5 cm running gel with 10% acrylamide. The stacking gel is responsible for the concentration of the proteins, whereas the running gel separates the proteins. After complete polymerization of the gel, the chamber was set up according to the manufacturer's protocol. Prior to analysis, the protein samples were heated for 5 min at 95 °C in a sample buffer and shortly centrifuged. The samples were loaded with a maximum volume of 20 µl in the 15 pockets of the gel. A pre stained protein ladder was also applied, as a molecular weight standard and to validate the transfer in a subsequent Western blot. Afterwards, the gel was run at constant voltage of 75 V for 20 min, then at 120 V for 20 min and finally at 150 V for about 55 min until the bromphenol blue line migrated to the end of the gel. After completion of the procedure, gels were either stained or subjected to Western blot analysis.

3.2.3 **Coomassie-staining of SDS-polyacrylamide gels** (Ausrubel, 1996)

After SDS-PAGE, the gels were stained in staining solution for 1h at RT with constant agitation. The gels were incubated in destaining solution until the background of the gel appeared nearly transparent. Afterwards, the gel could be stored a couple of days in ddH_2O.

3.2.4 **Western blot** (Towbin et al., 1979; Burnette, 1981)

3.2.4.1 Electrophoretic transfer

Proteins were transferred from the SDS-polyacrylamide gel on a nitrocellulose membrane (Protran Nitrocellulose BA 85, 0.45 µm, Schleicher & Schüll) using a Mini Trans-blot apparatus (*BioRad*). The blotting sandwich was assembled in blot buffer as described in the manufacturer's protocol. Proteins were transferred electrophoretically at 4°C in blot buffer at a constant voltage (80 V for 120 min).

3.2.4.2 Immunological detection of proteins on nitrocellulose membranes

After the electrophoretic transfer, the membranes were placed protein-binding side up in glass vessels. The membranes were washed shortly in TBST and incubated in 10 ml blocking buffer for at least 1 h at room temperature on a shaking platform. Afterwards, the primary antibody diluted in 10 ml blocking buffer was added in the appropriate dilution either for 1 h at RT or overnight at 4°C. The primary antibody was removed by washing the membrane 5 times for 5 min with TBST. The appropriate horseradish peroxidase (HRP) coupled secondary antibody diluted 1:10.000 in 10 ml washing buffer was applied for 1 h at RT. Incubation of the membrane always took place under constant agitation. The membrane was washed again 5 times for 5 min with TBST, and immunoreactive bands were visualized using the enhanced chemiluminescence (ECL) detection system (*Pierce*). The membrane was covered for 1 min with detection solution (1:1 mixture of solutions I and II). The solution was discarded, and the blot was placed between two plastic foils. The membrane was exposed to X-ray film (*Kodak*) for various time periods, starting with a 1 min exposure, followed by development and fixation of the film.

3.2.4.3 Densitometric evaluation of band intensity

The developed film was scanned, and the digitalized picture was quantified by the image processing software TINA 2.09. Band densities were evaluated according to the manual.

3.2.5 Recombinant expression of proteins in *Escherichia coli* (Ausrubel, 1996)

For recombinant expression of proteins in *E. coli*, the appropriate cDNA was cloned into the pQE30 expression plasmid and transformed into *E. coli* M15 (pREP4) bacteria. The protein was expressed with an N-terminal poly His-tag for purification. After transformation of the expression plasmid, the bacteria were streaked on LB plates supplemented with kanamycin and ampicillin. A single colony was inoculated in a 100 ml LB culture with antibiotics and incubated overnight at 37°C with constant agitation. Afterwards, the 100 ml were transferred into a 2 l culture and incubated at 37°C under constant agitation until the culture had reached an optic density of 0.6-0.7. Protein expression was induced by adding 2 ml 1 M IPTG (1 mM final concentration) to the culture with further incubation for 2-4 h at 30°C. Bacteria were collected by centrifugation (4000 x g, 20 min, 4°C) and stored at –20°C. The frozen cell pellet was thawed 15 min on ice and afterwards resuspended in lysis buffer. Subsequently, the cells were broken open by French press treatment. After centrifugation (10,000 x g, 20 min, 4°C), proteins were purified in soluble form under native conditions using nickel-chelate-resin (Ni-NTA beads) according to the QIAexpressionist™ manual (*Qiagen*). The beads were washed twice with wash buffer for 30 min at 4°C and after that eluted thrice with elution buffer while inverting. Protein solutions were concentrated to 2-8 mg/ml using Centricon filter devices (*Millipore*) and stored at -20°C.

3.2.6 French press

The cell suspension was transferred into a precooled French-*Pressure*-20K-cylinder (capacity: 40 ml). Bacteria were compressed (Spectronic Instruments/SLM Aminco, 10000 psi, 5 min) and lysed by opening the valve carefully. The procedure was repeated thrice, and then the suspension was centrifuged (10.000 x g, 20 min, 4°C) in a Beckman centrifuge to get rid of the cellular debris.

3.2.7 Enzyme-linked immunosorbent assay (ELISA)

All ELISAs were performed with either recombinantly expressed proteins, purchased proteins (*Novartis*) or purchased peptides (*Schafer-N*).

3.2.7.1 General ELISA

The indicated proteins and peptides were immobilized on a polyvinylchloride surface in 96-well microtiter plate (*Nunc*) at a concentration of 10-20 µg/ml in case of proteins, and 10-100 µg/ml in case of peptides, overnight at 4°C under constant agitation. After removal of unbound proteins/peptides by washing three times for 5 min at RT with TBST, the wells were blocked for 1 h at RT with blocking buffer. From this point on, all steps were performed at room temperature and under constant agitation. Potential binding proteins were diluted in TBST prior to incubation at certain concentrations (2.5-100 µg/ml) overnight. Unspecifically bound proteins were removed by five washing steps of 5 min with TBST. Specific primary antibodies and their respective HRP-coupled secondary antibodies were used for the detection of bound proteins. Primary antibodies were incubated for 1 h followed by five washing steps of 5 min with TBST. After an incubation

of 1 h with secondary antibodies, a series of five final washes of 5 min with TBST and one with TBS followed.

For visualization of protein binding in all ELISA experiments, 50 µl of freshly prepared ABTS staining solution was applied and incubated for 10 min at room temperature. The detection reaction of HRP was quantified by measuring the absorbance at 405 nm using an ELISA reader.

3.2.7.2 Biotin ELISA

Peptides, coupled to biotin as potential binding partners for the immobilized proteins/peptides, were incubated at certain concentrations (12.5-100 µg/ml) overnight. Unspecifically bound peptides were removed by five washing steps of 5 min with TBST. Diluted HRP-coupled Neutravidin (*Pierce*), used for the detection of bound biotin coupled peptides, was incubated for 1 h. Apart from that, all biotin ELISAs were performed as described for the general ELISA.

3.2.7.3 Competitive ELISA

In case of competitive ELISAs, the respective competitor was pre-incubated for 10 min at different concentrations (2.5-400 µg/ml), and a constant amount (25-50 µg/ml) of the binding partner was applied in succession. All other steps were performed as described for the general ELISA.

.

3.2.8 Immunoprecipitation

The immunoprecipitations were performed either in murine brain homogenate, in murine brain homogenate subfractions or in transiently transfected cell lines 48 h after transfection.

3.2.8.1 Co-immunoprecipitation using protein A/G agarose beads

The respective cell lysate (supplemented with COMPLETE^{TM} Protease inhibitor) was pre-cleared by incubation with Protein A/G agarose Plus (*Santa Cruz Biotechnology*). An appropriate antibody was applied at a certain concentration for precipitation, and samples were incubated for 3 h on a rotating wheel at 4°C. Prewashed Protein A/G agarose beads were added and incubated overnight at 4°C under constant agitation. Beads then were washed three times with RIPA buffer or TBS(T). Attached proteins were extracted by applying 2x SDS-PAGE sample buffer to the beads and cooking for 5 min at 95°C.

3.2.8.2 Co-immunoprecipitation using anti-phosphotyrosine agarose beads

After harvesting and lysing transfected CHO cells in RIPA buffer (supplemented with COMPLETE^{TM} Protease inhibitor and Phosphatase Inhibitor Cocktail 1 and 2), prewashed anti-phosphotyrosine agarose beads (*Upstate*) were applied, and the mixture was incubated overnight at 4°C under constant agitation. Beads then were washed three times with RIPA buffer or TBS(T). Attached proteins were extracted by applying 2x SDS-PAGE sample buffer to the beads and cooking for 5 min at 95°C.

3.2.9 Cell surface biotinylation

The transfected CHO cells were washed once with ice-cold PBSCM. Surface proteins were biotinylated by incubating cells with 0.5 mg/ml Sulfo-NHS-LS-biotin (*Pierce*) in PBSCM for 10 min at 4°C. Biotinylation was terminated by incubation with 20 mM glycine in PBSCM at 4°C for 10 min followed by extensive washing with PBSCM. Biotinylated cells were lysed directly in RIPA buffer and centrifuged at 4°C for 10 min at 700 x g to get rid of the nuclei. The lysed cells were incubated with pre-washed Strepdavidin magnetic beads (*Pierce*) and incubated overnight at 4°C on a rotating wheel. Beads were then washed three times with RIPA buffer. Attached proteins were extracted by applying 2x SDS-PAGE sample buffer to the beads and cooking for 5 min at 95°C.

3.2.10 Biochemical cross-linking

About 100 µl of the purified bait protein was diluted to 1 mg/ml in PBS and transferred into a foil-covered tube. The trifunctional cross-linker sulfo-SBED (*Pierce*), containing a biotin moiety, a Sulfo-NHS active ester, and a photoactive aryl azide, was dissolved in DMSO, and a 1- to 5-fold molar excess over the purified bait protein was applied. Since the cross-linker was light-sensitive, the whole procedure was performed in darkness until after photoactivation by using UV light. The reaction was gently mixed and incubated for 1 h at RT or for 4 h at 4 °C. After that Zeba^{TM} Desalt Spin Columns (*Pierce*) were used to remove nonreacted cross-linker from the reaction. The labeled bait protein could be stored protected from light at -80°C for later use. The biotin-labeled bait protein was added to about 20 µg of prey protein sample and the whole mixture incubated for 1 h at RT. Then the solution was photoactivated with a UV-light source (365 nm) for 15 min on ice to transfer the biotin label to the potentially bound prey protein. Sample buffer was added to the sample and was heated for 5 min at 70°C. Following analyzes were performed by SDS-PAGE and Western blot.

3.3 Cell biology

3.3.1 Continuous cell culture

3.3.1.1 Culture of CHO cells

The respective cells were cultured with 10 ml of their appropriate medium in 75 cm^2 flasks (*Nunc*) at 37°C, 5 % CO_2 and 90 % relative humidity. Cells were passaged when they were confluent (usually after 3-4 days). Medium was removed, and the cells were shortly washed with washing solution. Cells were detached by treatment with 3 ml Trypsine for 3 min at 37°C and afterwards resuspended in 7 ml fresh medium. Cells were split 1:10 for maintenance or seeded 1:4 in 6-well plates (d = 35 mm; area = 9.69 cm^2) (*Nunc*) for transfection.

3.3.1.2 Transfection of CHO cells

For transfection of CHO cells, the FuGENE® 6 Transfection Reagent (*Roche*) was used. One day before transfection, 1-3 x 10^5 cells were seeded per 35 mm dish of a 6-well plate. When cell density had reached 50-80% (usually after 18-24 h), the cells were washed with washing buffer. For the transfection, 3 µl FuGENE® 6 Reagent and 1 µg total DNA per 35 mm well was used. In case of double transfection, equal amounts of DNA were used. The expression plasmids, used for the transfection, were in all cases pcDNA3 vectors (*Invitrogen*). The transfection procedure was performed as described in the manufacturer's protocol.

3.3.1.3 Lysis of CHO cells

After maintenance or 48 h after transfection of CHO cells in 35 mm-culture dishes, the medium was removed, and cells were lysed in 200-400 µl RIPA buffer per 35 mm well with constant agitation (1 h, 4°C). Cells were scraped of the wells and transferred into a 1.5 ml Eppendorf tube. Debris was removed by centrifugation (15000 x g, 4°C, 10 min), and the supernatant was stored at –20°C for further experiments.

3.3.2 Primary cell culture

3.3.2.1 Culture of primary hippocampal neurons

For preparation of dissociated hippocampal cultures, several C57BL/6J mice of postnatal day 1-2 were used. First, the mice were decapitated, their brains removed from the skulls and cut along the midline. The dissected hippocampi were split into 1 mm thick pieces, washed once with dissection solution and digested with papain and DNAseI for 8-15 min at 30°C. After removal of the digestion solution, hippocampi were washed twice with dissection solution and resolved in dissection solution containing DNaseI. Various glass pasteur pipettes with successively smaller diameters were used to dissociate hippocampal cells by trituration to a homogeneous suspension. The last step of the procedure was the removal of cell debris and the plating of the cells. The hippocampal suspension was centrifuged (80 x g, 10 min, RT) and the pellet resuspended in dissection solution. Cells were counted in a Neubauer cell chamber and transfected with the SCN Nucleofactor® kit (*Amaxa*) before being plated on previously prepared (i.e. coated) cover slips within primary culture medium.

3.3.2.2 Transfection of primary hippocampal neurons

For transfection of primary hippocampal neurons, the SCN Nucleofactor® kit (*Amaxa*) was used. About 2 x 10^5 cells were used for transfection. For each sample either 0.1-0.6 µg DNA and 0.4 µg pmax EGFP® or 40 nM siRNA and 0.4 µg pmax EGFP® were diluted in 3 µl Basic Neuron SCN Nucleofactor® Solution. The expression plasmids used for the transfection were in all cases pcDNA3 vectors (*Invitrogen*) and the siRNA was Stealth™ RNAi (*Invitrogen*). Cells were resuspended in 20µl Basic Neuron SCN Nucleofactor® Solution and mixed with the pre-diluted DNA/siRNA. The sample was transferred into an amaxa cuvette, and program 7 according to the manufacturer's protocol was performed. Afterwards, 80 µl of the primary culture medium was applied to the sample in the cuvette, and the whole mixture was transferred to formerly prepared cover slips in a 96-well plate with the provided plastic pipettes. Transfected cells were incubated at 37°C, 5 % CO_2 and 90 % relative humidity in an incubator. Primary culture medium was exchanged after 4 h, and cells were fixed 48 h later.

Transfection of primary hippocampal neurons were in part performed in cooperation with Dr. Alexander Dityatev in the group of Melitta Schachner.

.

3.3.2.3 Fixation of primary hippocampal neurons

The medium was removed from the coverslips, and cells were fixed with 1 ml of 4 % para-formaldehyde in PBS for 10 min at RT. Cells were either washed twice with PBS and stored in PBS at 4°C or stained with 1 % toluidine blue and 1 % methylene blue in 1 % borax (pH 7.4) for 1 h at RT. After three final washes with H_2O, the cells were dried at RT.

The fixed hippocampal neurons were imaged with a Kontron microscope (*Zeiss*) and analysed with Carl Zeiss Vision KS 400 V2.2 software. For each experimental value, the length of total neurites per cell was measured. In each experiment at least 100 neurites longer than the cell body diameter were separately measured on two coverslips. Analysis only included cells that were not in contact with other cells.

3.3.3 Oocyte cell culture

3.3.3.1 Heterologous expression in *Xenopus laevis* oocytes

For recombinant protein expression in *Xenopus* oocytes, cDNAs of NCAM, Trk and Kir3 isoforms were subcloned into the polyadenylation vector pSGEM. N-terminal fusion of EGFP to rat Kir3.3 was generated by insertion of an EGFP-coding PCR product without a stop codon into the 5' NotI-site of rKir3.3 cDNA. The resulting fusion construct (GFP-Kir3.3) seperates both entire ORFs by three in frame alanine codons. Capped run-off poly $(A)^+$ cRNA transcripts were synthesized from linearized cDNA and subsequently injected into defolliculated oocytes. Xenopus oocytes were incubated at 20°C in ND96 solution (pH 7.4) supplemented with 100 µg/ml gentamicin and 2.5 mM sodium pyruvat, and 48 hours after injection either two electrode voltage clamp recordings or fluorescence measurements were performed. The injection of the oocytes was performed in cooperation with Dr. Erhard Wischmeyer, Göttingen.

3.3.3.2 Electrophysiological recordings from transfected *Xenopus laevis* oocytes

Currents were recorded with a Turbo Tec-10 amplifier (*npi*) and sampled through an EPC9 (*Heka*) interface using Pulse/Pulsefit software (*Heka*). For rapid exchange of external solution, oocytes were placed in a small perfusion chamber with a constant flow of ND96 (pH 7.4). Electrophysiological recordings of oocytes were performed in cooperation with Dr. Erhard Wischmeyer, Göttingen.

3.3.3.3 Cell-surface expression measurements of transfected *Xenopus laevis* oocytes

Cell-surface fluorescence in oocytes was measured with a Nikon C1 laser scanning microscope equipped with a 10x water-immersion objective. For quantification of fluorescence intensity, confocal images were taken under constant parameters from ten different oocytes for each experiment. These measurements were performed in cooperation with Dr. Erhard Wischmeyer, Göttingen.

3.4 Computer based sequence analysis

Computer based sequence analysis and alignments of DNA sequences and protein sequences were performed using the Lasergene-programe (DNASTAR, Inc., www.dnastar.com). The following databases were used: Medline-, BLASTN- and BLASTP-Server of NCBI (National Center for Biotechnology Information, www.ncbi.nlm.nih.gov).

3.5 Statistical analysis

All numerical data are presented as group mean values with standard deviation (SD). Parametric tests (*t*-test or analysis of variance, ANOVA, with subsequent Tukey's *post-hoc* test) were used to compare group mean values as appropriate. Data conformed to the requirement for normal distribution ('normality' test, SigmaStat 2.0, SPSS, Chicago, IL, USA). The threshold value for acceptance of differences between group mean values was 5%.

4 Results

4.1 Identification of an interaction between the intracellular domains of TrkB and NCAM

4.1.1 Phage display analysis of NCAM180 intracellular domain

In search of binding partners for the intracellular domain of NCAM a random 12mer peptide library was screened by phage display using the recombinant intracellular domain of the 180 kDa isoform of NCAM (NCAM180-ID) as substrate-coated bait. The screening was performed by Dr. Jens Lütjohann. A phage expressing an NCAM180-ID binding peptide with similarity to a sequence stretch within the intracellular domain of the tyrosine kinase TrkB (TrkB-ID) was identified (Fig. 5). This short stretch comprising amino acids 668-679 is present in the membrane proximal catalytic domain of TrkB and contains the functionally pivotal aspartic acid which is required for the enzymatic activity of TrkB.

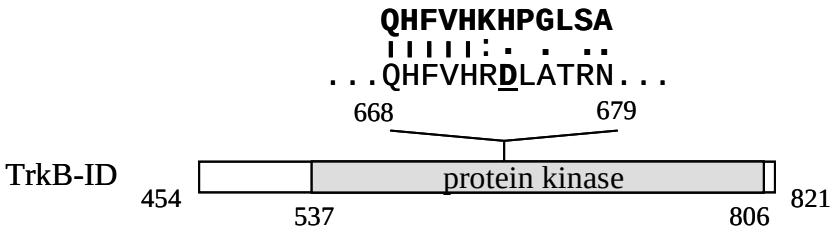

Figure 5 Similarity of phage display sequence binding to NCAM180-ID and TrkB-ID sequence.

The sequence of a peptide (bold letters) identified in a phage display analysis using NCAM180-ID as bait shows significant similarity to a sequence in TrkB-ID. The active site of the tyrosine kinase domain (D), identical amino acids (|), highly conserved amino acids (**:**) and weakly conserved amino acids (**.**) are shown. Numbers designate amino acid positions.

4.1.2 Binding studies of NCAM and TrkB by ELISA experiments

To ascertain, whether the intracellular domain of NCAM binds to a synthetic TrkB peptide (2.10.2) comprising of the amino acids 668-679 found in the phage display analysis and/or to the entire TrkB-ID, an ELISA was performed. Native TrkB-ID was prepared in a baculovirus expression system (Iwasaki et al., 1997). The intracellular domain of the close homolog of L1 (CHL1-ID), an immunoglobulin superfamily member like NCAM, and the intracellular domains of NCAM140 and NCAM180 (NCAM140-ID and NCAM180-ID) were recombinantly expressed and produced in *E. coli*. The synthetic TrkB peptide and the native TrkB-ID were substrate-coated at a constant concentration. Both recombinant NCAM140-ID and NCAM180-ID, but not CHL1-ID, bound to the substrate-coated synthetic TrkB peptide (Fig. 6A) and, in addition, to the substrate-coated recombinantly expressed TrkB-ID (Fig. 6B) in a concentration dependent manner.

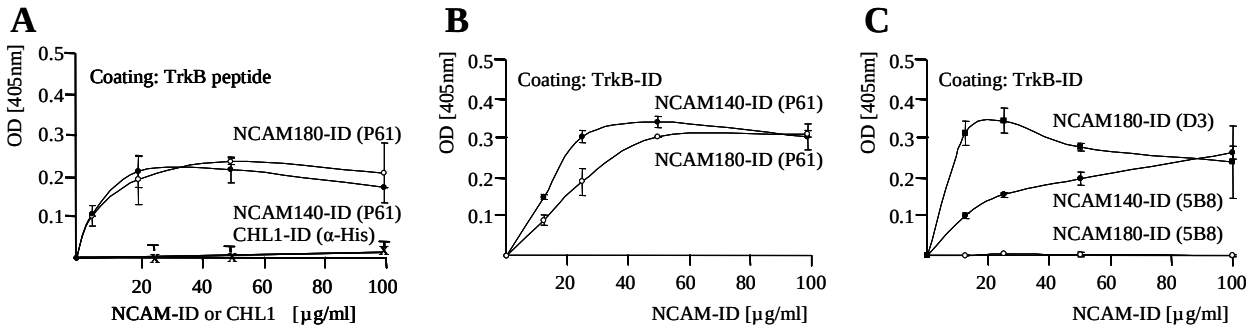

Figure 6 Binding between NCAM-IDs and TrkB peptide or TrkB-ID.

10 µg/ml of substrate-coated TrkB peptide, encompassing the sequence identified by phage display, (**A**) and 10 µg/ml of substrate-coated TrkB-ID (**B, C**) were incubated with increasing amounts of NCAM140-ID (**A-C**), NCAM180-ID (**A-C**) or CHL1-ID (**A**). Binding of the NCAM-IDs was detected by using the antibody P61 (**B, C**), 5B8 (**C**) and D3 (**C**), and binding of CHL1-ID was detected by using a His-tag antibody (**A**). All experiments (**A-C**) were performed at least three times. Error bars represent SD.

Interestingly, the antibody P61 showed a binding for both NCAM isoforms to TrkB-ID (Fig. 6B) and the NCAM180 specific antibody D3 showed a binding for NCAM180-ID to TrkB-ID (Fig. 6C), whereas the antibody 5B8 showed a binding only for NCAM140-ID, and not NCAM180-ID, to TrkB-ID (Fig. 6C). It is known that the 5B8 antibody binds to

the utmost C-terminus of NCAM (Fig 7) and this very region might be responsible for the binding to TrkB and thus is not accessible for the 5B8 antibody anymore. Still, such a conclusion remains to be validated and is remarkable since the binding of the 5B8 antibody to NCAM140-ID is not abolished.

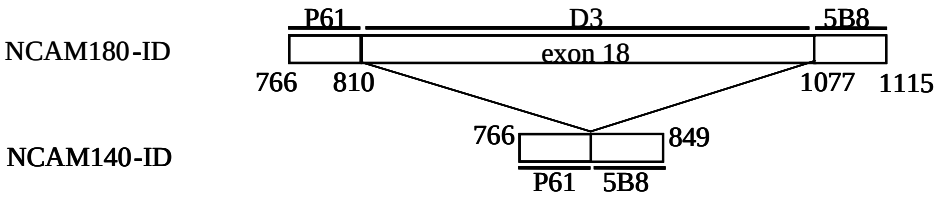

Figure 7 Schematic representation of NCAM140-ID and NCAM180-ID.

The epitopes for binding of the monoclonal antibodies P61 and 5B8 were mapped by using peptides covering amino acids 766-810 and 811-849/1077-1115 respectively. The monoclonal antibody D3 recognizes an epitope in exon 18.

4.1.3 Identification of TrkB binding site in NCAM by competitive ELISA experiments

To further identify the binding site for TrkB within NCAM140-ID and NCAM180-ID and to see, whether the utmost C-terminal region of NCAM is involved in the binding as suggested by the former ELISA experiments, peptides comprising consecutive sequences derived from NCAM140-ID and NCAM180-ID (peptides 1, 2, 3) (Fig. 8) were probed in a competitive ELISA for inhibition of binding of NCAM180-ID to substrate-coated TrkB peptide. The synthetic TrkB peptide was substrate-coated at a constant concentration, and the NCAM180-ID binding partner was also applied at a constant concentration. The NCAM peptides were preincubated at increasing concentrations before the application of the binding partner.

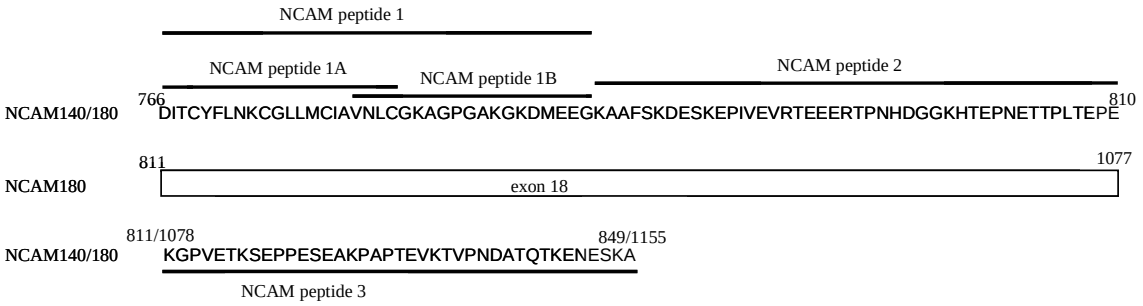

Figure 8 Amino acid sequence of NCAM intracellular domain.

Sequence of NCAM140-ID and NCAM180-ID showing the regions of the respective peptides used in ELISA experiments.

The peptide (NCAM peptide 1), comprising the membrane proximal sequences (amino acids 730-764) of NCAM140-ID and NCAM180-ID, but not the two other peptides (NCAM peptide 2 and 3) deduced from the more distal intracellular sequences, reduced binding of NCAM180-ID to the TrkB peptide in a concentration dependent manner (Fig. 9A).

In addition, to narrow down the binding region in NCAM to an even greater degree, two peptides comprising the N-terminal (peptide 1A) respectively the C-terminal (peptide 1B) part of the membrane proximal peptide 1 were probed in a competitive ELISA for inhibition of binding of biotinylated Kir3.3 peptide C to substrate-coated TrkB peptide (Fig. 9B). The synthetic TrkB peptide was substrate-coated at a constant concentration, and the biotinylated Kir3.3 peptide C binding partner was also applied at a constant concentration. The NCAM peptides were preincubated at increasing concentrations before the application of the binding partner.

The peptide 1A, which comprised the N-terminal part of peptide 1, reduced binding of biotinylated Kir3.3 peptide C to the TrkB peptide in in a concentration dependent manner similar to peptide 1 (Fig. 9B).

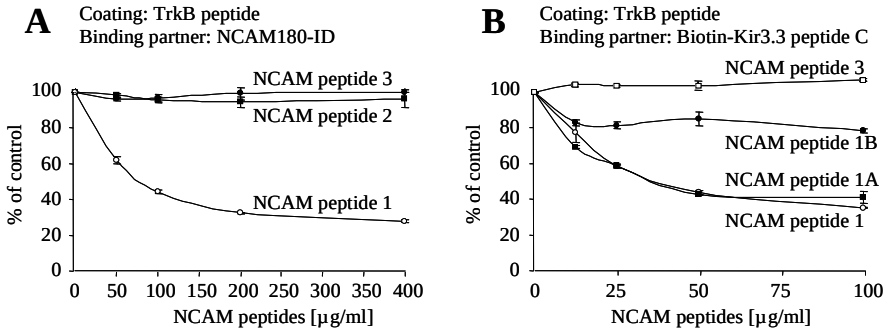

Figure 9 Competition of NCAM peptides to the binding between NCAM180-ID or Kir3.3 peptide C and TrkB peptide.

10 µg/ml of substrate-coated TrkB peptide was pre-incubated with increasing amounts of NCAM140-ID sequence-derived peptides 1, 2 and 3 and then incubated with 25µg/ml of NCAM180-ID (**A**) or 50 µg/ml of the biotin-Kir3.3 peptide C (**B**). Binding of the NCAM180-ID was detected by using the NCAM antibody P61 and binding of the biotinylated Kir3.3 peptide C (Biotin-Kir3.3 peptide C) was detected by using Neutravidin. Both experiments were performed three times. Error bars represent SD.

These observations indicate that the intracellular domains of TrkB and NCAM directly interact with each other in functionally important domains: The catalytic domain of TrkB and the membrane proximal part of NCAM140-ID and NCAM180-ID, that carries the functionally important tyrosine residue, which, when phosphorylated, has been implicated in neurite outgrowth (Diestel et al., 2004).

4.2 Determination of tyrosine phosphorylation of NCAM by TrkB

4.2.1 Generation of an NCAM140-Y734F mutant by site-directed mutagenesis

Considering the function of TrkB as a receptor tyrosine kinase, it was investigated whether TrkB is required for the phosphorylation of the intracellular domain of NCAM at the transmembrane proximal tyrosine that is important for neurite outgrowth, and whether this phosphorylation is dependent on BDNF. A mutation in full-length NCAM140 (NCAM140-

Y734F) was generated by site-directed mutagenesis, whereby the tyrosine at amino acid position 734 was exchanged by phenylalanine, mimicking a permanently unphosphorylated tyrosine. Therefore, the oligonucleotides NCAM-Y734F-up and NCAM-Y734F-dn were used for the site-directed mutagenesis in the NCAM140-pcDNA3 vector to obtain a single amino acid mutation at the mentioned amino acid position 734. These specific oligonucleotides bound to the sequence and changed the original triplet codon TTA (coding for tyrosine) to TTC (coding for phenylalanine) throughout the experimental procedure. After sequencing the mutated vector, a part of the vector CDS consisting of the mutated sequence was cut by the restriction enzymes EcoRI and NotI and ligated with the original NCAM140-pcDNA3 that was lacking the very same region through an EcoRI and NotI digestion (Fig. 10).

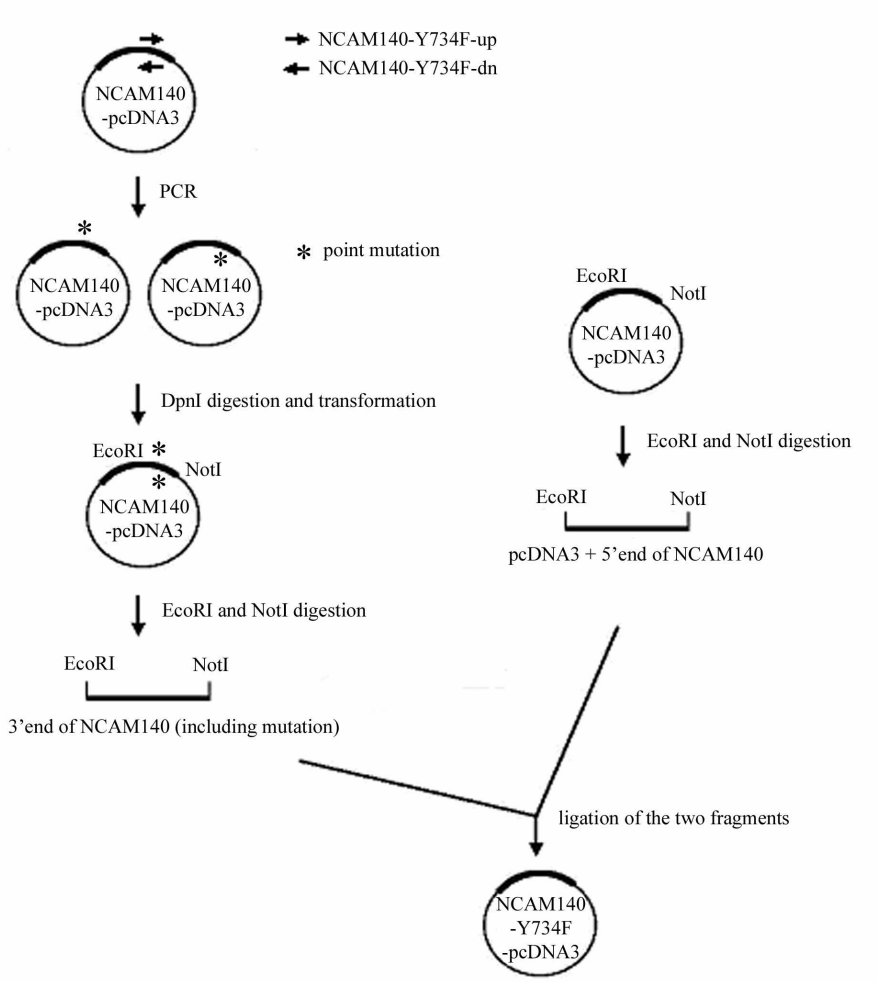

Figure 10 Cloning of the mutated NCAM140-Y734F.

A standard PCR reaction was performed with the oligonucleotides NCAM140-Y734F-up and NCAM140-Y734F-dn as primers and NCAM140-pcDNA3 as the template. The non mutated NCAM140 template DNA in the amplification reaction was digested by adding 1 µl of DpnI enzyme. The amplification reaction was transformed into competent XL1-Blue bacteria, and the plasmids from positive clones, as well as the original NCAM140-pcDNA3 vector, were digested with EcoRI and NotI for subsequent ligation with each other. Mutation was verified by sequencing.

To see, whether the mutated NCAM140-Y734F reaches the cell surface in the same way as the wild-type NCAM140, a cell surface biotinylation was performed. It could be shown, that the mutated NCAM140-Y734F is membrane bound in about the same way as the wild-type NCAM140 (Fig. 11).

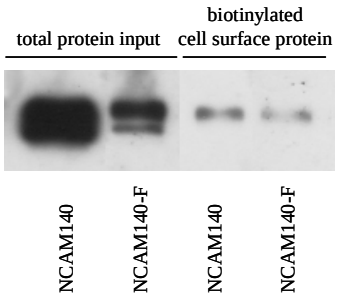

Figure 11 Cell surface delivery of the mutated NCAM140-Y734F.

CHO cells were transfected with NCAM140 and NCAM140-Y734F (NCAM140-F) and maintained for 24 h before biotinylation. For biotinylation of surface proteins, cells were incubated with a trifunctional cross-linker, and the biotinylation was terminated by incubation with glycine. Biotinylated cells were lysed and incubated with pre-washed Strepdavidin magnetic beads. After washing, the samples were subjected to SDS-PAGE and Western blot analysis using the NCAM specific antibody 5B8.

4.2.2 Generation of a eukaryotic expression vector for TrkB

For the construction of a eukaryotic expression vector of TrkB, the cDNA of TrkB was subloned from the cloning vector TrkB-pBluescript KS^+ into the pcDNA3 vector (Fig. 12). Therefore, the TrkB-pBluescript, as well as the empty pcDNA3 vector, was digested by the restriction enzymes EcoRI and NotI. The cut out TrkB cDNA was eluted from an agarose gel and ligated with the linearized pcDNA3 vector, and the ligation was transformed into DH5α cells. Positive clones were sequenced, and the finished TrkB-pcDNA3 vector was used for further experiments.

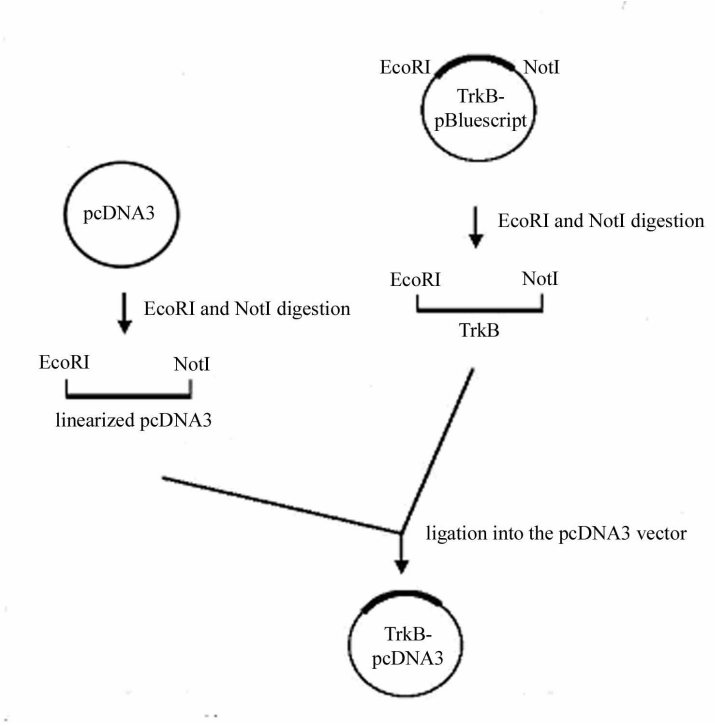

Figure 12 Cloning of TrkB.

TrkB-pBluescript and pcDNA3 were digested with EcoRI and NotI and subsequently ligated with each other. After transformation, positive clones were checked by sequencing.

4.2.3 TrkB dependent phosphorylation studies of NCAM by co-immunoprecipitation experiments

The tyrosine phosphorylation of NCAM140 was investigated in the presence and absence of BDNF after transfection of wild-type NCAM140 or NCAM140-Y734F mutant and/or TrkB into fibroblast-like CHO cells, which do not express detectable levels of NCAM. Upon co-transfection of TrkB and wild-type NCAM140 or NCAM140-Y734F, immunoprecipitation of tyrosine phosphorylated proteins by immobilized phosphotyrosine antibodies and Western blot analysis using NCAM antibodies showed co-immunoprecipitation of wild-type NCAM140 with the phosphotyrosine antibody in the presence of BDNF, but not in its absence (Fig. 13). However, even in the presence of BDNF and upon co-transfection of TrkB, the mutated NCAM140-Y734F was not co-immunoprecipitated by the phosphotyrosine antibody (Fig. 13). Furthermore, neither the

mutated NCAM140-Y734F nor the wild-type NCAM140 was co-immunoprecipitated by the phosphotyrosine antibody when transfected alone without TrkB (Fig. 13), indicating that TrkB was necessary for tyrosine phosphorylation of NCAM. However, the binding of TrkB to NCAM was not influenced by phosphorylation as they co-immunoprecipitated with or without BDNF-triggering of TrkB to the same degree (data not shown).

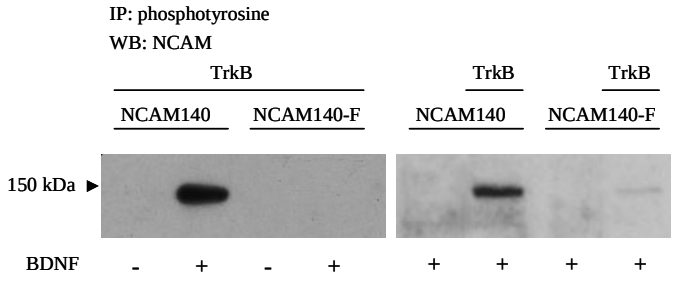

Figure 13 Phosphorylation of NCAM by co-transfection of TrkB and/or treatment of BDNF.

CHO cells were transfected with NCAM140 and NCAM140-Y734F (NCAM140-F) alone or in combination with TrkB. Transfected cells were maintained for 24 h and treated for 20 min with or without 100 ng/ml BDNF before lysis. The cell lysates were incubated with phosphotyrosine antibody coupled agarose. The immunoprecipitates were subjected to SDS-PAGE and Western blot analysis using the NCAM specific antibody 5B8. The experiment was performed thrice with identical results.

To exclude the possibility, that NCAM is co-immunoprecipitated with other tyrosine phosphorylated proteins, co-immunoprecipitations were also performed using an NCAM antibody, and the immunoprecipitates were probed with the phosphotyrosine antibodies. The first sets of these experiments were widely unsuccessful, as no phosphorylated protein could be co-immunoprecipitated with NCAM in any case. It was only, when phosphatase inhibitor cocktails were added to the buffers used in the experiment, that phosphorylated NCAM could be detected in the immunoprecipitate. Upon co-transfection of TrkB and wild-type NCAM140 or mutated NCAM140-Y734F, immunoprecipitation using NCAM antibodies and Western blot analysis using phosphotyrosine antibodies revealed co-immunoprecipitation of tyrosine phosphorylated wild-type NCAM140, but not of mutated NCAM140-Y734F, even in the absence of BDNF (Fig. 14). In the presence of BDNF, the amount of tyrosine phosphorylated wild-type NCAM140 significantly increased (Fig. 14). When cells were mock-transfected or transfected with wild-type NCAM140 alone, no co-

immunoprecipitation of tyrosine phosphorylated NCAM140 was detectable independent on the presence of BDNF (Fig. 14).

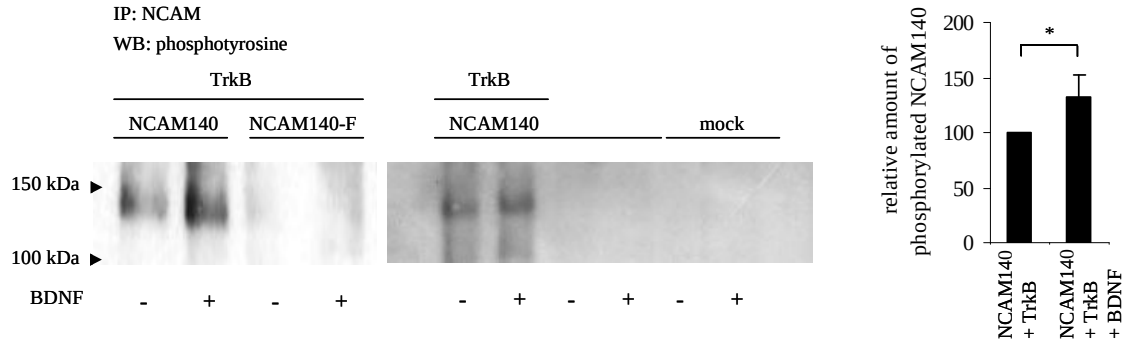

Figure 14 Phosphorylation of NCAM by co-transfection of TrkB and/or treatment of BDNF (II).

CHO cells were transfected with NCAM140 and NCAM140-Y734F (NCAM140-F) alone or in combination with TrkB or were mock-transfected. Transfected cells were maintained for 24 h and treated for 20 min with or without 100 ng/ml BDNF before lysis. The cell lysates were incubated with NCAM specific antibody (1B2) followed by incubation with Protein A/G agarose. The immunoprecipitates were subjected to SDS-PAGE and Western blot analysis using the phosphotyrosine specific antibody PY20. Bar graph showing the relative increase of phosphorylated NCAM140 after treatment with BDNF. The experiment was performed thrice with similar results. Bar graphs show average from three independent experiments with the asterisks indicating a statistically significant difference (Student's t-test; * $p<0.05$). Error bar represents SD.

In summary, these results clearly show a TrkB-dependent tyrosine phosphorylation of NCAM that is at least increased by, if not dependent on, activation of BDNF.

4.3 Effect of knock-down of TrkB expression on NCAM-mediated neurite outgrowth

4.3.1 Neurite outgrowth measurement of TrkB siRNA transfected hippocampal neurons

Since NCAM-mediated neurite outgrowth depends on NCAM phosphorylation (Diestel et al., 2004) and NCAM phosphorylation, on the other hand, depends on the activity of TrkB, the functional relationship between NCAM-dependent neurite outgrowth and TrkB expression was investigated. Therefore, neurite outgrowth on substrate-coated NCAM was determined, upon ablation of TrkB expression in dissociated early postnatal hippocampal neurons, by using TrkB siRNA. In parallel, control siRNA was applied. Also, poly-L-lysine or laminin were used as negative or positive control substrate-coats, respectively. Cultures were maintained in the absence or presence of BDNF to investigate whether activation of TrkB affected neurite outgrowth. Before measuring the neurite outgrowth of the siRNA transfected hippocampal neurons, it was checked whether the application of TrkB siRNA leads to an ablation of TrkB protein expression. Therefore, the cells were maintained for 36 h after transfection and then harvested and lysed in RIPA buffer. The protein amount was checked by Western blot analysis using a TrkB antibody (H-181). The amount of GAPDH protein was measured as a loading control and used for normalization of the total protein amount. The transfection of TrkB siRNA led to a relative reduction of full-length TrkB protein expression in the hippocampal neurons to a value of 49.6 % (5 nM siRNA) and 47.7 % (20 nM siRNA) respectively (Fig 15). The truncated splice variant of TrkB was not detectable in any of the cell lysates, since its expression increases remarkably not until after birth (Escandon et al., 1994) and the hippocampal neurons, used in this experiment, were from newborn mice. On the other hand, the brain homogenate, used as a positive control, was from adult mice, where the truncated splice variant of TrkB becomes the most abundant form (Escandon et al., 1994).

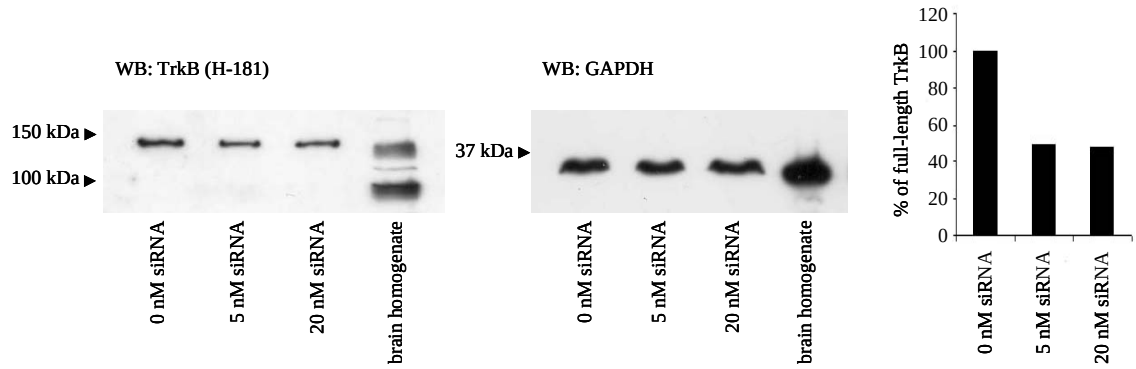

Figure 15 Relative TrkB protein amount of hippocampal neurons after transfection of TrkB siRNA in vitro.

Dissociated hippocampal neurons were transfected with different amounts of TrkB siRNA (5 nM and 20 nM). The cells were maintained for 36 h and then harvested and lysed. The cell lysates, and brain homogenate as a control, were subjected to SDS-PAGE and Western blot analysis using the TrkB specific antibody H-181 and, as a loading control, the GAPDH specific antibody 6C5. Bar graph showing the relative decrease of full-length TrkB after transfection with different amounts of TrkB siRNA.

As it could be shown, that the transfection of TrkB siRNA leads to a strong reduction of TrkB protein expression already at 5 nM siRNA (Fig. 15), the following transfections were always performed with a concentration of 5 nM TrkB siRNA and 5 nM control siRNA.

In the absence of BDNF, neurons, transfected with control siRNA, showed an enhanced neurite outgrowth on NCAM or laminin substrate-coats relative to that observed on poly-L-lysine (Fig. 16). In the presence of BDNF neurite lengths were slightly but not significantly increased on poly-L-lysine relative to that observed in the absence of BDNF, while application of BDNF led to a significant increase in neurite outgrowth on NCAM but not on laminin (Fig. 16). In contrast, the enhanced neurite outgrowth on NCAM in the presence and absence of BDNF was completely abolished upon transfection of neurons with TrkB siRNA. Presence of TrkB siRNA did not change the extent of neurite outgrowth on poly-L-lysine nor on laminin when compared to the negative control siRNA values (Fig. 16).

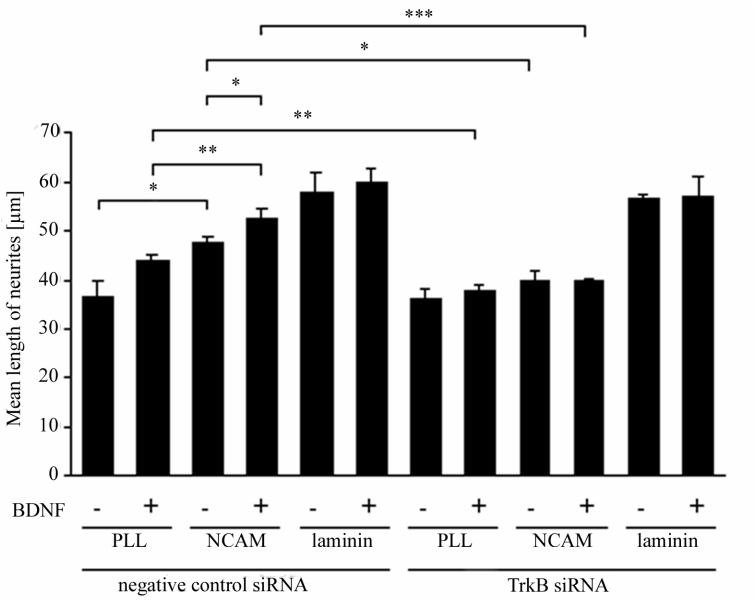

Figure 16 Neurite outgrowth from hippocampal neurons transfected with TrkB siRNA in vitro.

Dissociated hippocampal neurons were transfected with negative control siRNA or TrkB siRNA. The cells were plated on either poly-L-lysine, NCAM-Fc or laminin as coated substrates and maintained for 36 h. Cells were treated with or without 100 ng/ml BDNF after transfection. The lengths of neurites of transfected neurons were measured with a Zeiss Kontron KS 400 microscope. Bar graphs show a significant reduction of total neurite length only when TrkB siRNA transfected neurons are maintained on substrate-coated NCAM-Fc. Data represent means from three independent experiments with asterisks indicating statistically significant differences (Student's t-test; *** $p<0.005$, ** $p<0.01$, * $p<0.05$). Error bars represent SEM.

These observations indicate that there is a functional interdependence of NCAM and TrkB in enhancement of NCAM-mediated neurite outgrowth. Integrin-dependent neurite outgrowth, as triggered by laminin, was not affected by reduced expression of TrkB.

4.4 Identification of an interaction between the intracellular domains of TrkB and the inwardly rectifying K^+ channel subunit Kir3.3

4.4.1 Sequence analysis of NCAM intracellular domain

To see whether other proteins could be potential binding partners of TrkB, a sequence analysis of the intracellular domain of NCAM was performed. In this sequence analysis the amino acid sequence of the intracellular domain of NCAM was compared to the amino acid sequence of other cytosolic domains in proteins. This comparison led to the following discovery. Within the C-terminal region of NCAM140-ID and NCAM180-ID a short sequence stretch was found to show similarity to sequences present in the C-terminal intracellular domain of the inwardly rectifying K^+ channel subunit Kir3.3 and, to a lesser degree, to the Kir3.2 subunit (Fig. 17).

Figure 17 Similarity of NCAM intracellular domain and Kir3 intracellular domain.

A short stretch within the intracellular domain of NCAM140 and NCAM180 shows sequence similarity to the intracellular domain of Kir3.3 and, to a lesser extent, with the intracellular domain of Kir3.2. Dark grey bars feature the same amino acids and light grey bars similar amino acids. –OH designates C-terminus of each protein and numbers designate amino acid positions.

Although the previously performed competitive ELISA (Fig. 9) did not indicate, that this specific region of NCAM mediates the direct interaction between the intracellular domains of NCAM and TrkB, the possibility was considered that Kir3.3 or, and less so, Kir3.2 may interact with TrkB. To verify the possibility of an interaction between TrkB and Kir3.3, different binding studies were carried out.

4.4.2 Binding studies of TrkB and Kir3.3 by co-immunoprecipitation experiments

Co-immunopreciptiation was chosen as an initial method to confirm a possible interaction between TrkB and Kir3.3. In this co-immunoprecipitation a panTrk antibody (C-14) was used to precipitate TrkB from different mouse brain fractions. The Kir channel subunit Kir3.3 could be co-immunoprecipitated with the panTrk antibody from synaptosomal fractions of wild-type and NCAM-deficient mice, whereas no co-immunoprecipitation of Kir3.3 could be observed when a control non-immune IgG was used for immunoprecipitation (Fig. 18).

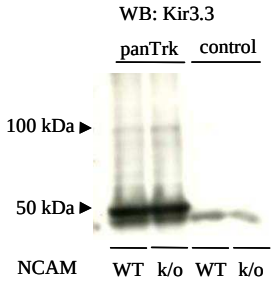

Figure 18 Interaction between TrkB and Kir3.3.

Synaptosomal fractions from brain of NCAM+/+ and NCAM-/- mice were incubated with panTrk antibody or with a non-specific IgG followed by incubation with Protein A/G agarose. SDS-PAGE and Western blot analysis of the immunoprecipitates were performed using the Kir3.3 antibody C-18, showing a Kir3.3 monomer and faintly a putative dimer. The experiment was performed twice with identical results.

4.4.3 Generation of a prokaryotic expression vector for the intracellular domain of Kir3.3 and Kir3.2

The co-immunoprecipitation experiments confirmed an interaction between TrkB and Kir3.3, but to substantiate a direct interaction between these two molecules, further biochemical experiments, requiring purified proteins, were necessary. Therefore, the intracellular domain of the Kir3.3 channel (Kir3.3-ID) and, as a control, the intracellular

domain of the Kir3.2 channel (Kir3.2-ID) was cloned into the prokaryotic expression vector pQE30 (Fig. 19). The oligonucleotides Kir3.3-ID-up-BamHI and Kir3.3-ID-dn-HindIII, respectively Kir3.2-ID-up-BamHI and Kir3.2-ID-dn-HindIII, were used for the amplification by linker PCR or touchdown PCR. The eukaryotic expression vector Kir3.1/3.3-pcDNA3 and Kir3.1/3.2-pcDNA3 were used as the template DNA for the PCR. After amplification, the amplicons were subjected to T/A cloning and were subcloned into the cloning vector pGEM-T Easy. The Kir3.3-ID-pGEM-T and Kir3.2-ID-pGEM-T constructs were digested with the restriction enzymes BamHI and HindIII, as was the empty pQE30 vector. Finally, the cut out Kir3.3-ID and Kir3.2-ID inserts were ligated into the linearized pQE30 vector and the ligation was transformed into DH5α cells. Positive clones were sequenced, and the finished Kir3.3-ID-pQE30 and Kir3.2-ID-pQE30 vectors could be used for recombinant expression in bacteria.

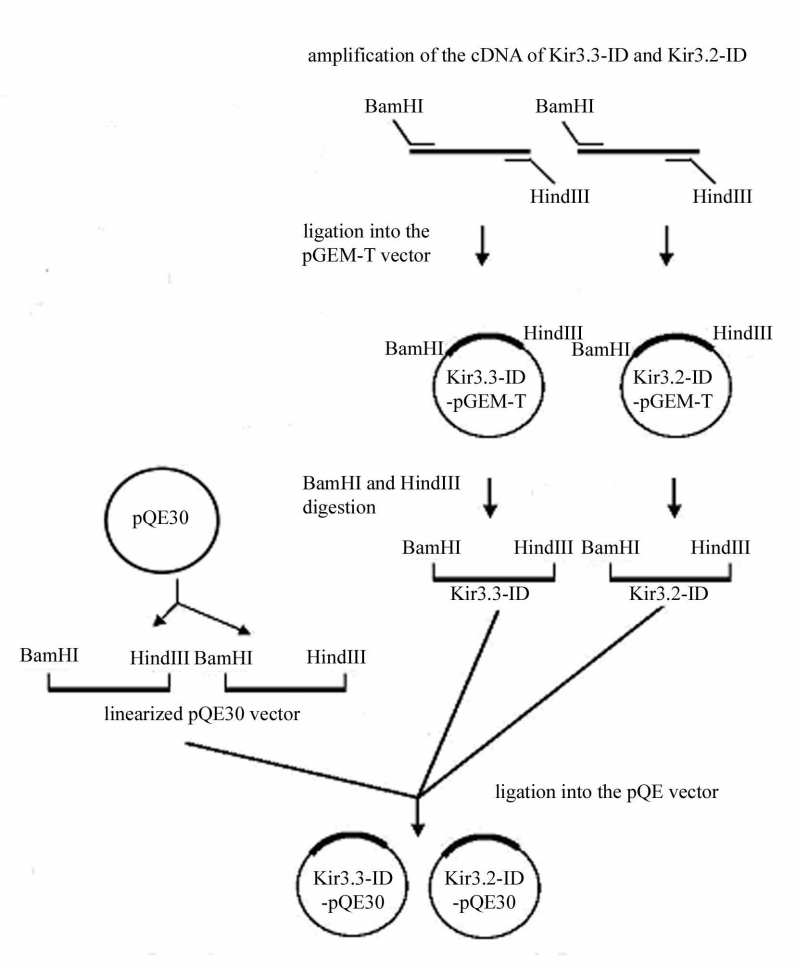

Figure 19 Cloning of Kir3.3-ID and Kir3.2-ID.

The Kir3.3-ID and Kir3.2-ID cDNA were amplified and subcloned into the pGEM-T vector. Kir3.3-ID-pGEM-T, Kir3.2-ID-pGEM-T, and pQE30 were digested with BamHI and HindIII, and subsequently the inserts were ligated into the vector. After transformation, positive clones were checked by sequencing.

4.4.4 Binding studies of TrkB and NCAM by cross-linking experiments

To further characterize the interaction between TrkB and Kir3.3, a chemical cross-linking approach was taken. Kir3.3-ID was recombinantly expressed and produced in *E. coli*. This recombinant Kir3.3-ID was coupled to the trifunctional cross-linker sulfo-SBED, containing a biotin moiety, and this conjugate was incubated as bait with native TrkB-ID or, as a control, PBS. After UV-cross-linking, TrkB-ID that bound to the bait protein Kir3.3-ID was isolated using streptavidin magnetic beads and separated by SDS-PAGE

under reducing conditions leading to a transfer of the biotin label from the bait protein to the bound target protein. Western blot analysis, using streptavidin conjugated to horseradish peroxidase, allowed to detect biotinylated binding partners. No band was detectable when the Kir3.3-ID bait was incubated with a PBS control instead of the TrkB-ID prey, while a biotinylated protein with an apparent molecular weight of approximately 30 kDa was detected as binding partner of the Kir3.3-ID bait when incubated with native TrkB-ID (Fig. 20). This molecular weight resembled that of TrkB-ID and, by Western blot analysis using a panTrk antibody (C-14), it was verified that the cross-linked 30 kDa protein was indeed TrkB-ID (Fig. 20).

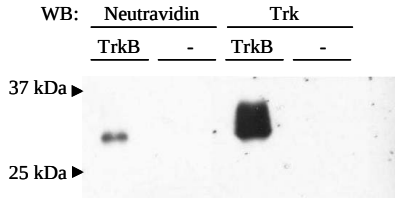

Figure 20 Association of TrkB and Kir3.3.

The cross-linker sulfo-SBED containing a biotin moiety was coupled to Kir3.3-ID and native TrkB-ID was added to the protein-cross-linker complexes. After UV-cross-linking, the potential binding partners were isolated and separated by SDS-PAGE under reducing conditions resulting in a transfer of the biotin group to the cross-linked partner molecule. Western blot analysis (WB) was performed using Neutravidin and a panTrk antibody (C-14).

4.4.5 Binding studies of TrkB and Kir3.3 by ELISA experiments

Next, to test whether Kir3.3 and perhaps Kir3.2 binds to TrkB via those sequences which show similarity to NCAM sequences (Fig. 17), the synthetic peptides Kir3.3 peptide C and Kir3.2 peptide C, carrying the particular C-terminal sequences of Kir3.3 and Kir3.2 (Fig. 21), and recombinant Kir3.3-ID and Kir3.2-ID were used as substrate-coat in an ELISA to detect binding of TrkB-ID.

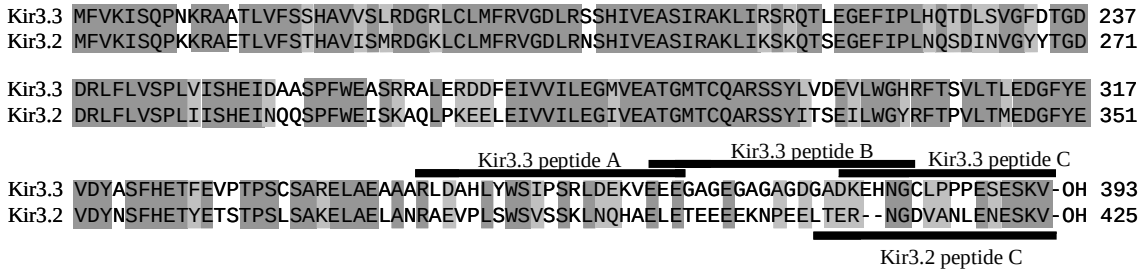

Figure 21 Similarity of Kir3.3 intracellular domain and Kir3.2 intracellular domain.

Amino acid sequences of Kir3.3-ID and Kir3.2-ID showing the regions of the peptides used in ELISA experiments. Dark grey bars feature the same amino acids and light grey bars similar amino acids. –OH designates C-terminus of each protein and numbers designate amino acid positions.

The synthetic Kir3.3 and Kir3.2 peptides and the recombinant Kir3.3-ID and Kir3.2-ID were substrate-coated at a constant concentration. TrkB-ID bound to the Kir3.3-ID and to the Kir3.3 peptide C, but neither to the Kir3.2-ID nor to the Kir3.2 peptide C in a concentration dependent manner as detected by the panTrk antibody C-14 (Fig. 22A). In addition to the above ELISA, further biotin ELISAs were performed. In these biotin ELISAs either the TrkB-ID and, as a control, the NCAM140-ID and NCAM180-ID were used as a substrate-coat to detect binding of biotinylated Kir3.3 peptide C, or the synthetic TrkB peptide was used as a substrate-coat to detect binding of biotinylated Kir3.3 peptide C and, as a control, the biotinylated NCAM peptide 3 carrying the sequences showing similarity to the C-terminal Kir3.3 and Kir3.2. The TrkB-ID, the recombinant NCAM140-ID and NCAM180-ID, and the synthetic TrkB peptide were substrate-coated at a constant concentration. The biotinylated Kir3.3 peptide C bound to substrate-coated TrkB-ID, but not to substrate-coated NCAM140-ID nor to NCAM180-ID (Fig. 22B), in a concentration dependent manner. Furthermore, the Kir3.3 peptide C also bound to the TrkB peptide in a concentration dependent manner, whereas the biotinylated NCAM peptide 3 sequences did not bind to the TrkB peptide (Fig. 22C).

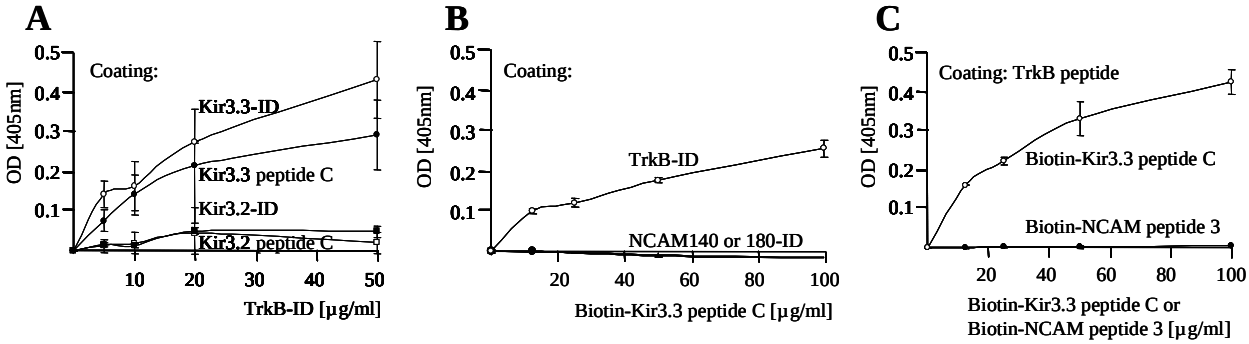

Figure 22 Binding between Kir3.3-ID or Kir3.3 peptide C and TrkB-ID or TrkB peptide.

10 µg/ml of substrate-coated Kir3.3-ID and Kir3.2-ID, 100 µg/ml Kir3.3 peptide C and Kir3.2 peptide C (**A**), 20 µg/ml of substrate-coated TrkB-ID, NCAM140-ID and NCAM180-ID (**B**), and 10 µ/ml of substrate-coated TrkB peptide (**C**) were incubated with increasing amounts of TrkB-ID (**A**), biotinylated Kir3.3 peptide C (Biotin-Kir3.3 peptide C) (**B, C**) or biotinylated NCAM peptide 3 (Biotin-NCAM peptide 3) (**C**). Binding of TrkB-ID was detected by using a panTrk antibody (C-14) (**A**). Binding of the biotinylated peptides was determined by using Neutravidin (**B, C**). All experiments were performed at least three times. Error bars represent SD.

4.4.6 Verification of Kir3.3 binding site in TrkB by competitive ELISA experiments

To further verify the results of the aforementioned biotin ELISA regarding the Kir3.3 binding to the synthetic TrkB peptide, Kir3.3-ID and Kir3.2-ID were probed in a competitive ELISA for inhibition of binding of NCAM140-ID or NCAM180-ID to substrate-coated TrkB peptide. The synthetic TrkB peptide was substrate-coated at a constant concentration and the NCAM140-ID and NCAM180-ID binding partners were also applied at a constant concentration. The Kir3.3-ID and Kir3.2-ID were preincubated at increasing concentrations before the application of the binding partner. Binding of both NCAM140-ID and NCAM180-ID to the TrkB peptide was inhibited by Kir3.3-ID, but not by Kir3.2-ID, in a concentration dependent manner (Fig. 23A and 23B).

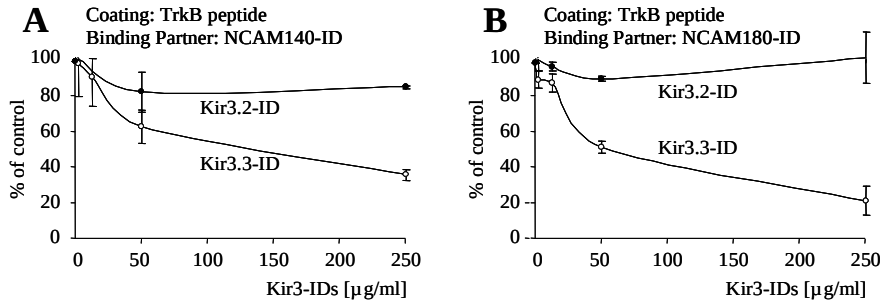

Figure 23 Competition of NCAM peptides to the binding between NCAM180-ID and TrkB peptide.

10 µg/ml of substrate-coated TrkB peptide was pre-incubated with increasing amounts of Kir3.3-ID or Kir3.2-ID and then incubated with 50 µg/ml of NCAM140-ID (**A**) or NCAM180-ID (**B**). Binding of NCAM-IDs was detected by using the antibody P61. Both experiments (**A, B**) were performed at least three times. Error bars represent SD.

These results show a direct interaction between the intracellular domains of TrkB and Kir3.3, but not Kir3.2. This interaction is mediated by amino acids 668-679 of TrkB which also mediate the binding to amino acids 729-765 of NCAM and amino acids 377-393 of Kir3.3. These observations indicate that TrkB-ID not only binds directly to NCAM140-ID and NCAM180-ID, but also to the intracellular domain of the Kir3.3 subunit of the inwardly rectifying K^+ channel. Interestingly, this binding is only seen for the Kir3.3, but not Kir3.2 subunit.

4.5 TrkB and NCAM dependent cell surface localization of Kir3.3

4.5.1 Current recordings from *Xenopus* oocytes expressing Kir3 channels, TrkB and NCAM

Since the above described binding experiments showed that Kir3.3-ID, but not Kir3.2-ID, interacts directly with TrkB-ID, and since it was shown in a previous study that NCAM influences Kir3 mediated currents (Delling et al., 2002), the influence of TrkB and/or

NCAM140 or NCAM180 on Kir3.3 mediated K^+ currents was investigated in *Xenopus* oocytes. This experiment was performed in cooperation with Dr. Erhard Wischmeyer. The oocytes were injected with concatameric Kir3.1/3.3 cRNA, concatameric Kir3.1/3.3 cRNA + TrkB cRNA, concatameric Kir3.1/3.3 cRNA + TrkB cRNA + NCAM180 cRNA and concatameric Kir3.1/3.3 cRNA + TrkB cRNA + NCAM140 cRNA. In addition, controls were performed for either co-expression with TrkA cRNA instead of TrkB cRNA or single- and co-expression of concatameric Kir3.1/3.2 cRNA and concatameric Kir3.1/3.4 cRNA instead of concatameric Kir3.1/3.3 cRNA. Oocytes were clamped at -80 mV, perfused with 'high K^+' (96 mM external K^+) solution and the amplitude currents were recorded.

Co-expression of TrkB and a concatamer of Kir3.1/Kir3.3 resulted in an increase in the current via Kir3.1/3.3 in comparison to the current observed when only Kir3.1/Kir3.3 was expressed (Fig. 24A and 24B). Co-expression of Kir3.1/Kir3.3 with TrkA did not enhance the current (Fig. 24A). The enhancement of current via Kir3.1/3.3 by TrkB was decreased by concomitant expression of NCAM140 or NCAM180 (Fig. 24A and 24B). The concatameric expression of Kir3.1/Kir3.4 or Kir3.1/3.2 did not show enhanced currents when co-expressed with TrkB (Fig. 24C), indicating that the enhancement of K^+ currents by TrkB is specific for Kir3.3.

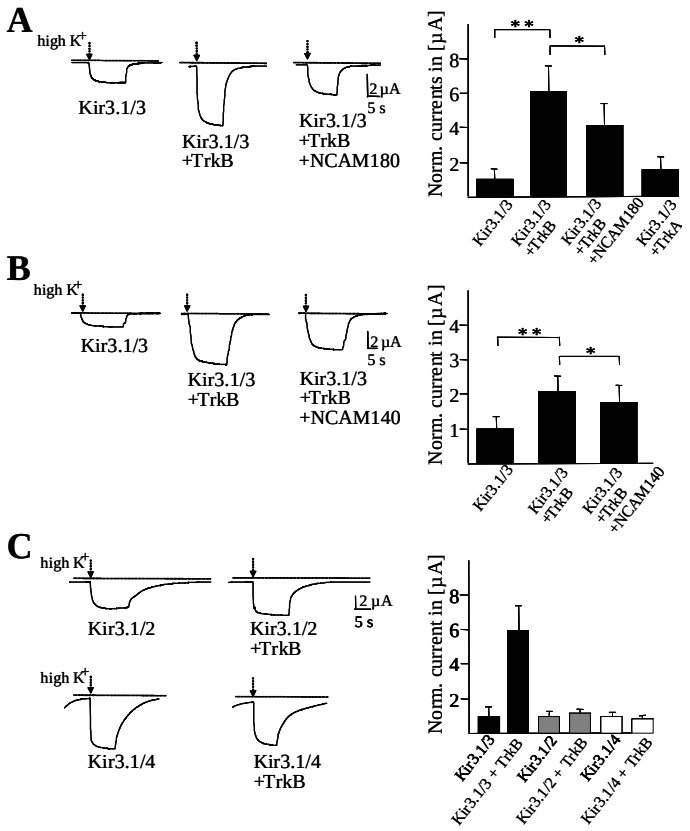

Figure 24 Current recordings from *Xenopus* oocytes expressing Kir3 channels, TrkB and NCAM.

(**A**) Oocytes were injected with concatameric Kir3.1/3.3 cRNA, concatameric Kir3.1/3.3 cRNA + TrkB cRNA (cRNA ratio 1:0.25), and concatameric Kir3.1/3.3 cRNA + TrkB cRNA + NCAM180 cRNA (cRNA ratio 1:0.25:1). Oocytes were clamped at -80 mV and perfused with 'high K^+' (96 mM external K^+) solution as indicated by arrows. Bar graph in the right panel shows current amplitude ratios of measurements shown in the left panel. In addition, current amplitude ratio is given for co-expression with TrkA. (**B**) Current recordings as shown in (**A**), but triple injection is displayed for Kir3.1/3.3 cRNA + TrkB cRNA + NCAM140 cRNA (cRNA ratio 1:0.25:4) instead of Kir3.1/3.3 cRNA + TrkB cRNA + NCAM180 cRNA. Bar graph in the right panel shows current amplitude ratios of measurements shown in the left panel. (**C**) Current recordings from oocytes injected with concatameric Kir3.1/3.2 cRNA, concatameric Kir3.1/3.2 cRNA + TrkB cRNA (left panel, upper part), concatameric Kir3.1/3.4 cRNA and concatameric Kir3.1/3.4 cRNA + TrkB cRNA (left panel, lower part). Bar graphs in the right panel show current amplitude ratios from measurements depicted in the left panel. The Kir3.1/3.3 data are from five independent experiments, and the Kir3.1/3.2 and Kir3.1/3.4 data are from two independent experiments each. Data are shown as mean with asterisks indicating statistically significant differences (Student's t-test; ** $p<0.01$, * $p<0.05$). Error bars represent SD.

4.5.2 Cell surface localization of *Xenopus* oocytes expressing Kir3.1/EGFP-Kir3.3 channels

To test, whether the increase in K^+ currents appeared due to a direct modulation of the channel properties or due to a higher cell surface expression of the channel, an EGFP-tagged Kir3.1/3.3 concatamer was used for injection into oocytes. These experiments were performed in cooperation with Dr. Erhard Wischmeyer. The EGFP-tagged Kir3.3-subunits targeted to the plasma membrane, and the resulting surface fluorescence of the respective oocytes, were quantified by laser scanning microscopy. The oocytes were injected with concatameric Kir3.1/3.3 cRNA, concatameric Kir3.1/3.3 cRNA + TrkB cRNA and concatameric Kir3.1/3.3 cRNA + TrkB cRNA + NCAM180 cRNA.

The co-expression of Kir3.1/3.3 with TrkB enhanced the cell surface expression of Kir3.1/Kir3.3 (Fig. 25A and 25B), and this enhanced cell surface expression was reduced when NCAM180 was co-expressed with Kir3.1/Kir3.3 and TrkB (Fig. 25A and 25B). The presence or absence of BDNF had no effect on the K^+ currents and on the cell surface localization of the Kir3 channels for all subunits studied (data not shown).

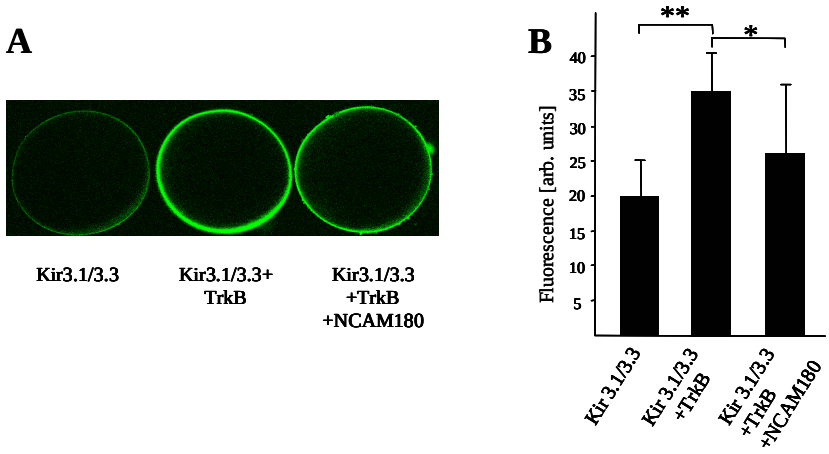

Figure 25 Cell surface localization of Kir3.1/EGFP-Kir3.3 channels.

(**A**) Representative confocal images are shown of *Xenopus* oocytes injected with cRNAs of Kir3.1/3.3 (left panel), Kir3.1/3.3 with TrkB (cRNA ratio 1:0.25) (middle panel), and Kir3.1/3.3 with TrkB and NCAM180 (cRNA ratio 1:0.25:1) (right panel). Surface fluorescence of oocytes results from EGFP-tagged Kir3.3-subunits targeted to the plasma membrane. (**B**) Bar graphs show average fluorescence intensities of 10 oocytes injected with cRNAs as indicated in (**A**). Data are shown as mean with asterisks indicating statistically significant differences (ANOVA and Tukey (**D, E**); ** $p<0.01$, * $p<0.05$). Error bars represent SD.

These observations indicate that surface localization of Kir3.1/Kir3.3 and, thus, the basic electric features of the plasma membrane depend on levels of TrkB and NCAM expression.

4.6 Identification of an interaction between the intracellular domains of NCAM and Kir3.3

4.6.1 Binding studies of NCAM and Kir3.3 by ELISA experiments

As NCAM inhibits the cell surface expression of Kir3.3, it was checked whether the NCAM-IDs and Kir3.3 are not only functionally associated with each other via TrkB, but also interact directly. Therefore ELISA experiments were performed as an approach to test for a possible direct binding of NCAM and Kir3.3. Recombinant Kir3.3-ID and recombinant Kir3.2-ID were substrate-coated at a constant concentration. Both recombinant NCAM140-ID and NCAM180-ID showed binding to substrate-coated Kir3.3-ID, but not Kir3.2-ID, in a concentration dependent manner (Fig. 26A and 26B).

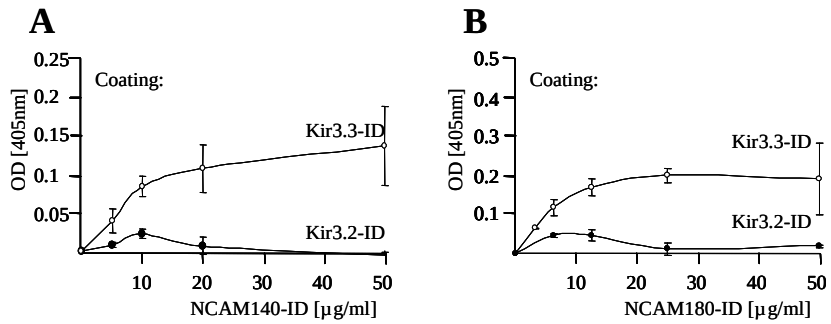

Figure 26 Binding between NCAM-IDs and Kir3.3-ID.

10 µg/ml of substrate-coated Kir3.3-ID and Kir3.2-ID were incubated with NCAM140-ID (**A**) or NCAM180-ID (**B**). Binding of the NCAM-IDs was detected by using the antibody P61. Both experiments were performed at least three times. Error bars represent SD.

Since NCAM-IDs bind to Kir3.3-ID, but not Kir3.2-ID, and since Kir3.3-ID and Kir3.2-ID show significant sequence differences mainly over a stretch of approximately 50 amino acids at the C-terminus (Fig 21), overlapping peptides spanning the C-terminal stretch of Kir3.3, that is different from Kir3.2, were used in an ELISA to identify the binding site for NCAM-ID on Kir3.3-ID. The synthetic Kir3.3 peptides A, B and C (Fig. 21) were substrate-coated at a constant concentration. Peptide A, but not the more C-terminal peptides B and C, comprising of amino acids 344-364 of Kir3.3 bound to NCAM140-ID (Fig. 27A) and NCAM180-ID (Fig. 27B and 27C) in a concentration dependent manner.

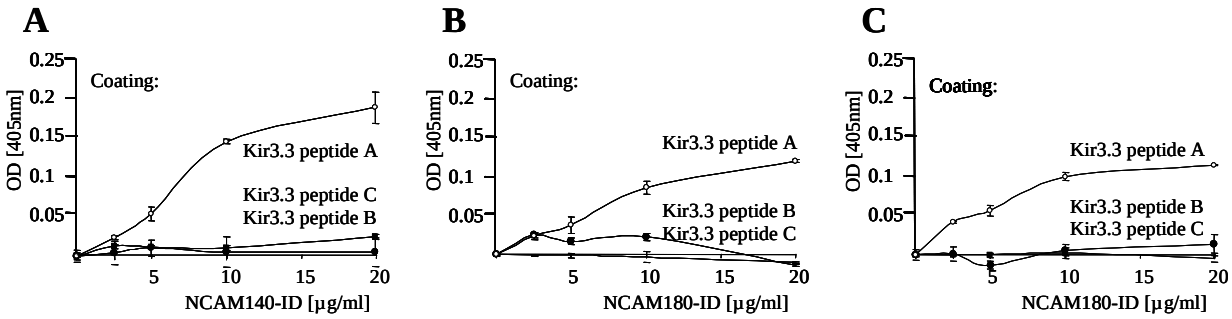

Figure 27 Binding between NCAM-IDs and Kir3.3 peptide C.

25 µg/ml substrate-coated Kir3.3 peptides A, B and C (Fig. 21) were incubated with NCAM140-ID (**A**) or NCAM180-ID (**B, C**). Binding of the NCAM-IDs was detected by using the antibody P61 (**A, B**) or D3 (**C**). Both experiments were performed at least three times. Error bars represent SD.

4.6.2 Identification of Kir3.3 binding site in NCAM by competitive ELISA experiments

To identify the site on NCAM responsible for the binding of Kir3.3, a competitive ELISA was performed using NCAM peptides matching the consecutive sequences of NCAM140-ID and NCAM180-ID for inhibition of binding of NCAM180-ID to substrate-coated Kir3.3-ID. The recombinant Kir3.3-ID was substrate-coated at a constant concentration, and the NCAM180-ID binding partner was also applied at a constant concentration. The NCAM peptides were preincubated at increasing concentrations before the application of the binding partner.

The peptide 1 comprising the membrane proximal sequences of NCAM140-ID and NCAM180-ID (amino acids 730-764), but not the two other peptides deduced from the more distal intracellular sequences, reduced binding of NCAM180-ID to the substrate-coated Kir3.3-ID in a concentration dependent manner (Fig. 28).

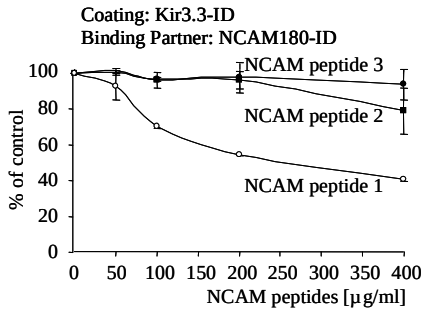

Figure 28 Competition of NCAM peptides to the binding of NCAM180-ID to TrkB peptide.

10 µg/ml of substrate-coated Kir3.3-ID was pre-incubated with increasing amounts of NCAM140-ID sequence-derived peptides 1, 2 and 3 and then incubated with 25 µg/ml of NCAM180-ID. Binding of the NCAM180-ID was detected by using the antibody P61 (**A**-**E**). All experiments (**A**-**E**) were performed at least three times. Error bars represent SD.

These observations showed that not only TrkB, but also NCAM interacts with the Kir3.3 subunit at a site different from the one involved in binding of Kir3.3 to TrkB-ID. In addition, the binding of NCAM to Kir3.3 and to TrkB involves the same membrane proximal region of NCAM.

4.7 Effect of Kir3.3 expression on neurite outgrowth of cultured hippocampal neurons

4.7.1 Neurite outgrowth measurement of Kir3.1/3.3 transfected hippocampal neurons

As previously shown, substrate-coated NCAM enhances neurite outgrowth of dissociated early postnatal hippocampal neurons in comparison to substrate-coated poly-L-lysine (Doherty et al., 1990). Therefore, it was investigated whether NCAM-dependent neurite outgrowth is affected by the interaction between the intracellular domains of NCAM and Kir3.3. Since Kir3.3 is not expressed in early postnatal neurons (Grosse et al., 2003), hippocampal neurons were transfected with concatameric Kir3.1/3.3, or as a negative control Kir3.1/3.2, and measured neurite outgrowth on NCAM versus poly-L-lysine, as a negative control, or laminin, as a positive control. These experiments were performed in cooperation with Dr. Alexander Dityatev. When hippocampal neurons were plated on poly-L-lysine expression of Kir3.1/3.2 or Kir3.1/3.3 did not change the mean length of neurites when compared to mock-transfected neurons (Fig. 29). Similarly, no difference in neurite outgrowth was seen with mock-, Kir3.1/3.2- or Kir3.1/3.3-transfected neurons when plated on laminin, which enhances neurite length relative to poly-L-lysine (Fig. 29). Interestingly, however, overexpression of Kir3.1/3.3 in neurons maintained on substrate-coated NCAM led to reduced neurite outgrowth when compared to mock- and Kir3.1/3.2-transfected neurons (Fig. 29).

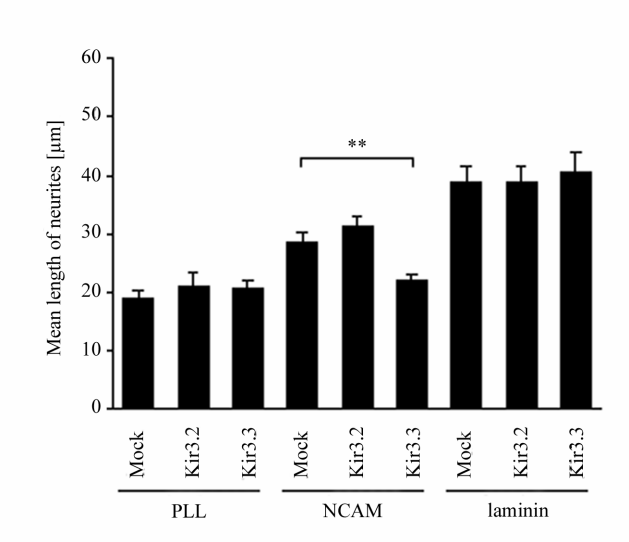

Figure 29 Neurite outgrowth from hippocampal neurons transfected with Kir3 in vitro.

Dissociated hippocampal neurons were transfected with either a mock vector, concatameric Kir3.1/3.2 or concatameric Kir3.1/3.3. The cells were plated on either poly-L-lysine, NCAM-Fc or laminin as coated substrates and maintained for 24 h. The lengths of neurites of transfected neurons were measured using the laser-scanning confocal microscope LSM510-based imaging system. Bar graphs show a significant reduction of total neurite length only when Kir3.1/3.3 transfected neurons are maintained on substrate-coated NCAM-Fc. Data represent means from three independent experiments with asterisks indicating statistically significant differences (Student's t-test; ** $p<0.01$). Error bars represent SEM.

These observations indicate that the previously proven homophilic enhancement of neurite outgrowth via NCAM is negatively modified by Kir3.3. This is noteworthy in view of the fact that Kir3.3 only becomes expressed later in development of the mouse brain (Grosse et al., 2003), namely within the second postnatal week, when neurite outgrowth ceases.

5 Discussion

This study has revealed direct associations of three developmentally and functionally important molecules: The neural cell adhesion molecule NCAM, the tyrosine receptor kinase TrkB, and the inwardly rectifying K^+ channel subunit Kir3.3 (Fig. 30). It provides evidence that the intracellular domains of NCAM and TrkB interact directly with each other and both NCAM and TrkB bind to sites in the C-terminal, intracellular domain of Kir3.3, but not to the structurally similar subunit Kir3.2. The binding sites for NCAM and TrkB on Kir3.3 are distinct, but closely localized next to each other, such that binding of NCAM to Kir3.3 can block the direct binding of TrkB to Kir3.3 and vice versa. The intracellular domains of NCAM and Kir3.3 bind to the same binding site on TrkB. This binding site is localized within the protein kinase domain of TrkB and carries the aspartic acid that is essential for the kinase activity of TrkB (Kaplan and Miller, 2000). A membrane proximal site on NCAM was identified to mediate the binding to Kir3.3 and TrkB. This membrane proximal site is a region of great interest, as it features the palmitoylation sites responsible for membrane attachment and lipid raft targeting of NCAM (Little et al., 1998; Niethammer et al., 2002), as well as a tyrosine known to influence NCAM-mediated neurite outgrowth (Diestel et al., 2004). In addition, the sequence of this region shows a high degree of homology between the different species mouse, rat and human. Whether a binding of TrkB to NCAM has any influence on lipid raft targeting remains to be seen and lies beyond the scope and focus of this study.

The interaction of TrkB with Kir3.3 drastically enhances the cell surface expression of Kir3.1/3.3 and thus the Kir3.1/3.3-mediated K^+ currents. On the other hand, TrkB does not trigger the cell surface expression of other Kir channels, namely Kir3.1/3.2 and Kir3.1/3.4. TrkA, which is structurally and functionally related to TrkB, does not affect the surface expression of Kir3.3. It is noteworthy that the only tyrosine of the C-terminal intracellular domain of Kir3.3 is within the region binding to TrkB. Furthermore, this very region features a lysosomal targeting sequence (aa YWSI) that is reported to be responsible for the unique trafficking pattern of Kir3.3 consisting channels effectively reducing the number of functional Kir3 channels on the cell surface (Ma et al., 2002). The binding of TrkB to this lysosomal targeting sequence, or even a putative phosphorylation of this lone tyrosine, could lead to an ablation of the lysosomal targeting and an increase of cell surface delivery.

It is known from the other Kir3 channel subunits, that they are influenced in trafficking by tyrosine phosphorylation of the N-terminal region, leading to a remarkable increase of cell surface expression (Ippolito et al., 2002).

The TrkB-dependent increase in cell surface expression of Kir3.3, and the increase in Kir3.3-mediated K^+ currents were reduced by co-expression of NCAM, indicating that NCAM competes with Kir3.3 for binding to TrkB. Interestingly, it was previously reported that NCAM also reduces the cell surface expression of Kir3.1/3.2 and thus the Kir3.1/3.2-mediated K^+ currents (Delling et al., 2002). Still, it is likely that this inhibiting effect of NCAM on Kir3 channel surface expression appears through different molecular mechanism in both Kir3 subunit types, as the Kir3.2 subunit shows no direct binding to NCAM and is in addition not regulated by TrkB. NCAM binds to the utmost C-terminus of Kir3.3 and this very region features a class I PDZ-binding motif (aa ESKV) that is known to be responsible for the binding of the PDZ domain containing trafficking molecule sorting nexin 27 (SNX27) to Kir3 channels and for the delivery of Kir3.3 to the cell surface (Lunn et al., 2007). Furthermore, it is known that the two inwardly rectifying K^+ channels, Kir2.1 and Kir2.3, bind to the PDZ domain containing protein PSD-95 (Cohen et al., 1996). The binding of NCAM could lead to a masking of this PDZ-binding region, so that certain PDZ domain containing trafficking proteins like SNX27 cannot bind anymore, and hence the delivery to the cell surface is decreased.

The functional relationship between TrkB and NCAM is evidenced by the ability of TrkB, particularly in the presence of its ligand BDNF, to enhance tyrosine phosphorylation of NCAM. Two different kinds of co-immunoprecpitations showed that either the phosphorylation of NCAM by TrkB is dependent on BDNF or almost independent of BDNF. In view of the fact that one kind of co-immunoprecipitation approach needed the application of phosphatase inhibitors, it might well be that, due to the lacking of phosphatases and thus kinase antagonists, a basal phosphorylation of NCAM took place irrespective of BDNF. On the other hand, without the phosphatase inhibitors, the phosphatases got rid of all NCAM phosphorylations throughout the course of the experiment even after the induction by BDNF in this co-immunoprecipitation approach. In the other kind of co-immunoprecipitation, which made use of the phosphotyrosine antibody coupled agarose beads, the once phosphorylated NCAM seemed to be protected from the phosphatases by the direct binding of the antibody to the phosphorylated tyrosine, and

hence the phosphatase inhibitors were unnecessary in this co-immunoprecipitation approach.

Homophilic interaction of NCAM in a *trans*-position promotes neurite outgrowth from hippocampal neurons (Doherty et al., 1990). This NCAM-induced neurite outgrowth depends on TrkB, since ablation of TrkB expression does not allow neurite outgrowth triggered by the homophilic NCAM interaction. Considering these effects, it remains to be seen whether TrkB is an upstream effector of NCAM that phosphorylates NCAM and thereby activates NCAM-mediated neurite outgrowth, or whether NCAM is an upstream effector of TrkB by inducing signal transduction events through phosphorylation by TrkB when NCAM is bound in a homophilic *trans*-interaction. Hereby, the modulation of BDNF responsiveness to TrkB through PSA-NCAM (Muller et al., 2000; Kiss et al., 2001; Vutskits et al., 2001; Burgess and Aubert, 2006) could be a key factor in the possible upstream regulation of NCAM phosphorylation and hence NCAM-mediated neurite outgrowth. PSA-NCAM can modulate homophilic NCAM-mediated interactions (Cunningham et al., 1983; Sadoul et al., 1983), and it is furthermore known that the expression of PSA is reduced when developmental events cease (Hekmat et al., 1990; Durbec and Cremer, 2001). So, PSA on NCAM could regulate the accessibility of BDNF to TrkB as well as the preference of a homophilic *trans*-interaction of NCAM throughout early neuronal development, thereby promoting neurite outgrowth processes taking place. Later in development, when the expression of PSA is reduced, BDNF binding to TrkB starts to decrease, and also the homophilic interaction of NCAM in *trans*-position becomes less prevalent, and thus neurite outgrowth begins to abate. Furthermore, the preferred binding of NCAM in a *cis*-position, when PSA is absent, could also lead to increasing difficulties for TrkB to bind, and hence to phosphorylate, NCAM due to steric reasons.

The mechanism for NCAM activation through BDNF and TrkB seems to be quite distinct from the formerly described activation of NCAM through the glia cell line-derived neurotrophic factor GDNF (Paratcha et al., 2003). GDNF can bind directly to NCAM, thereby bypassing its usual signaling cascade via GPI-linked GDNF receptor GFRα and the receptor tyrosine kinase RET. Normally, upon GFL-GFRα complex formation, the complex brings together two molecules of RET, triggering trans-autophosphorylation of specific tyrosine residues within the tyrosine kinase domain of each RET molecule (Durbec et al., 1996; Jing et al., 1996; Treanor et al., 1996; Trupp et al., 1996). Phosphorylation of

these tyrosines then initiates intracellular signal transduction processes. When RET is lacking in cells, NCAM can take over GDNF signaling by direct binding of this neurotrophin and signal transduction along the cytoplasmic protein tyrosine kinases Fyn and FAK (Paratcha et al., 2003). BDNF on the other hand is not known to bind to NCAM directly, even though the PSA on NCAM is known to influence its ability to bind to TrkB (Muller et al., 2000; Kiss et al., 2001; Burgess and Aubert, 2006). Furthermore, the BDNF receptor TrkB is a transmembrane protein that is capable to transduce signals through the membrane without needing a co-receptor like in the case of the GFRα-RET complex.

Interestingly enough, Diestel et al. (2004) could observe an increased neurite outgrowth of B35 neuroblastoma cells transfected with an NCAM180-Y734F mutant. These results seem to contradict the observation of this study, but since neuroblastoma cell lines are known for their peculiar behaviour, and since NCAM180 is known to be less responsible for neurite outgrowth than NCAM140, these results are hardly comparable. In addition, Diestel et al. could describe enhanced neurite outgrowth even on poly-L-lysine, and the neurite outgrowth increasing effect was an FGFR dependent one. It is known, that cosignaling of NCAM via lipid rafts and the FGFR is essential for neuritogenesis (Niethammer et al., 2002) and also that TrkB is recruited to neuronal lipid rafts by BDNF and $p59^{fyn}$ (Suzuki et al., 2004; Pereira and Chao, 2007), where NCAM signaling via $p59^{fyn}$ is independent of the FGFR (Niethammer et al., 2002). One might therefore conclude that TrkB mediated NCAM signaling is independent of FGFR, but dependent of $p59^{fyn}$ and limited to lipid rafts. So the differing effects in neurite outgrowth come into play due to the different signaling pathways involved and responsible. In addition, preliminary results of neurite outgrowth experiments in primary hippocampal neurons of NCAM knock-out mice transfected with the mutated NCAM140-Y734F showed a reduction of NCAM-mediated neurite outgrowth (data not shown) and thus supports above assumption that different signaling pathways for NCAM are involved.

Whether there is some cross-talk between the activation of NCAM through TrkB and the known signaling of NCAM via the FGFR remains to be seen. The two ligands BDNF (Muller et al., 2000; Kiss et al., 2001; Burgess and Aubert, 2006) and FGF (Francavilla et al., 2007) are both known to be influenced in the binding capabilities to their respective receptor by the presence of NCAM. Still, the FGFR is proven to be a downstream effector of NCAM (Saffell et al., 1997), whereas this role is so far not proven for TrkB.

Premature expression of Kir3.1/3.3, but not the expression of Kir3.1/3.2, in neonatal hippocampus neurons in vitro, which at that point in time do not express Kir3.3 channels (Grosse et al., 2003), inhibits NCAM-dependent neurite outgrowth. This observation suggests that Kir3.3 disturbs the interaction between TrkB and NCAM (Fig. 8) which is required for the TrkB-dependent NCAM-induced neurite outgrowth. This is noteworthy especially regarding the fact that Kir3.3 binds to the region of NCAM that is bound and phosphorylated by TrkB and thus essential for the neurite outgrowth promoting effect of NCAM.

These observations bring together the interdependence of three important players in neural development during embryogenesis and in the adult and entail important consequences in central nervous system development of neuronal network: a) during the formative stages of neural development TrkB modulates the neurite outgrowth functions of NCAM via a direct binding to NCAM and tyrosine phosphorylation of NCAM, b) later on in the development, when expression of Kir3.3 arises, the direct interaction between TrkB and NCAM is disturbed by binding of Kir3.3 to TrkB and NCAM and c) in the late phases of central nervous system development when Kir3.3 expression is upregulated (Grosse et al., 2003), the inhibition of the direct binding of TrkB and NCAM by Kir3.3 no more allows NCAM-dependent neurite outgrowth and d) in the adult, when the Kir3.3 expression reaches the highest level, the binding of TrkB to Kir3.3 results in an enhanced surface expression of channels composed of Kir3.3 subunits, which constitute K^+ currents of functionally matured neurons.

Thus, the study has identified a molecular mechanism by which the neurite outgrowth is promoted by interaction between TrkB and NCAM. It is no more functional when an important player in regulating the neuronal membrane potential in the adult, namely Kir3.3, is upregulated in its expression. The observations reveal a novel role for an interplay between three functionally important molecules (NCAM, TrkB and Kir3.3) during different stages of neuronal development. First, the finding that TrkB binds directly to NCAM through its intracellular domain and triggers, through activation by its ligand BDNF, tyrosine phosphorylation of NCAM and thus NCAM-mediated neurite outgrowth in early stages of development, puts into focus the important triggering role of TrkB for NCAM-specific neurite outgrowth. The triggering of NCAM through tyrosine phosphorylation of TrkB is the important signal for neurite outgrowth during early stages of neuronal

development. Although the results indicate that BDNF binding to TrkB is required for phosphorylation of NCAM, NCAM-induced neurite outgrowth is less dependent on addition of BDNF to the culture medium. Bearing in mind that it cannot be excluded that low amounts of BDNF are probably expressed by the cultured neurons and that this endogenously produced BDNF is sufficient to trigger NCAM phosphorylation by TrkB, it is not surprising that TrkB promotes NCAM-mediated neurite outgrowth at a basal level even without applying exogenous BDNF. In contrast, it is highly unlikely that CHO cells produce BDNF, and therefore the TrkB-mediated phosphoylation of NCAM depends on the addition of exogenous BDNF. Aside from that, TrkB has a lot more time to phosphorylate, and thereby activate, NCAM at a basal level throughout the 24-36 hours of maintenance of the primary hippocampal neurons in culture in comparison to the biochemical snap-shot-like measurement of the NCAM phosphorylation amount after BDNF induction in CHO cells.

The finding, that TrkB binds to and directly phosphorylates NCAM, is the first evidence that a neurotrophin receptor with its well-known neurite outgrowth promoting activity (Huang and Reichardt, 2003) in the presence of its ligand can trigger the functions of a neural cell adhesion molecule. This relationship is a functionally extremely intriguing one, since the neurite outgrowth promoting activities of both molecules is now defined by NCAM being the effector of a neurotrophin receptor which has long been known to have important functions not only during nervous system development, but also in synaptic plasticity and regeneration after injury (Huang and Reichardt, 2001). This cooperation between NCAM and TrkB in regulating neurite outgrowth thus appears to be different from the previously reported regulation of neurite outgrowth via homophilic interaction involving the immunoglobulin family molecules TrkA and TrkB (Tannahill et al., 1995).

It is evident, that the relationship between TrkB and NCAM would be counterproductive in the adult, when both molecules continue to be expressed after cessation of nervous system development, since strongly continued neurite outgrowth in the adult would lead to disturbances in the maintenance of once formed and viable neuronal networks. It is at this time of later neuronal development that expression of the truncated splice variant of TrkB is remarkably increased becoming the most abundant adult form of TrkB (Allendoerfer et al., 1994; Escandon et al., 1994; Eide et al., 1996). The truncated TrkB receptor, lacking most of the intracellular domain including the kinase domain, can bind and internalize

neurotrophins in the same way as the full-length TrkB receptor, but it does not initiate the phosphorylation events required for signal transduction of NCAM and other molecules. As a result, the truncated receptor modulates neurotrophin activity by restricting the availability of the ligand for full-length receptors (Biffo et al., 1995; Eide et al., 1996; Fryer et al., 1997; Li et al., 1998; Haapasalo et al., 2002) and thus restricting also the phosphorylation of NCAM in later ontogeny. At the same time a new player emerges in the relationship between NCAM and TrkB, namely the Kir3.3 subunit of the inwardly rectifying K^+ channel, which is suggested to have important roles in maintenance of membrane potential and excitability of neurons (Jelacic et al., 2000; Torrecilla et al., 2002; Koyrakh et al., 2005). This channel disrupts the neurite outgrowth promoting relationship between TrkB and NCAM by binding via specific and distinct sites at the C-terminal intracellular domain to TrkB and NCAM, thereby inhibiting neurite outgrowth. Kir3.3 is affected by TrkB and NCAM in opposite directions: TrkB enhances surface localization of Kir3.3, while NCAM decreases surface localization of Kir3.3.

Thus, the developmentally co-active pair of TrkB and NCAM, ensuring neurite outgrowth during development, becomes no more functional since the developmentally late appearing Kir3.3 subunit disturbs their relationship and, in addition, the developmentally late appearing truncated splice variant of TrkB is not able to bind and phosphorylate NCAM, but competes with its full-length counterpart for binding to BDNF. In the adult, TrkB and NCAM become counterplayers in the sense that TrkB enhances K^+ currents independent of BDNF, while NCAM diminishes those via regulation of cell surface expression of this channel. An interesting relationship between NCAM and Kir3.3 emerges by the finding that Kir3.3 mediates the acute inhibitory effects of opioids on locus coeruleus neurons, as seen in mice that are ablated in Kir3.3 subunit expression. Kir3.3 subunit ablated mice are impaired in their ability to mediate the acute inhibitory effect of opioids on locus coeruleus neurons (Torrecilla et al., 2002). The relevance of Kir3.3 to neuronal Kir3 channels remains an interesting and important topic, particularly in light of the impact of Kir3.3 ablation on drug reward behavior (Morgan et al., 2003). These findings are noteworthy in view of the fact that mice constitutively deficient in NCAM expression show abnormal responses in fear-conditioning and addictive responses (Stork et al., 1997; Stork et al., 1999; Mackowiak et al., 2005). Whether opioid receptors enter into the relationship between NCAM and TrkB in modulating K^+ currents by direct or indirect association with

the three molecules, and whether there is a link between these molecules and behaviour, remains to be seen.

In addition, mossy fibers normally show a prominent expression of polysialylated NCAM, and most of them grow superficial to the CA3 pyramidal neurons in the suprapyramidal bundle, which forms the major constituent of stratum lucidum (Seki and Arai, 1993a; Seki and Arai, 1993b). This ordered organization is severely altered in the NCAM-deficient situation, despite the fact that all axons initially grow in the right direction and appear to make synapses with their correct target neurons, the CA3 pyramidal cells (Cremer et al., 1997). Interestingly, Kir3.3 is selectively enriched in the stratum lucidum of the CA3 area, especially in the distal parts of the pyramidal axons (Grosse et al., 2003). This separate set of axons extends across the pyramidal cell layer into the stratum lucidum and mingles there with bona fide mossy fibers, sending branches in either direction of the mossy fiber tract. The neurons showing axonal sorting of Kir3.3 are characterized by a GABAergic phenotype and are proposed to belong to the group of mossy fiber-associated interneurons (Grosse et al., 2003). In addition, also in the absence of TrkB, the thickness of the stratum lucidum as well as the density of mossy fiber terminals, and their synaptic contacts, are reduced (Otal et al., 2005; Danzer et al., 2008). This appears due to a significant reduction of the surface area and the perimeter of mossy terminals. So, the lack of TrkB signaling results in smaller and less complex mossy axon terminals and in reduced numbers of synaptic vesicles. Because these parameters increase with postnatal ages (Amaral and Dent, 1981), one could conclude that NCAM and TrkB signaling is necessary for the presynaptic maturation of mossy fiber terminals in a region where Kir3.3 is strongly present.

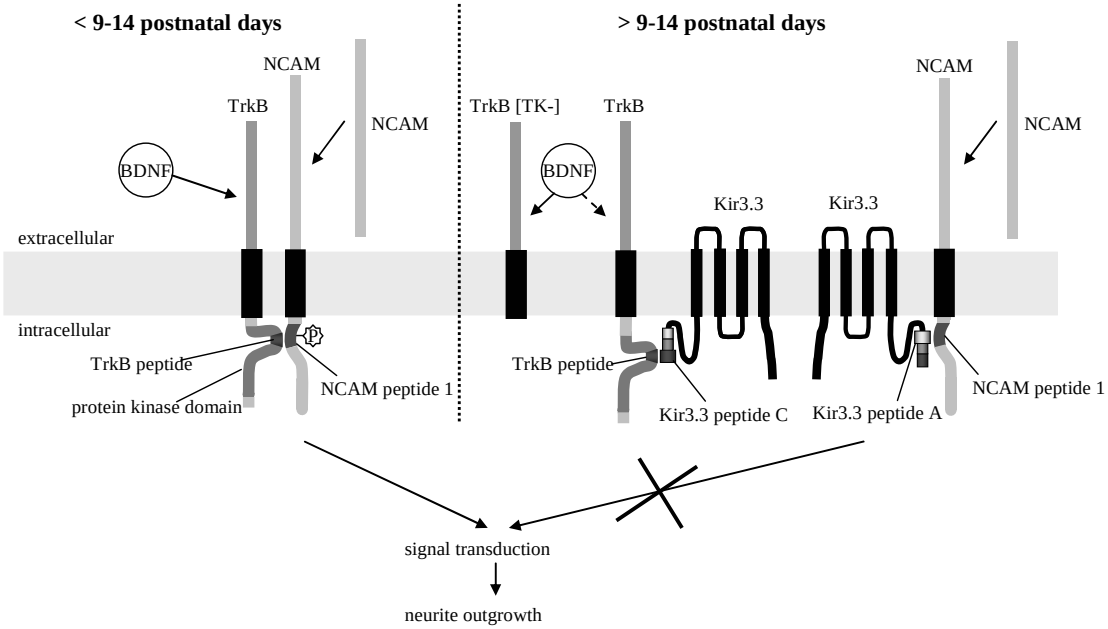

Figure 30 Scheme of proposed functional interplay of NCAM, TrkB and Kir3.3.

Up to postnatal days 9-14 homophilic NCAM *trans*-interaction induces phosphorylation of NCAM by TrkB activated by BDNF and, in the absence of Kir3.3, promotes *cis*-interaction between NCAM and TrkB. This leads to increased neurite outgrowth due to the activation of signal transduction cascades. From postnatal days 9-14 onward Kir3.3 is increasingly expressed in the hippocampus and binds in turn to NCAM and TrkB, thus leading to a reduction of NCAM-TrkB interaction and a decrease in NCAM-induced and TrkB-dependent signal transduction and neurite outgrowth. Furthermore, the increased expression of the truncated splice variant of TrkB (TrkB [TK-]) at this time leads to a reduced BDNF activation of full-length TrkB, thereby contributing to a diminished activation by phosphorylation of NCAM.

6 Summary

This study provides evidence that the intracellular domains of the neural cell adhesion molecule NCAM and the receptor protein tyrosine kinase TrkB directly interact, and that both molecules bind to distinct sites at the C-terminal intracellular domain of the inwardly rectifying K^+ channel subunit Kir3.3. TrkB, but not the closely related Trk-family member TrkA, increases K^+ currents mediated by Kir3.1/3.3 channels, through increased cell surface expression. TrkB does not increase the K^+ currents mediated by channels made up by other functional Kir3 subunits like Kir3.1/3.2 or Kir3.1/3.4. TrkB-dependent Kir3.1/3.3-mediated currents are reduced by co-expression with NCAM due to reduced cell surface expression of Kir3.1/3.3. Expression of Kir3.1/3.3, but not Kir3.1/3.2, inhibits NCAM-induced neurite outgrowth. A further functional relationship between TrkB and NCAM was seen in experiments showing that TrkB, triggered by its ligand BDNF, enhances tyrosine phosphorylation of NCAM. Moreover, the knock-down of TrkB leads to a reduction of NCAM-, but not laminin- induced neurite outgrowth. The observations indicate a decisive role for a neuronal K^+ channel in mediating TrkB- and NCAM-interdependent regulation of neurite outgrowth and attribute a physiologically meaningful interplay for these molecules in limiting neurite outgrowth in ontogenetic development.

7 Zusammenfassung

Diese Studie zeigt, dass die intrazellulären Domänen des neuralen Zelladhäsionsmoleküls NCAM und der Rezeptor-Tyrosinkinase TrkB direkt miteinander interagieren und dass beide Moleküle an unterschiedlichen Stellen der intrazellulären C-terminalen Domäne des G-Protein-aktivierten Kaliumkanals Kir3.3 binden. TrkB, im Gegensatz zu dem eng verwandten TrkA, erhöht Kir3.1/3.3-Kanal vermittelte K^+-Ströme aufgrund von erhöhter Zelloberflächenexpression der Kir3.1/3.3-Kanäle. TrkB erhöht jedoch nicht Ströme, die durch Kir3.1/3.2- und Kir3.1/3.4-Kanäle vermittelt werden. Durch TrkB erhöhte Kir3.1/3.3 vermittelte Ströme werden durch zusätzliche Expression von NCAM reduziert. Dies geschieht aufgrund einer geringeren Zelloberflächenexpression der Kir3.1/3.3-Kanäle. Expression von Kir3.1/3.3, nicht jedoch von Kir3.1/3.2, inhibiert NCAM-induziertes Neuritenwachstum. Ein weiterer funktioneller Zusammenhang zwischen TrkB und NCAM wurde in Experimenten gesehen, die zeigen, dass BDNF-aktiviertes TrkB die Phosphorylierung von NCAM steigert. Darüber hinaus führt der *knock-down* von TrkB zu einer Reduktion des NCAM-induzierten, aber nicht Laminin-induzierten Neuritenwachstums. Diese Beobachtungen zeigen, dass ein neuronaler Kaliumkanal die voneinander abhängige Regulation von TrkB und NCAM in Bezug auf das Neuritenwachstum modulieren kann, und sie beschreiben einen physiologisch bedeutungsvollen Einfluss von Kir3.3 durch das Einschränken von Neuritenwachstum in der ontogenetischen Entwicklung.

8 Reference List

Allendoerfer,K.L., Cabelli,R.J., Escandon,E., Kaplan,D.R., Nikolics,K., and Shatz,C.J. (1994). Regulation of neurotrophin receptors during the maturation of the mammalian visual system. J. Neurosci. *14*, 1795-1811.

Amaral,D.G. (2000). The Anatomical Organization of the Central Nervous System. In Principles of neural science, E.R.Kandel, J.H.Schwartz, and T.M.Jessell, eds. (New York: McGraw-Hill), pp. 317-336.

Amaral,D.G. and Dent,J.A. (1981). Development of the mossy fibers of the dentate gyrus: I. A light and electron microscopic study of the mossy fibers and their expansions. J. Comp Neurol. *195*, 51-86.

Anderson,A.A., Kendal,C.E., Garcia-Maya,M., Kenny,A.V., Morris-Triggs,S.A., Wu,T., Reynolds,R., Hohenester,E., and Saffell,J.L. (2005). A peptide from the first fibronectin domain of NCAM acts as an inverse agonist and stimulates FGF receptor activation, neurite outgrowth and survival. J. Neurochem. *95*, 570-583.

Angata,K., Long,J.M., Bukalo,O., Lee,W., Dityatev,A., Wynshaw-Boris,A., Schachner,M., Fukuda,M., and Marth,J.D. (2004). Sialyltransferase ST8Sia-II assembles a subset of polysialic acid that directs hippocampal axonal targeting and promotes fear behavior. J. Biol. Chem. *279*, 32603-32613.

Armanini,M.P., McMahon,S.B., Sutherland,J., Shelton,D.L., and Phillips,H.S. (1995). Truncated and catalytic isoforms of trkB are co-expressed in neurons of rat and mouse CNS. Eur. J. Neurosci. *7*, 1403-1409.

Ausrubel,F.M. (1996). Current Protocols in Molecular Biology. (Brooklyn, New York: Greene Publishing Associates, Inc.).

Barbacid,M. (1994). The Trk family of neurotrophin receptors. J. Neurobiol. *25*, 1386-1403.

Barbacid,M., Lamballe,F., Pulido,D., and Klein,R. (1991). The trk family of tyrosine protein kinase receptors. Biochim. Biophys. Acta *1072*, 115-127.

Beggs,H.E., Baragona,S.C., Hemperly,J.J., and Maness,P.F. (1997). NCAM140 interacts with the focal adhesion kinase p125(fak) and the SRC-related tyrosine kinase p59(fyn). J. Biol. Chem. *272*, 8310-8319.

Beggs,H.E., Soriano,P., and Maness,P.F. (1994). NCAM-dependent neurite outgrowth is inhibited in neurons from Fyn-minus mice. J. Cell Biol. *127*, 825-833.

Bibel,M., Hoppe,E., and Barde,Y.A. (1999). Biochemical and functional interactions between the neurotrophin receptors trk and p75NTR. EMBO J. *18*, 616-622.

Biffo,S., Offenhauser,N., Carter,B.D., and Barde,Y.A. (1995). Selective binding and internalisation by truncated receptors restrict the availability of BDNF during development. Development *121*, 2461-2470.

Blednov,Y.A., Stoffel,M., Alva,H., and Harris,R.A. (2003). A pervasive mechanism for analgesia: activation of GIRK2 channels. Proc. Natl. Acad. Sci. U. S. A *100*, 277-282.

Boeshore,K.L., Luckey,C.N., Zigmond,R.E., and Large,T.H. (1999). TrkB isoforms with distinct neurotrophin specificities are expressed in predominantly nonoverlapping populations of avian dorsal root ganglion neurons. J. Neurosci. *19*, 4739-4747.

Brackenbury,R., Thiery,J.P., Rutishauser,U., and Edelman,G.M. (1977). Adhesion among neural cells of the chick embryo. I. An immunological assay for molecules involved in cell-cell binding. J. Biol. Chem. *252*, 6835-6840.

Brennaman,L.H. and Maness,P.F. (2008). NCAM in Neuropsychiatric and Neurodegenerative Disorders. Neurochem. Res.

Brodmann,K. (1908). Vergleichende Lokalisationslehre der Grosshirnrinde in ihren Prinzipien dargestellt auf Grund des Zellenbaues. Ambrosius Barth Verlag).

Burgess,A. and Aubert,I. (2006). Polysialic acid limits choline acetyltransferase activity induced by brain-derived neurotrophic factor. J. Neurochem. *99*, 797-806.

Burnette,W.N. (1981). "Western blotting": electrophoretic transfer of proteins from sodium dodecyl sulfate--polyacrylamide gels to unmodified nitrocellulose and radiographic detection with antibody and radioiodinated protein A. Anal. Biochem. *112*, 195-203.

Chan,K.W., Langan,M.N., Sui,J.L., Kozak,J.A., Pabon,A., Ladias,J.A., and Logothetis,D.E. (1996a). A recombinant inwardly rectifying potassium channel coupled to GTP-binding proteins. J. Gen. Physiol *107*, 381-397.

Chan,K.W., Sui,J.L., Vivaudou,M., and Logothetis,D.E. (1996b). Control of channel activity through a unique amino acid residue of a G protein-gated inwardly rectifying K+ channel subunit. Proc. Natl. Acad. Sci. U. S. A *93*, 14193-14198.

Chao,M.V. (1992). Neurotrophin receptors: a window into neuronal differentiation. Neuron *9*, 583-593.

Chao,M.V. (1994). The p75 neurotrophin receptor. J. Neurobiol. *25*, 1373-1385.

Chao,M.V. (2003). Neurotrophins and their receptors: a convergence point for many signalling pathways. Nat. Rev. Neurosci. *4*, 299-309.

Chao,M.V. and Hempstead,B.L. (1995). p75 and Trk: a two-receptor system. Trends Neurosci. *18*, 321-326.

Cohen,N.A., Brenman,J.E., Snyder,S.H., and Bredt,D.S. (1996). Binding of the inward rectifier K+ channel Kir 2.3 to PSD-95 is regulated by protein kinase A phosphorylation. Neuron *17*, 759-767.

Cremer,H., Chazal,G., Goridis,C., and Represa,A. (1997). NCAM is essential for axonal growth and fasciculation in the hippocampus. Mol. Cell Neurosci. *8*, 323-335.

Crossin,K.L. and Krushel,L.A. (2000). Cellular signaling by neural cell adhesion molecules of the immunoglobulin superfamily. Dev. Dyn. *218*, 260-279.

Cunningham,B.A., Hemperly,J.J., Murray,B.A., Prediger,E.A., Brackenbury,R., and Edelman,G.M. (1987). Neural cell adhesion molecule: structure, immunoglobulin-like domains, cell surface modulation, and alternative RNA splicing. Science *236*, 799-806.

Cunningham,B.A., Hoffman,S., Rutishauser,U., Hemperly,J.J., and Edelman,G.M. (1983). Molecular topography of the neural cell adhesion molecule N-CAM: surface orientation and location of sialic acid-rich and binding regions. Proc. Natl. Acad. Sci. U. S. A *80*, 3116-3120.

Cunningham,M.E., Stephens,R.M., Kaplan,D.R., and Greene,L.A. (1997). Autophosphorylation of activation loop tyrosines regulates signaling by the TRK nerve growth factor receptor. J. Biol. Chem. *272*, 10957-10967.

Danzer,S.C., Kotloski,R.J., Walter,C., Hughes,M., and McNamara,J.O. (2008). Altered morphology of hippocampal dentate granule cell presynaptic and postsynaptic terminals following conditional deletion of TrkB. Hippocampus.

Dechant,G., Biffo,S., Okazawa,H., Kolbeck,R., Pottgiesser,J., and Barde,Y.A. (1993). Expression and binding characteristics of the BDNF receptor chick trkB. Development *119*, 545-558.

Delling, M. Schematic drawing of a Kir3 channel. 2002.
Ref Type: Art Work

Delling,M., Wischmeyer,E., Dityatev,A., Sytnyk,V., Veh,R.W., Karschin,A., and Schachner,M. (2002). The neural cell adhesion molecule regulates cell-surface delivery of G-protein-activated inwardly rectifying potassium channels via lipid rafts. J. Neurosci. *22*, 7154-7164.

Diestel,S., Laurini,C., Traub,O., and Schmitz,B. (2004). Tyrosine 734 of NCAM180 interferes with FGF receptor-dependent signaling implicated in neurite growth. Biochem. Biophys. Res. Commun. *322*, 186-196.

Doherty,P., Fruns,M., Seaton,P., Dickson,G., Barton,C.H., Sears,T.A., and Walsh,F.S. (1990). A threshold effect of the major isoforms of NCAM on neurite outgrowth. Nature *343*, 464-466.

Doherty,P., Williams,G., and Williams,E.J. (2000). CAMs and axonal growth: a critical evaluation of the role of calcium and the MAPK cascade. Mol. Cell Neurosci. *16*, 283-295.

Durbec,P. and Cremer,H. (2001). Revisiting the function of PSA-NCAM in the nervous system. Mol. Neurobiol. *24*, 53-64.

Durbec,P., Marcos-Gutierrez,C.V., Kilkenny,C., Grigoriou,M., Wartiowaara,K., Suvanto,P., Smith,D., Ponder,B., Costantini,F., Saarma,M., and . (1996). GDNF signalling through the Ret receptor tyrosine kinase. Nature *381*, 789-793.

Eckhardt,M., Bukalo,O., Chazal,G., Wang,L., Goridis,C., Schachner,M., Gerardy-Schahn,R., Cremer,H., and Dityatev,A. (2000). Mice deficient in the polysialyltransferase ST8SiaIV/PST-1 allow discrimination of the roles of neural cell adhesion molecule protein and polysialic acid in neural development and synaptic plasticity. J. Neurosci. *20*, 5234-5244.

Eide,F.F., Vining,E.R., Eide,B.L., Zang,K., Wang,X.Y., and Reichardt,L.F. (1996). Naturally occurring truncated trkB receptors have dominant inhibitory effects on brain-derived neurotrophic factor signaling. J. Neurosci. *16*, 3123-3129.

Escandon,E., Soppet,D., Rosenthal,A., Mendoza-Ramirez,J.L., Szonyi,E., Burton,L.E., Henderson,C.E., Parada,L.F., and Nikolics,K. (1994). Regulation of neurotrophin receptor expression during embryonic and postnatal development. J. Neurosci. *14*, 2054-2068.

Fakler,B., Brandle,U., Glowatzki,E., Weidemann,S., Zenner,H.P., and Ruppersberg,J.P. (1995). Strong voltage-dependent inward rectification of inward rectifier K+ channels is caused by intracellular spermine. Cell *80*, 149-154.

Foehr,E.D., Lin,X., O'Mahony,A., Geleziunas,R., Bradshaw,R.A., and Greene,W.C. (2000). NF-kappa B signaling promotes both cell survival and neurite process formation in nerve growth factor-stimulated PC12 cells. J. Neurosci. *20*, 7556-7563.

Francavilla,C., Loeffler,S., Piccini,D., Kren,A., Christofori,G., and Cavallaro,U. (2007). Neural cell adhesion molecule regulates the cellular response to fibroblast growth factor. J. Cell Sci. *120*, 4388-4394.

Fryer,R.H., Kaplan,D.R., Feinstein,S.C., Radeke,M.J., Grayson,D.R., and Kromer,L.F. (1996). Developmental and mature expression of full-length and truncated TrkB receptors in the rat forebrain. J. Comp Neurol. *374*, 21-40.

Fryer,R.H., Kaplan,D.R., and Kromer,L.F. (1997). Truncated trkB receptors on nonneuronal cells inhibit BDNF-induced neurite outgrowth in vitro. Exp. Neurol. *148*, 616-627.

Grosse,G., Eulitz,D., Thiele,T., Pahner,I., Schroter,S., Takamori,S., Grosse,J., Wickman,K., Tapp,R., Veh,R.W., Ottersen,O.P., and Ahnert-Hilger,G. (2003). Axonal sorting of Kir3.3 defines a GABA-containing neuron in the CA3 region of rodent hippocampus. Mol. Cell Neurosci. *24*, 709-724.

Haapasalo,A., Sipola,I., Larsson,K., Akerman,K.E., Stoilov,P., Stamm,S., Wong,G., and Castren,E. (2002). Regulation of TRKB surface expression by brain-derived neurotrophic factor and truncated TRKB isoforms. J. Biol. Chem. *277*, 43160-43167.

Harkins,A.B., Dlouhy,S., Ghetti,B., Cahill,A.L., Won,L., Heller,B., Heller,A., and Fox,A.P. (2000). Evidence of elevated intracellular calcium levels in weaver homozygote mice. J. Physiol *524 Pt 2*, 447-455.

Hekmat,A., Bitter-Suermann,D., and Schachner,M. (1990). Immunocytological localization of the highly polysialylated form of the neural cell adhesion molecule during development of the murine cerebellar cortex. J. Comp Neurol. *291*, 457-467.

Hess,E.J. (1996). Identification of the weaver mouse mutation: the end of the beginning. Neuron *16*, 1073-1076.

Heumann,R. (1994). Neurotrophin signalling. Curr. Opin. Neurobiol. *4*, 668-679.

Hille,B. (1992). G protein-coupled mechanisms and nervous signaling. Neuron *9*, 187-195.

Ho,K., Nichols,C.G., Lederer,W.J., Lytton,J., Vassilev,P.M., Kanazirska,M.V., and Hebert,S.C. (1993). Cloning and expression of an inwardly rectifying ATP-regulated potassium channel. Nature *362*, 31-38.

Hoffman,S. and Edelman,G.M. (1983). Kinetics of homophilic binding by embryonic and adult forms of the neural cell adhesion molecule. Proc. Natl. Acad. Sci. U. S. A *80*, 5762-5766.

Huang,C.L., Slesinger,P.A., Casey,P.J., Jan,Y.N., and Jan,L.Y. (1995). Evidence that direct binding of G beta gamma to the GIRK1 G protein-gated inwardly rectifying K+ channel is important for channel activation. Neuron *15*, 1133-1143.

Huang,E.J. and Reichardt,L.F. (2001). Neurotrophins: roles in neuronal development and function. Annu. Rev. Neurosci. *24*, 677-736.

Huang,E.J. and Reichardt,L.F. (2003). Trk receptors: roles in neuronal signal transduction. Annu. Rev. Biochem. *72*, 609-642.

Inagaki,N., Thoenen,H., and Lindholm,D. (1995). TrkA tyrosine residues involved in NGF-induced neurite outgrowth of PC12 cells. Eur. J. Neurosci. *7*, 1125-1133.

Inanobe,A., Yoshimoto,Y., Horio,Y., Morishige,K.I., Hibino,H., Matsumoto,S., Tokunaga,Y., Maeda,T., Hata,Y., Takai,Y., and Kurachi,Y. (1999). Characterization of G-protein-gated K+ channels composed of Kir3.2 subunits in dopaminergic neurons of the substantia nigra. J. Neurosci. *19*, 1006-1017.

Inoue,H., Nojima,H., and Okayama,H. (1990). High efficiency transformation of Escherichia coli with plasmids. Gene *96*, 23-28.

Ippolito,D.L., Temkin,P.A., Rogalski,S.L., and Chavkin,C. (2002). N-terminal tyrosine residues within the potassium channel Kir3 modulate GTPase activity of Galphai. J. Biol. Chem. *277*, 32692-32696.

Isomoto,S., Kondo,C., and Kurachi,Y. (1997). Inwardly rectifying potassium channels: their molecular heterogeneity and function. Jpn. J. Physiol *47*, 11-39.

Iwasaki,Y., Nishiyama,H., Suzuki,K., and Koizumi,S. (1997). Sequential cis/trans autophosphorylation in TrkB tyrosine kinase. Biochemistry *36*, 2694-2700.

Iwase,T., Jung,C.G., Bae,H., Zhang,M., and Soliven,B. (2005). Glial cell line-derived neurotrophic factor-induced signaling in Schwann cells. J. Neurochem. *94*, 1488-1499.

Jelacic,T.M., Kennedy,M.E., Wickman,K., and Clapham,D.E. (2000). Functional and biochemical evidence for G-protein-gated inwardly rectifying K+ (GIRK) channels composed of GIRK2 and GIRK3. J. Biol. Chem. *275*, 36211-36216.

Jessell,T.M. and Sanes,J.R. (2000). The Induction and Patterning of the Nervous System. In Principles of neural science, E.R.Kandel, J.H.Schwartz, and T.M.Jessell, eds. (New York: McGraw-Hill), pp. 1019-1038.

Jessen,U., Novitskaya,V., Pedersen,N., Serup,P., Berezin,V., and Bock,E. (2001). The transcription factors CREB and c-Fos play key roles in NCAM-mediated neuritogenesis in PC12-E2 cells. J. Neurochem. *79*, 1149-1160.

Jing,S., Wen,D., Yu,Y., Holst,P.L., Luo,Y., Fang,M., Tamir,R., Antonio,L., Hu,Z., Cupples,R., Louis,J.C., Hu,S., Altrock,B.W., and Fox,G.M. (1996). GDNF-induced activation of the ret protein tyrosine kinase is mediated by GDNFR-alpha, a novel receptor for GDNF. Cell *85*, 1113-1124.

Johnson,C.P., Fragneto,G., Konovalov,O., Dubosclard,V., Legrand,J.F., and Leckband,D.E. (2005). Structural studies of the neural-cell-adhesion molecule by X-ray and neutron reflectivity. Biochemistry *44*, 546-554.

Johnson,C.P., Fujimoto,I., Perrin-Tricaud,C., Rutishauser,U., and Leckband,D. (2004). Mechanism of homophilic adhesion by the neural cell adhesion molecule: use of multiple domains and flexibility. Proc. Natl. Acad. Sci. U. S. A *101*, 6963-6968.

Johnson,H., Hokfelt,T., and Ulfhake,B. (1999). Expression of p75(NTR), trkB and trkC in nonmanipulated and axotomized motoneurons of aged rats. Brain Res. Mol. Brain Res. *69*, 21-34.

Kaplan,D.R., Hempstead,B.L., Martin-Zanca,D., Chao,M.V., and Parada,L.F. (1991). The trk proto-oncogene product: a signal transducing receptor for nerve growth factor. Science *252*, 554-558.

Kaplan,D.R. and Miller,F.D. (2000). Neurotrophin signal transduction in the nervous system. Curr. Opin. Neurobiol. *10*, 381-391.

Karschin,C. and Karschin,A. (1997). Ontogeny of gene expression of Kir channel subunits in the rat. Mol. Cell Neurosci. *10*, 131-148.

Kennedy,M.E., Nemec,J., and Clapham,D.E. (1996). Localization and interaction of epitope-tagged GIRK1 and CIR inward rectifier K+ channel subunits. Neuropharmacology *35*, 831-839.

Kennedy,M.E., Nemec,J., Corey,S., Wickman,K., and Clapham,D.E. (1999). GIRK4 confers appropriate processing and cell surface localization to G-protein-gated potassium channels. J. Biol. Chem. *274*, 2571-2582.

Kiselyov,V.V., Soroka,V., Berezin,V., and Bock,E. (2005). Structural biology of NCAM homophilic binding and activation of FGFR. J. Neurochem. *94*, 1169-1179.

Kiss,J.Z., Troncoso,E., Djebbara,Z., Vutskits,L., and Muller,D. (2001). The role of neural cell adhesion molecules in plasticity and repair. Brain Res. Brain Res. Rev. *36*, 175-184.

Kleene,R. and Schachner,M. (2004). Glycans and neural cell interactions. Nat. Rev. Neurosci. *5*, 195-208.

Klein,R., Conway,D., Parada,L.F., and Barbacid,M. (1990). The trkB tyrosine protein kinase gene codes for a second neurogenic receptor that lacks the catalytic kinase domain. Cell *61*, 647-656.

Klein,R., Nanduri,V., Jing,S.A., Lamballe,F., Tapley,P., Bryant,S., Cordon-Cardo,C., Jones,K.R., Reichardt,L.F., and Barbacid,M. (1991). The trkB tyrosine protein kinase is a receptor for brain-derived neurotrophic factor and neurotrophin-3. Cell *66*, 395-403.

Klein,R., Parada,L.F., Coulier,F., and Barbacid,M. (1989). trkB, a novel tyrosine protein kinase receptor expressed during mouse neural development. EMBO J. *8*, 3701-3709.

Kofuji,P., Davidson,N., and Lester,H.A. (1995). Evidence that neuronal G-protein-gated inwardly rectifying K+ channels are activated by G beta gamma subunits and function as heteromultimers. Proc. Natl. Acad. Sci. U. S. A *92*, 6542-6546.

Kofuji,P., Hofer,M., Millen,K.J., Millonig,J.H., Davidson,N., Lester,H.A., and Hatten,M.E. (1996). Functional analysis of the weaver mutant GIRK2 K+ channel and rescue of weaver granule cells. Neuron *16*, 941-952.

Koyrakh,L., Lujan,R., Colon,J., Karschin,C., Kurachi,Y., Karschin,A., and Wickman,K. (2005). Molecular and cellular diversity of neuronal G-protein-gated potassium channels. J. Neurosci. *25*, 11468-11478.

Krapivinsky,G., Gordon,E.A., Wickman,K., Velimirovic,B., Krapivinsky,L., and Clapham,D.E. (1995). The G-protein-gated atrial K+ channel IKACh is a heteromultimer of two inwardly rectifying K(+)-channel proteins. Nature *374*, 135-141.

Krushel,L.A., Cunningham,B.A., Edelman,G.M., and Crossin,K.L. (1999). NF-kappaB activity is induced by neural cell adhesion molecule binding to neurons and astrocytes. J. Biol. Chem. *274*, 2432-2439.

Kubo,Y., Baldwin,T.J., Jan,Y.N., and Jan,L.Y. (1993). Primary structure and functional expression of a mouse inward rectifier potassium channel. Nature *362*, 127-133.

Laemmli,U.K. (1970). Cleavage of structural proteins during the assembly of the head of bacteriophage T4. Nature *227*, 680-685.

Ledda,F., Paratcha,G., Sandoval-Guzman,T., and Ibanez,C.F. (2007). GDNF and GFRalpha1 promote formation of neuronal synapses by ligand-induced cell adhesion. Nat. Neurosci. *10*, 293-300.

Lei,Q., Jones,M.B., Talley,E.M., Schrier,A.D., McIntire,W.E., Garrison,J.C., and Bayliss,D.A. (2000). Activation and inhibition of G protein-coupled inwardly rectifying potassium (Kir3) channels by G protein beta gamma subunits. Proc. Natl. Acad. Sci. U. S. A *97*, 9771-9776.

Lei,Q., Talley,E.M., and Bayliss,D.A. (2001). Receptor-mediated inhibition of G protein-coupled inwardly rectifying potassium channels involves G(alpha)q family subunits, phospholipase C, and a readily diffusible messenger. J. Biol. Chem. *276*, 16720-16730.

Lesage,F., Guillemare,E., Fink,M., Duprat,F., Heurteaux,C., Fosset,M., Romey,G., Barhanin,J., and Lazdunski,M. (1995). Molecular properties of neuronal G-protein-activated inwardly rectifying K+ channels. J. Biol. Chem. *270*, 28660-28667.

Li,Y.X., Xu,Y., Ju,D., Lester,H.A., Davidson,N., and Schuman,E.M. (1998). Expression of a dominant negative TrkB receptor, T1, reveals a requirement for presynaptic signaling in BDNF-induced synaptic potentiation in cultured hippocampal neurons. Proc. Natl. Acad. Sci. U. S. A *95*, 10884-10889.

Liao,Y.J., Jan,Y.N., and Jan,L.Y. (1996). Heteromultimerization of G-protein-gated inwardly rectifying K+ channel proteins GIRK1 and GIRK2 and their altered expression in weaver brain. J. Neurosci. *16*, 7137-7150.

Lindholm,D., Hamner,S., and Zirrgiebel,U. (1997). Neurotrophins and cerebellar development. Perspect. Dev. Neurobiol. *5*, 83-94.

Little,E.B., Edelman,G.M., and Cunningham,B.A. (1998). Palmitoylation of the cytoplasmic domain of the neural cell adhesion molecule N-CAM serves as an anchor to cellular membranes. Cell Adhes. Commun. *6*, 415-430.

Lunn,M.L., Nassirpour,R., Arrabit,C., Tan,J., McLeod,I., Arias,C.M., Sawchenko,P.E., Yates,J.R., III, and Slesinger,P.A. (2007). A unique sorting nexin regulates trafficking of potassium channels via a PDZ domain interaction. Nat. Neurosci. *10*, 1249-1259.

Luscher,C., Jan,L.Y., Stoffel,M., Malenka,R.C., and Nicoll,R.A. (1997). G protein-coupled inwardly rectifying K+ channels (GIRKs) mediate postsynaptic but not presynaptic transmitter actions in hippocampal neurons. Neuron *19*, 687-695.

Ma,D., Zerangue,N., Raab-Graham,K., Fried,S.R., Jan,Y.N., and Jan,L.Y. (2002). Diverse trafficking patterns due to multiple traffic motifs in G protein-activated inwardly rectifying potassium channels from brain and heart. Neuron *33*, 715-729.

Mackowiak,M., Markowicz-Kula,K., Fijal,K., and Wedzony,K. (2005). Acute and repeated administration of cocaine differentially regulates expression of PSA-NCAM-positive neurons in the rat hippocampus. Brain Res. *1055*, 149-155.

Maness,P.F. and Schachner,M. (2007). Neural recognition molecules of the immunoglobulin superfamily: signaling transducers of axon guidance and neuronal migration. Nat. Neurosci. *10*, 19-26.

Mark,M.D. and Herlitze,S. (2000). G-protein mediated gating of inward-rectifier K+ channels. Eur. J. Biochem. *267*, 5830-5836.

Martin-Zanca,D., Barbacid,M., and Parada,L.F. (1990). Expression of the trk proto-oncogene is restricted to the sensory cranial and spinal ganglia of neural crest origin in mouse development. Genes Dev. *4*, 683-694.

Martin-Zanca,D., Hughes,S.H., and Barbacid,M. (1986a). A human oncogene formed by the fusion of truncated tropomyosin and protein tyrosine kinase sequences. Nature *319*, 743-748.

Martin-Zanca,D., Mitra,G., Long,L.K., and Barbacid,M. (1986b). Molecular characterization of the human trk oncogene. Cold Spring Harb. Symp. Quant. Biol. *51 Pt 2*, 983-992.

Mendiratta,S.S., Sekulic,N., Lavie,A., and Colley,K.J. (2005). Specific amino acids in the first fibronectin type III repeat of the neural cell adhesion molecule play a role in its recognition and polysialylation by the polysialyltransferase ST8Sia IV/PST. J. Biol. Chem. *280*, 32340-32348.

Middlemas,D.S., Lindberg,R.A., and Hunter,T. (1991). trkB, a neural receptor protein-tyrosine kinase: evidence for a full-length and two truncated receptors. Mol. Cell Biol. *11*, 143-153.

Minichiello,L. and Klein,R. (1996). TrkB and TrkC neurotrophin receptors cooperate in promoting survival of hippocampal and cerebellar granule neurons. Genes Dev. *10*, 2849-2858.

Morgan,A.D., Carroll,M.E., Loth,A.K., Stoffel,M., and Wickman,K. (2003). Decreased cocaine self-administration in Kir3 potassium channel subunit knockout mice. Neuropsychopharmacology *28*, 932-938.

Muhlenhoff,M., Eckhardt,M., Bethe,A., Frosch,M., and Gerardy-Schahn,R. (1996). Polysialylation of NCAM by a single enzyme. Curr. Biol. *6*, 1188-1191.

Muller,D., Djebbara-Hannas,Z., Jourdain,P., Vutskits,L., Durbec,P., Rougon,G., and Kiss,J.Z. (2000). Brain-derived neurotrophic factor restores long-term potentiation in polysialic acid-neural cell adhesion molecule-deficient hippocampus. Proc. Natl. Acad. Sci. U. S. A *97*, 4315-4320.

Mullis,K., Faloona,F., Scharf,S., Saiki,R., Horn,G., and Erlich,H. (1986). Specific enzymatic amplification of DNA in vitro: the polymerase chain reaction. Cold Spring Harb. Symp. Quant. Biol. *51 Pt 1*, 263-273.

Nichols,C.G. and Lopatin,A.N. (1997). Inward rectifier potassium channels. Annu. Rev. Physiol *59*, 171-191.

Niethammer,P., Delling,M., Sytnyk,V., Dityatev,A., Fukami,K., and Schachner,M. (2002). Cosignaling of NCAM via lipid rafts and the FGF receptor is required for neuritogenesis. J. Cell Biol. *157*, 521-532.

Ohira,K., Shimizu,K., and Hayashi,M. (1999). Change of expression of full-length and truncated TrkBs in the developing monkey central nervous system. Brain Res. Dev. Brain Res. *112*, 21-29.

Otal,R., Martinez,A., and Soriano,E. (2005). Lack of TrkB and TrkC signaling alters the synaptogenesis and maturation of mossy fiber terminals in the hippocampus. Cell Tissue Res. *319*, 349-358.

Paratcha,G., Ibanez,C.F., and Ledda,F. (2006). GDNF is a chemoattractant factor for neuronal precursor cells in the rostral migratory stream. Mol. Cell Neurosci. *31*, 505-514.

Paratcha,G., Ledda,F., and Ibanez,C.F. (2003). The neural cell adhesion molecule NCAM is an alternative signaling receptor for GDNF family ligands. Cell *113*, 867-879.

Patapoutian,A. and Reichardt,L.F. (2001). Trk receptors: mediators of neurotrophin action. Curr. Opin. Neurobiol. *11*, 272-280.

Pawson,T. and Nash,P. (2000). Protein-protein interactions define specificity in signal transduction. Genes Dev. *14*, 1027-1047.

Pereira,D.B. and Chao,M.V. (2007). The tyrosine kinase Fyn determines the localization of TrkB receptors in lipid rafts. J. Neurosci. *27*, 4859-4869.

Persohn,E., Pollerberg,G.E., and Schachner,M. (1989). Immunoelectron-microscopic localization of the 180 kD component of the neural cell adhesion molecule N-CAM in postsynaptic membranes. J. Comp Neurol. *288*, 92-100.

Petridis,A.K., El Maarouf,A., and Rutishauser,U. (2004). Polysialic acid regulates cell contact-dependent neuronal differentiation of progenitor cells from the subventricular zone. Dev. Dyn. *230*, 675-684.

Polo-Parada,L., Bose,C.M., Plattner,F., and Landmesser,L.T. (2004). Distinct roles of different neural cell adhesion molecule (NCAM) isoforms in synaptic maturation revealed by analysis of NCAM 180 kDa isoform-deficient mice. J. Neurosci. *24*, 1852-1864.

Polo-Parada,L., Plattner,F., Bose,C., and Landmesser,L.T. (2005). NCAM 180 acting via a conserved C-terminal domain and MLCK is essential for effective transmission with repetitive stimulation. Neuron *46*, 917-931.

Qian,X., Riccio,A., Zhang,Y., and Ginty,D.D. (1998). Identification and characterization of novel substrates of Trk receptors in developing neurons. Neuron *21*, 1017-1029.

Rabacchi,S.A., Kruk,B., Hamilton,J., Carney,C., Hoffman,J.R., Meyer,S.L., Springer,J.E., and Baird,D.H. (1999). BDNF and NT4/5 promote survival and neurite outgrowth of pontocerebellar mossy fiber neurons. J. Neurobiol. *40*, 254-269.

Rao,Y., Zhao,X., and Siu,C.H. (1994). Mechanism of homophilic binding mediated by the neural cell adhesion molecule NCAM. Evidence for isologous interaction. J. Biol. Chem. *269*, 27540-27548.

Rico,B., Xu,B., and Reichardt,L.F. (2002). TrkB receptor signaling is required for establishment of GABAergic synapses in the cerebellum. Nat. Neurosci. *5*, 225-233.

Rogalski,S.L., Appleyard,S.M., Pattillo,A., Terman,G.W., and Chavkin,C. (2000). TrkB activation by brain-derived neurotrophic factor inhibits the G protein-gated inward rectifier Kir3 by tyrosine phosphorylation of the channel. J. Biol. Chem. *275*, 25082-25088.

Ruppersberg,J.P. (2000). Intracellular regulation of inward rectifier K+ channels. Pflugers Arch. *441*, 1-11.

Ruppersberg,J.P. and Fakler,B. (1996). Complexity of the regulation of Kir2.1 K+ channels. Neuropharmacology *35*, 887-893.

Sadoul,R., Hirn,M., Deagostini-Bazin,H., Rougon,G., and Goridis,C. (1983). Adult and embryonic mouse neural cell adhesion molecules have different binding properties. Nature *304*, 347-349.

Saffell,J.L., Williams,E.J., Mason,I.J., Walsh,F.S., and Doherty,P. (1997). Expression of a dominant negative FGF receptor inhibits axonal growth and FGF receptor phosphorylation stimulated by CAMs. Neuron *18*, 231-242.

Sambrook,J., Fritsch,E.F., and and Maniatis,T. (1989). Molecular cloning: A Laboratory Manual.

Saragovi,H.U., Zheng,W., Maliartchouk,S., DiGugliemo,G.M., Mawal,Y.R., Kamen,A., Woo,S.B., Cuello,A.C., Debeir,T., and Neet,K.E. (1998). A TrkA-selective, fast internalizing nerve growth factor-antibody complex induces trophic but not neuritogenic signals. J. Biol. Chem. *273*, 34933-34940.

Schmid,R.S., Graff,R.D., Schaller,M.D., Chen,S., Schachner,M., Hemperly,J.J., and Maness,P.F. (1999). NCAM stimulates the Ras-MAPK pathway and CREB phosphorylation in neuronal cells. J. Neurobiol. *38*, 542-558.

Schuch,U., Lohse,M.J., and Schachner,M. (1989). Neural cell adhesion molecules influence second messenger systems. Neuron *3*, 13-20.

Segal,R.A. and Greenberg,M.E. (1996). Intracellular signaling pathways activated by neurotrophic factors. Annu. Rev. Neurosci. *19*, 463-489.

Segal,R.A., Pomeroy,S.L., and Stiles,C.D. (1995). Axonal growth and fasciculation linked to differential expression of BDNF and NT3 receptors in developing cerebellar granule cells. J. Neurosci. *15*, 4970-4981.

Seki,T. and Arai,Y. (1993a). Distribution and possible roles of the highly polysialylated neural cell adhesion molecule (NCAM-H) in the developing and adult central nervous system. Neurosci. Res. *17*, 265-290.

Seki,T. and Arai,Y. (1993b). Highly polysialylated neural cell adhesion molecule (NCAM-H) is expressed by newly generated granule cells in the dentate gyrus of the adult rat. J. Neurosci. *13*, 2351-2358.

Shimada,A., Mason,C.A., and Morrison,M.E. (1998). TrkB signaling modulates spine density and morphology independent of dendrite structure in cultured neonatal Purkinje cells. J. Neurosci. *18*, 8559-8570.

Signorini,S., Liao,Y.J., Duncan,S.A., Jan,L.Y., and Stoffel,M. (1997). Normal cerebellar development but susceptibility to seizures in mice lacking G protein-coupled, inwardly rectifying K+ channel GIRK2. Proc. Natl. Acad. Sci. U. S. A *94*, 923-927.

Sjostrand,D., Carlsson,J., Paratcha,G., Persson,B., and Ibanez,C.F. (2007). Disruption of the GDNF binding site in NCAM dissociates ligand binding and homophilic cell adhesion. J. Biol. Chem. *282*, 12734-12740.

Slesinger,P.A., Reuveny,E., Jan,Y.N., and Jan,L.Y. (1995). Identification of structural elements involved in G protein gating of the GIRK1 potassium channel. Neuron *15*, 1145-1156.

Smith,P.K., Krohn,R.I., Hermanson,G.T., Mallia,A.K., Gartner,F.H., Provenzano,M.D., Fujimoto,E.K., Goeke,N.M., Olson,B.J., and Klenk,D.C. (1985). Measurement of protein using bicinchoninic acid. Anal. Biochem. *150*, 76-85.

Sofroniew,M.V., Howe,C.L., and Mobley,W.C. (2001). Nerve growth factor signaling, neuroprotection, and neural repair. Annu. Rev. Neurosci. *24*, 1217-1281.

Stephens,R.M., Loeb,D.M., Copeland,T.D., Pawson,T., Greene,L.A., and Kaplan,D.R. (1994). Trk receptors use redundant signal transduction pathways involving SHC and PLC-gamma 1 to mediate NGF responses. Neuron *12*, 691-705.

Stevens,E.B., Woodward,R., Ho,I.H., and Murrell-Lagnado,R. (1997). Identification of regions that regulate the expression and activity of G protein-gated inward rectifier K+ channels in Xenopus oocytes. J. Physiol *503 (Pt 3)*, 547-562.

Stoilov,P., Castren,E., and Stamm,S. (2002). Analysis of the human TrkB gene genomic organization reveals novel TrkB isoforms, unusual gene length, and splicing mechanism. Biochem. Biophys. Res. Commun. *290*, 1054-1065.

Stork,O., Welzl,H., Cremer,H., and Schachner,M. (1997). Increased intermale aggression and neuroendocrine response in mice deficient for the neural cell adhesion molecule (NCAM). Eur. J. Neurosci. *9*, 1117-1125.

Stork,O., Welzl,H., Wotjak,C.T., Hoyer,D., Delling,M., Cremer,H., and Schachner,M. (1999). Anxiety and increased 5-HT1A receptor response in NCAM null mutant mice. J. Neurobiol. *40*, 343-355.

Strohmaier,C., Carter,B.D., Urfer,R., Barde,Y.A., and Dechant,G. (1996). A splice variant of the neurotrophin receptor trkB with increased specificity for brain-derived neurotrophic factor. EMBO J. *15*, 3332-3337.

Suzuki,S., Numakawa,T., Shimazu,K., Koshimizu,H., Hara,T., Hatanaka,H., Mei,L., Lu,B., and Kojima,M. (2004). BDNF-induced recruitment of TrkB receptor into neuronal lipid rafts: roles in synaptic modulation. J. Cell Biol. *167*, 1205-1215.

Sytnyk,V., Leshchyns'ka,I., Delling,M., Dityateva,G., Dityatev,A., and Schachner,M. (2002). Neural cell adhesion molecule promotes accumulation of TGN organelles at sites of neuron-to-neuron contacts. J. Cell Biol. *159*, 649-661.

Tannahill,L., Klein,R., and Schachner,M. (1995). The neurotrophin receptors TrkA and TrkB are inhibitory for neurite outgrowth. Eur. J. Neurosci. *7*, 1424-1428.

Torrecilla,M., Marker,C.L., Cintora,S.C., Stoffel,M., Williams,J.T., and Wickman,K. (2002). G-protein-gated potassium channels containing Kir3.2 and Kir3.3 subunits mediate the acute inhibitory effects of opioids on locus ceruleus neurons. J. Neurosci. *22*, 4328-4334.

Towbin,H., Staehelin,T., and Gordon,J. (1979). Electrophoretic transfer of proteins from polyacrylamide gels to nitrocellulose sheets: procedure and some applications. Proc. Natl. Acad. Sci. U. S. A *76*, 4350-4354.

Treanor,J.J., Goodman,L., de Sauvage,F., Stone,D.M., Poulsen,K.T., Beck,C.D., Gray,C., Armanini,M.P., Pollock,R.A., Hefti,F., Phillips,H.S., Goddard,A., Moore,M.W., Buj-Bello,A., Davies,A.M., Asai,N., Takahashi,M., Vandlen,R., Henderson,C.E., and Rosenthal,A. (1996). Characterization of a multicomponent receptor for GDNF. Nature *382*, 80-83.

Trupp,M., Arenas,E., Fainzilber,M., Nilsson,A.S., Sieber,B.A., Grigoriou,M., Kilkenny,C., Salazar-Grueso,E., Pachnis,V., and Arumae,U. (1996). Functional receptor for GDNF encoded by the c-ret proto-oncogene. Nature *381*, 785-789.

Ultsch,M.H., Wiesmann,C., Simmons,L.C., Henrich,J., Yang,M., Reilly,D., Bass,S.H., and de Vos,A.M. (1999). Crystal structures of the neurotrophin-binding domain of TrkA, TrkB and TrkC. J. Mol. Biol. *290*, 149-159.

Urfer,R., Tsoulfas,P., O'Connell,L., Hongo,J.A., Zhao,W., and Presta,L.G. (1998). High resolution mapping of the binding site of TrkA for nerve growth factor and TrkC for neurotrophin-3 on the second immunoglobulin-like domain of the Trk receptors. J. Biol. Chem. *273*, 5829-5840.

Vutskits,L., Djebbara-Hannas,Z., Zhang,H., Paccaud,J.P., Durbec,P., Rougon,G., Muller,D., and Kiss,J.Z. (2001). PSA-NCAM modulates BDNF-dependent survival and differentiation of cortical neurons. Eur. J. Neurosci. *13*, 1391-1402.

Weinhold,B., Seidenfaden,R., Rockle,I., Muhlenhoff,M., Schertzinger,F., Conzelmann,S., Marth,J.D., Gerardy-Schahn,R., and Hildebrandt,H. (2005). Genetic ablation of polysialic acid causes severe neurodevelopmental defects rescued by deletion of the neural cell adhesion molecule. J. Biol. Chem. *280*, 42971-42977.

Wickman,K. and Clapham,D.E. (1995). Ion channel regulation by G proteins. Physiol Rev. *75*, 865-885.

Wickman,K., Nemec,J., Gendler,S.J., and Clapham,D.E. (1998). Abnormal heart rate regulation in GIRK4 knockout mice. Neuron *20*, 103-114.

Wickman,K., Pu,W.T., and Clapham,D.E. (2002). Structural characterization of the mouse Girk genes. Gene *284*, 241-250.

Wischmeyer,E., Doring,F., Wischmeyer,E., Spauschus,A., Thomzig,A., Veh,R., and Karschin,A. (1997). Subunit interactions in the assembly of neuronal Kir3.0 inwardly rectifying K+ channels. Mol. Cell Neurosci. *9*, 194-206.

Woodward,R., Stevens,E.B., and Murrell-Lagnado,R.D. (1997). Molecular determinants for assembly of G-protein-activated inwardly rectifying K+ channels. J. Biol. Chem. *272*, 10823-10830.

Wooten,M.W. (1999). Function for NF-kB in neuronal survival: regulation by atypical protein kinase C. J. Neurosci. Res. *58*, 607-611.

Wooten,M.W., Vandenplas,M.L., Seibenhener,M.L., Geetha,T., and Diaz-Meco,M.T. (2001). Nerve growth factor stimulates multisite tyrosine phosphorylation and activation of the atypical protein kinase C's via a src kinase pathway. Mol. Cell Biol. *21*, 8414-8427.

Yamada,M., Inanobe,A., and Kurachi,Y. (1998). G protein regulation of potassium ion channels. Pharmacol. Rev. *50*, 723-760.

Yan,Q., Radeke,M.J., Matheson,C.R., Talvenheimo,J., Welcher,A.A., and Feinstein,S.C. (1997). Immunocytochemical localization of TrkB in the central nervous system of the adult rat. J. Comp Neurol. *378*, 135-157.

York,R.D., Molliver,D.C., Grewal,S.S., Stenberg,P.E., McCleskey,E.W., and Stork,P.J. (2000). Role of phosphoinositide 3-kinase and endocytosis in nerve growth factor-induced extracellular signal-regulated kinase activation via Ras and Rap1. Mol. Cell Biol. *20*, 8069-8083.

9 Appendix

9.1 Abbreviations

°C	degree Celsius
x g	g-force
aa	amino acid(s)
A	ampere
Amp	ampicillin
ABTS	2,2'-azino-bis(3-ethylbenzthiazoline-6-sulphonic acid)
APS	ammonium persulfate
bp	base pairs
BSA	bovine serum albumine
cDNA	complementary deoxyribonucleic acid
CDS	coding sequence
C-terminal	carboxyterminal
C-terminus	carboxyterminus
dATP	2'-desoxyadenosine-5'-triphosphate
ddH_2O	double distilled H_2O
DNA	deoxyribonucleic acid
DNase	desoxyribonuclease
DMSO	dimethyl sulfoxide
dNTP	2'-desoxyribonucleotide-5'-triphosphate
E. coli	*Escherichia coli*
EDTA	ethylendiamintetraacetic acid
e.g.	exempli gratia
EGFP	enhanced green fluorescent protein
et al.	et aliter
FCS	fetal calf serum
FGF	fibroblast growth factor
Fig.	Figure
GABA	gamma-aminobutyric acid
GIRK	G protein-coupled inwardly rectifying potassium channel
GMEM	Glasgow modified eagle medium
h	hour(s)
H_2O	water
HEPES	4-(2-hydroxyethyl)-1-piperazineethanesulfonic acid
HRP	horseradish peroxidase
i.e.	id est
IP	immunoprecipitation
IPTG	isopropyl-β-D-thiogalactoside
K^+	potassium ions
kb	kilo base pairs
kDa	kilodalton

Kir	K^+ inwardly rectifying channel
l	liter
LB	luria broth
µg	microgram
M	molar
mA	milliampere
mg	milligram
min	minute(s)
ml	milliliter
mM	millimolar
MW	molecular mass
NCAM	neural cell adhesion molecule
N-terminal	aminoterminal
N-terminus	aminoterminus
o/n	overnight
OD_x	optical density – absorption bei x nm
ORF	open reading frame
p.a.	per analysis
PBS	phosphate buffered saline
PCR	polymerase chain reaction
Pfu	DNA polymerase *Pyrococcus furiosus*
RIPA buffer	radioimmunoprecipitation buffer
RNA	ribonucleic acid
RT	room temperature
SDS	sodium dodecyl sulfate
SDS-PAGE	sodium dodecyl sulfate polyacrylamide gel electrophoresis
siRNA	small interfering RNA
TBS	tris buffered saline
TAE	tris acetate EDTA
Taq	DNA polymerase *Thermus aquaticus*
TEMED	tetramethylethylenediamine
T_m	melting temerature
Trk	receptor protein tyrosine kinase
Tris	trishydroxymethylaminomethane
U	unit
UV	ultraviolet
V	volt
v/v	volume per volume
Vol.	volume
WB	Western blotting
w/v	weight per volume
ZMNH	Zentrum für Molekulare Neurobiologie Hamburg

Amino acids were abbreviated using the one letter code.

9.2 Accession numbers

Protein	Gene	Organism	Accession number
NCAM140	Ncam1	rat	P13596
NCAM180	Ncam1	rat	P13595
TrkA	Ntrk1	rat	P35739
TrkB	Ntrk2	mouse	P15209
Kir3.1 (GIRK1)	Kcnj3	mouse	P63250
Kir3.2 (GIRK2)	Kcnj6	mouse	P48550
Kir3.3 (GIRK3)	Kcnj9	mouse	P48543
Kir3.4 (GIRK4)	Kcnj5	mouse	P48545

9.3 Plasmids

9.3.1 NCAM and CHL1 plasmids

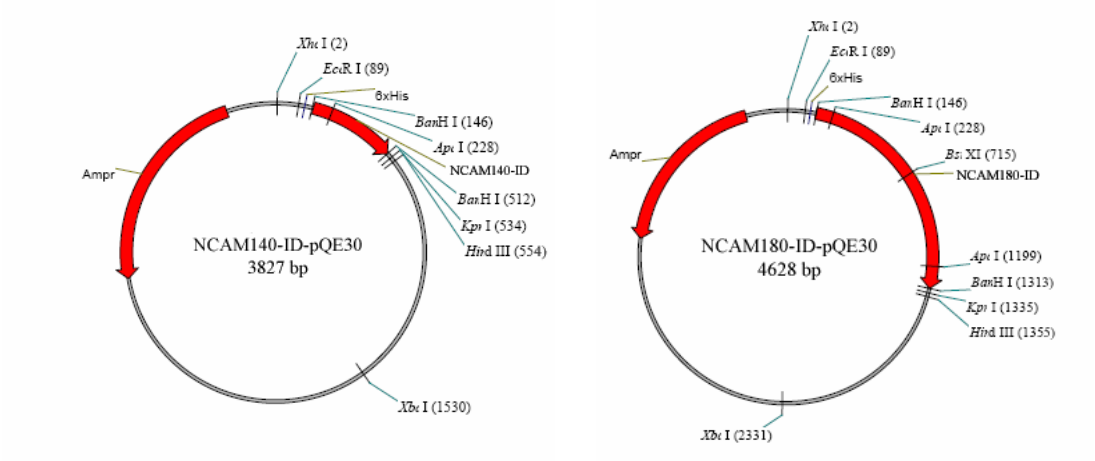

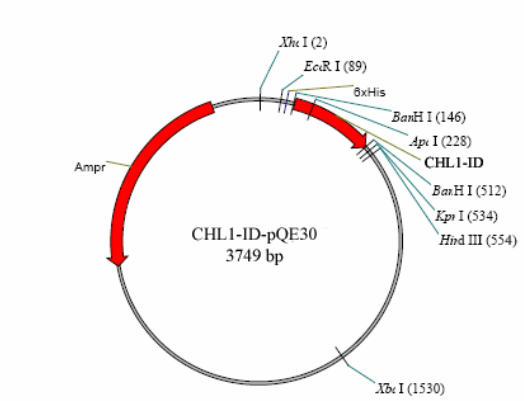
Xho I (2)
EcoR I (89)
6xHis
BanH I (146)
Apa I (228)
CHL1-ID
BanH I (512)
Kpn I (534)
Hind III (554)
Xba I (1530)
Ampr
CHL1-ID-pQE30
3749 bp

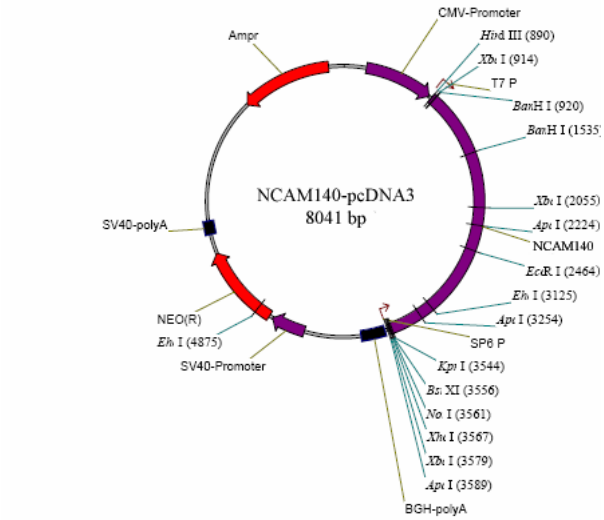
CMV-Promoter
Hind III (890)
Xba I (914)
T7 P
BanH I (920)
BanH I (1535)
Xba I (2055)
Apa I (2224)
NCAM140
EcoR I (2464)
Eha I (3125)
Apa I (3254)
SP6 P
Kpn I (3544)
Bst XI (3556)
Not I (3561)
Xho I (3567)
Xba I (3579)
Apa I (3589)
BGH-polyA
SV40-polyA
NEO(R)
Eha I (4875)
SV40-Promoter
Ampr
NCAM140-pcDNA3
8041 bp

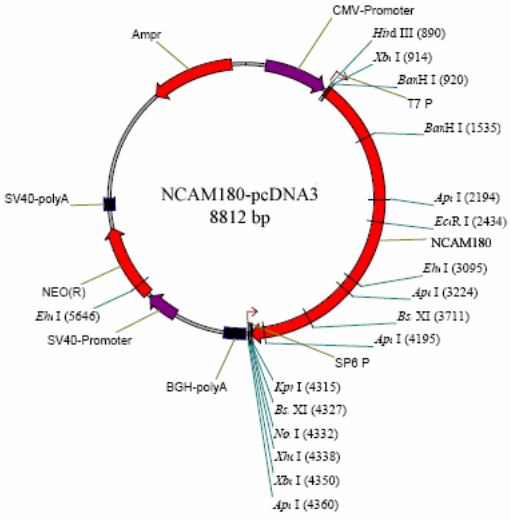
CMV-Promoter
Hind III (890)
Xba I (914)
BanH I (920)
T7 P
BanH I (1535)
Apa I (2194)
EcoR I (2434)
NCAM180
Eha I (3095)
Apa I (3224)
Bst XI (3711)
Apa I (4195)
SP6 P
Kpn I (4315)
Bst XI (4327)
Not I (4332)
Xho I (4338)
Xba I (4350)
Apa I (4360)
BGH-polyA
SV40-Promoter
NEO(R)
Eha I (5646)
SV40-polyA
Ampr
NCAM180-pcDNA3
8812 bp

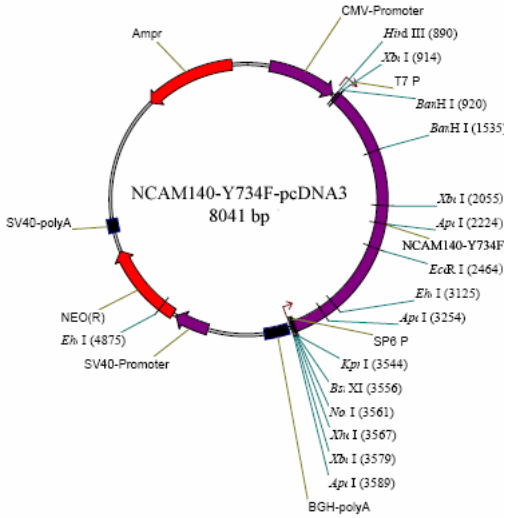
CMV-Promoter
Hind III (890)
Xba I (914)
T7 P
BanH I (920)
BanH I (1535)
Xba I (2055)
Apa I (2224)
NCAM140-Y734F
EcoR I (2464)
Eha I (3125)
Apa I (3254)
SP6 P
Kpn I (3544)
Bst XI (3556)
Not I (3561)
Xho I (3567)
Xba I (3579)
Apa I (3589)
BGH-polyA
SV40-polyA
NEO(R)
Eha I (4875)
SV40-Promoter
Ampr
NCAM140-Y734F-pcDNA3
8041 bp

9.3.2 TrkB plasmid

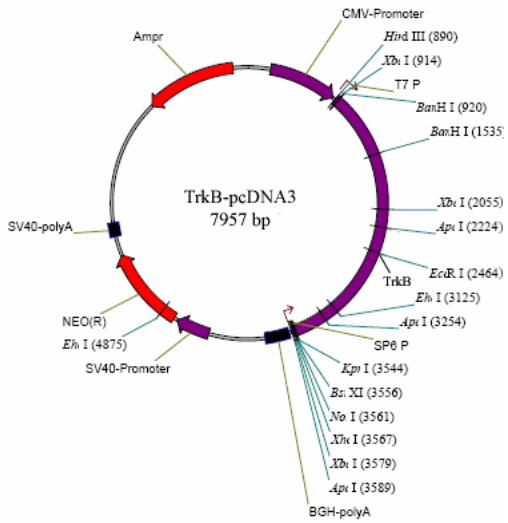

9.3.3 Kir3 plasmids

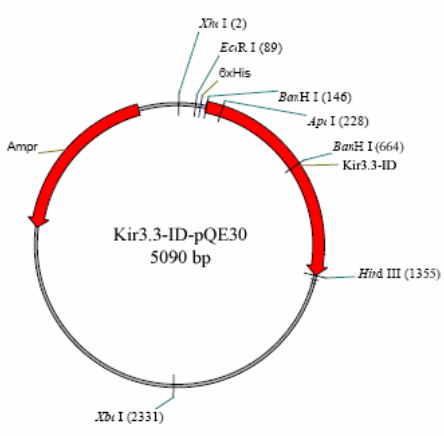

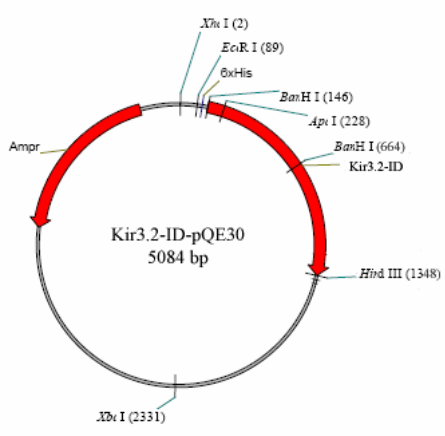

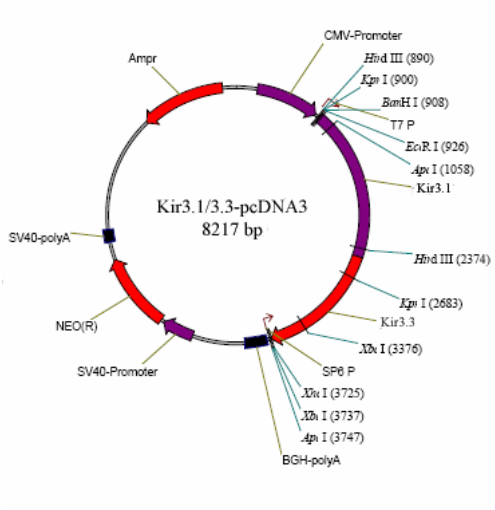
Kir3.1/3.3-pcDNA3
8217 bp
CMV-Promoter
Ampr
Hind III (890)
Kpn I (900)
BamH I (908)
T7 P
EcoR I (926)
Apa I (1058)
Kir3.1
Hind III (2374)
Kpn I (2683)
Kir3.3
Xba I (3376)
SP6 P
Xho I (3725)
Xba I (3737)
Apa I (3747)
BGH-polyA
SV40-polyA
NEO(R)
SV40-Promoter

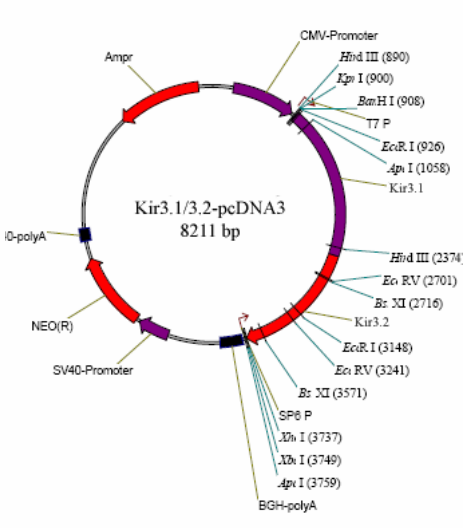
Kir3.1/3.2-pcDNA3
8211 bp
CMV-Promoter
Ampr
Hind III (890)
Kpn I (900)
BamH I (908)
T7 P
EcoR I (926)
Apa I (1058)
Kir3.1
Hind III (2374)
Eco RV (2701)
Bst XI (2716)
Kir3.2
EcoR I (3148)
Eco RV (3241)
Bst XI (3571)
SP6 P
Xho I (3737)
Xba I (3749)
Apa I (3759)
BGH-polyA
NEO(R)
SV40-Promoter

Danksagung

Sehr bedanken möchte ich mich bei Frau Professor Dr. Melitta Schachner für die Möglichkeit meine Doktorarbeit an ihrem Institut zu diesem spannenden und mannigfaltigen Thema gemacht zu haben sowie für die fachkundige Betreuung während der gesamten Zeit.

Bei Herrn Professor Dr. Konrad Wiese möchte ich mich für die Möglichkeit zu dieser externen Promotion bedanken und für die Freiheit bei der Ausgestaltung der Arbeit.

Ganz besonders möchte ich mich bedanken bei Herrn Dr. Ralf Kleene für die vielen fachlichen Diskussionen zu meiner Arbeit und für die stets zwanglose und hilfreiche Betreuung während der gesamten Zeit als Doktorand.

Bedanken möchte ich mich auch sehr bei Herrn Professor Dr. Erhard Wischmeyer, der mir mit den Daten zu den Experimenten an den *Xenopus* Oozyten und den ergiebigen Diskussionen hierzu sehr weitergeholfen hat.

Ebenfalls sehr bedanken möchte ich mich bei Frau Galina Dityateva und Herrn Dr. Alexander Dityatev, die mir bei der Durchführung und Interpretation der Primärkulturexperimente eine große Hilfe waren.

Allen Kolleginnen und Kollegen, deren namentliche Erwähnung den Platz dieser Seite sprengen würde, danke ich für die tolle Atmosphäre, die den manchmal beschwerlichen Weg zum Doktortitel bedeutend erleichterte.

Im speziellen danke ich meinem Labornachbarn und guten Freund Gerrit Wolters für die vielen spaßigen aber auch fachlichen Dialoge sowie für die gemeinsamen Mittagspausen, die häufigen Frustphasen und die manchmal etwas entrückten Nachtschichten.

Isabel danke ich von ganzem Herzen für ihre mich stets aufmunternde Art, für ihre unumstößliche Geduld und für ihre durchgehend liebevolle Unterstützung in und außerhalb des Labors.

Ganz besonderer Dank gebührt Nena für das schnelle Korrekturlesen meiner für sie fachfremden Arbeit und für die Diskussionen zu englischer Orthographie und Interpunktion.

Meinen Eltern und meinem Bruder danke ich für ihre Geduld und ihren Rückhalt während der gesamten Zeit der Promotion.